A Methodology for Assessment of Spatial Distribution of Flood Risk

by

Xinyu Jiang

A thesis submitted as partial fulfillment of requirements
for the degree of
Doctor of Philosophy in Informatics

Graduate School of Informatics
Kyoto university

2014

Chairperson of Supervisory Committee**:**
Professor Hirokazu Tatano
Graduate School of Informatics, Department of Social Informatics

Acknowledgement

First of all, I would like to give my sincere thanks to my respected supervisor, professor Hirokazu Tatano for his guidance, understanding, patience, encouragement, and most importantly, his friendship and kindness during my PhD research at Kyoto university. His guidance helped me find the right directions of research; his understanding made me confident of my own ideas and thoughts; his patience allowed me learn a lot of knowledge from him. I will always remember the day we spent more than 6 hours to discuss a small question; his encouragement cheered me up every time that I was lost in the hard research, depressed and upset; his friendship and kindness constructed a comfortable environment for my life and study in the foreign country. He taught me the necessary things for me becoming an independent researcher and how the attitude of a researcher should be. He instilled in me the concept of system solution and problem-oriented thinking which are the fortune of a lifetime.

Special thanks are also given to two of my advisors: professor Tomoharu Hori and professor Katsuya Yamori. Professor Hori is an excellent hydrologist and have much knowledge of hydrology, hydrodynamics, meteorology and modeling. He patiently answered a lot of questions I was asked, even some of them were quit stupid, and gave me many good advises which helped me dealing with complex hydrological problems, modeling flood and inundation process, and so on. Professor Yamori is an excellent psychologist who works in the field of disaster reduction system and have much knowledge of disaster education and risk communication. His advises from social sciences helped me understand the final purpose of my research and made my research more practical and useful. Without the two advisors respectively from natural science and social science, my research cannot be achieved.

I am deeply grateful to professor Michinori Hatayama and professor Yoshio Kajitani. As members of professor Tatano's team, they offered me many valuable comments on my researches which helped me format the idea of PhD thesis. Professor Hatayama always provide technical supports and software I needed. Professor Kajitani's guidance on R and statistics opened a window for me to deal with data.

I would like to thank professor Jiquan Zhang, my supervisor of master in China. He recommend me to Kyoto University and Tatano Lab for PhD course without any reservation. His help enable me pursuing PhD in such famous university. I am also indebted to professor Zhijun Tong, my advisor of master in China. He offered me the chance of writing a chapter in his book, which enriched my academic experiences and deepened the understanding of my research.

I also appreciate professor Norio Okada, professor Ana Maria Cruz, professor Muneta Yokomatsu. They always encourage me at meetings or joint seminars and gave me valuable comments. I also appreciate professor Kenji Kawaike. He taught me a lot about flood simulation using irregular meshes, even passed his paper and code to me. Discussing with professor Kawaike is always enjoyable.

Besides professors in Kyoto University, I am deeply grateful to professor Paul Bates, Head of the School of Geographical Sciences at the University of Bristol. He hosted me as a visiting scholar in the University of Bristol for three months and provided me his models of flood and inundation simulation for comparison with my model. And I also would like to thank Professor Dawei Han of the University of Bristol and Professor Qiuhua Liang of Newcastle University. During I visited the UK, they offered me many comments to improve my researches.

I would like to express my appreciation to Mr. Toshiaki Matsueda, the chief examiner of planning group, rivers preparation division, Osaka urban development section. He offered the data of case study area. Without his help, the case study was impossible to be conducted.

I would like to convey my heartfelt thanks to member of lab: Dr. Kazuyoshi Nakano, Ms. Hui Liu, Mr. Eisuke Imai, Mr. Seitarou Yukawa, Ms. Megumi Anto, Mr. Yusuke Yoshimura, Mr. Taiki Nishimura, Mr. Furuhashi Takayuki and Ms. Kobayakawa Yumi. Although they have graduated, I enjoyed the time studied and worked with them together in the lab. I will always remember my first birthday in Japan when Ms. Anto and Mr. Yoshimura gave me very surprised presents. I also thank Dr. Junho Choi, Dr. Reza Nourjou, Dr. Tetuya Tamaki. We have been together since I came to Japan. They helped me a lot. Especially, Dr. Choi helped me prepare many documents for the PhD application; Dr. Tamaki helped me in many aspects of daily life: wrote Japanese email, moved house, guided sightseeing, etc.. All of these helps are in my heart. I also thank Ms. Fuko Nakai, Ms. Xin Zhang, for their helps in daily life, and wish they could get more achievements both in academy and work in the future. And many thanks to Ms. Atsuyo Yamashita, the secretary of lab, for her warm supports in the daily life in laboratory.

I am very grateful for my big families: my mother, my father and my mother-in-law, my father-in-law. They constructed harmony family environment and took care of my baby so that my wife and I can concentrated ourselves on research. I am greatly indebted to my wife and my son. They form the backbone and origin of my happiness. Their love and support without any complaint or regret has enabled me to complete this PhD research. I owe my every achievement to them.

Abstract

Because of many reasons, flood risk management should become more integrated to deal with different types of countermeasures, multiple stakeholders and authorities. To provide scientific platform to assess present situation in a target river basin and to evaluate effectiveness of the integrated countermeasures, it is needed to know the flood risk distribution over the space in the basin.

Spatial flood risk assessment for basin area face challenge that how to assess flood risk from multiple sources. For a place in a river basin, it may be jointly affected by multiple flood sources: flood from a large river, flood from small rivers, inundation due to local rainfall. If the joint effects are ignored, it may lead to the flood risk in this place to be misestimated. The traditional method of flood risk assessment for the purpose of river management is mainly focus on flood risk of one river and one rainfall pattern is specified to conduct spatial flood risk assessment even when multiple flood sources are considered. The research objective of this study is developing a methodology for assessment of spatial distribution of flood risk considering multiple flood risk sources.

Comparing with the traditional flood risk assessment procedures, our proposed methodology emphasize on two key points: (1) estimation of the joint probability of occurrence of flood from multiple sources; (2) requirement of integrated simulation of process from multiple sources to inundated water depth.

For the first point, a copula based method is introduced to estimate the joint probability of occurrence of flood from multiple sources. Copulas are functions that join or “couple” multivariate distribution functions to their one-dimensional marginal distribution functions. Copula offers a way to scale-freely measure dependence as well as construct families of joint distribution. In the assessment of flood risk from multiple sources, occurrence of flood from single source could be treated as marginal distributions, through copula method, the joint probability of occurrence of flood from multiple sources could be achieved.

For the second point, an integrated rainfall-runoff-inundation model is developed for integrated simulation of process from multiple sources to inundated water depth. It is a Geographic information system (GIS) based visualized, simplified rainfall-runoff-inundation model. The hydrological analysis and spatial analysis of Geographic information system (GIS) provide basic data base and kinematic wave equations and simplified shallow water equations constitute the calculation framework. Runoff area is divided by hydrological analysis and a

kinematic wave equation is adopted according to sub basin and counter line based mesh. Inundation area is simulated by a simplified shallow water equations based 2D model. The integration of runoff and inundation is controlled by joining of runoff mesh and inundation mesh, and time steps are coordinated by interpolation. The model makes it possible to simulate runoff, flood and inundation together.

The flood risk assessment is realized through a Monte Carlo method. Through copula method, the joint probability of occurrence of flood from multiple resources can be analyzed and simulated. Given a return period, random rainfall event can be generated. For each of these generated rainfall events, the integrated rainfall-runoff-inundation model is used to simulate the inundation water depth over the risk assessment area and the corresponding loss could be calculated. The risk at each place is represented by probability distribution of loss.

The methodology was applied to Otsu river basin, Osaka, Japan. The case study demonstrate the feasibility of methodology proposed in my research and show the significance of flood risk assessment considering multiple sources.

Table of Contents

LIST OF FIGURES

LIST OF TABLES

Chapter 1 Introduction

1.1 Background

1.1.1 Flood disaster and flood risk management

Flooding, one of the most serious global disasters, affects approximately 520 million people and their livelihoods annually and claims approximately 25,000 lives worldwide. The annual cost to the global economy related to flooding and other water-related disasters is between $50 billion and $60 billion [1]. Data from the Emergency Events Database (EM-DAT) shows a clear increasing trend of reported flood events since the 1950s (Fig. 1). Furthermore, the effects of both climate change and global warming in recent years include observed intensification of heavy precipitation events over approximately two-thirds of the data-covered parts of land areas in the Northern Hemisphere [2], and global warming is very likely to have increased the probability of severe flooding in some areas [3]. Therefore, more severe challenges from flood disasters can be expected in future decades.

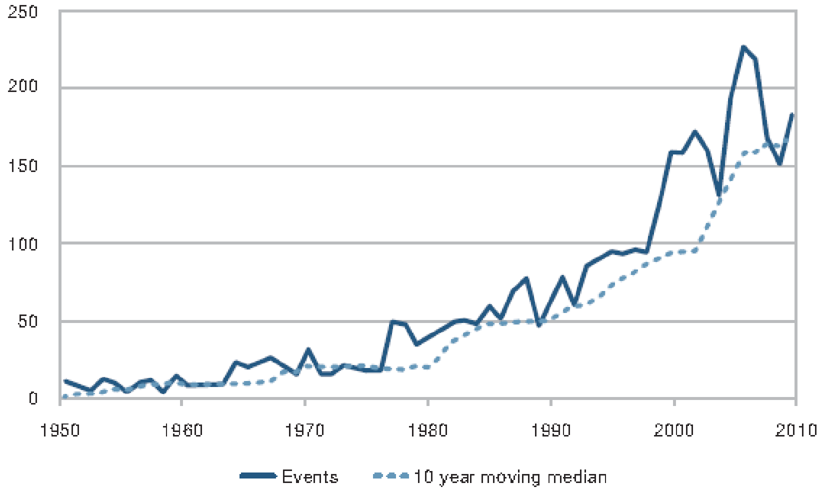

Figure 1 Numbers of reported flood events

As the continent with the largest area and population, Asia has incurred the most severe effects with more than 400 million people on average directly exposed to floods every year for the past two decades. Between 1987 and 1997, 44% of all flood disasters worldwide occurred in Asia, claiming 228,000 lives or roughly 93% of all flood-related deaths worldwide [4]. The majority of the victims lived in developing countries in Asia such as India and Bangladesh, where 1500 and 200 of victims, respectively, are counted per year. Developed countries have also incurred economic losses; Japan has reported annual losses of about 7.2 billion dollars. In China, severe losses have been reported in both human and economic losses of about 3,000 victims and 3 billion dollars annually [5].

To prevent or reduce both types of loss from flood disasters, people have continually updated their knowledge of flood behavior and treatment measures. Earliest recorded history shows attempts by society to deal with flooding until late in the twentieth century, when the principal means of mitigating the impacts of flooding was flood control. Levees, dykes, diversion channels, dams, and related structures have been constructed in an effort to control natural and periodic rising of rivers and coastal surges that accompany major storms. However, extreme events occurred and caused additional damage due to the concentrations of populations and properties in the protected areas. People then realized that flooding is a phenomenon of nature that should be managed rather than a natural disaster that can be completely controlled. Therefore, nonstructural methods and risk concepts began to play roles in flood management. Nowadays, flood risk management is widely accepted and has been adopted in many countries. Current measures take a whole-system view, which includes integrated structural and nonstructural techniques as well as policy instruments to deal with flood related challenges. The purpose is not to control floods but rather to accept them as risk events and adopt appropriate protocols for managing them.

1.1.2 Definition of flood risk

Although various perspectives result in differences in the definition of flood risk, the core definition of flood risk in flood risk management is described as

Flood Risk = f (probability of inundation and associated consequences).

Two components are involved in this definition: the probability of flood events and the associated consequences of the events [6]. Risk is the probability of potential consequences in nature. To describe flood risk, one must show the probability of flood events and the associated consequences of these events. This definition emphasizes the probabilistic characteristic of risk and provides basic concepts for modeling the risk.

Other definitions have been proposed that emphasize the mechanism of occurrence of the consequences. That is, disaster risk definitions in this group focus on the factors that determine the risk. Three different groups of definitions have been discussed in previous studies. The first definition can be described as

Risk = f (hazard and vulnerability).

Blaikie in 1994 proposed the Pressure and Release (PAR) model for understanding risk, in which risk is defined as the intersection of a hazard with some amount of vulnerability. Here, hazard is the potential threat of harm to humans and human systems by any condition or process, and vulnerability is the characteristics of a person or group in terms of capacity to anticipate, cope with, resist, and recover from the impact of a natural hazard [7]. Therefore, the mathematic expression is

Risk = hazard + vulnerability

However, arguments made on this mathematic expression stated that according to the expression, only hazard or vulnerability will cause risk, which is not true. Therefore, Blaikie amended the expression as [8]

Risk = hazard × vulnerability

This definition is consistent with risk expression of International Decade for Natural Disaster Reduction (IDNDR) and is widely used in flood risk assessment and management practice [9]. Under this concept, Zhou conducted flood risk assessment in the Liao River basin [10], Du conducted flood risk assessment in the Xiang River basin [11], and Tian conducted macro-scale flood risk assessment for the entire country of China [12].

The second definition is described as:

Risk = f (hazard, exposure, and vulnerability).

This definition is an extension of the former definition of risk. Here, exposure refers to the spatial distribution or frequency of an involved object agent exposed to the hazard [13]. Extraction of exposure as an explanatory variable of risk is meaningful because it reveals the cohesive process of hazard and vulnerability and better describes the formation mechanism of risk. In addition, it gives stronger spatial meaning to the definition of risk, and it facilitates risk management so people can more effectively handle hazards, exposure, and vulnerability. Okada and Tatano proposed and popularize these concepts [13][14], and Hori and Zhang applied them to flood risk assessment in Nagoya [15].

The third definition is described as

Risk = f (hazard, exposure, vulnerability, emergency response, and recovery capability). Based on the former definition, this definition considers emergency response and recovery capability in risk formation. It emphasizes the roles of emergency response and recovery capability, which are opposite risk formation. Davidson in 1997 proposed this concept in the study of earthquake risk assessment [16] and applied it to hurricane disaster risk assessment for the coast of the United States [17]. Moreover, Zhang applied this concept to flood risk assessment in the middle and lower basin of Liao River [18].

1.1.3 Flood risk assessment

Based on an understanding of the concept of disaster risk, the flood risk assessment and management measured have been developed. Flood risk management is a system project that includes many aspects. In this study, is the focus is flood risk assessment, which is an important step in the flood risk management process and consists of risk identification, risk analysis, and risk evaluation (Fig. 2) [19]. Risk assessment is the premise for other steps of flood risk management because it provides risk information for designing flood risk management countermeasures (Fig. 3). Only when the risk of a flood disaster is properly assessed can appropriate countermeasures be chosen. Therefore, it is necessary to investigate the methodology of flood risk assessment.

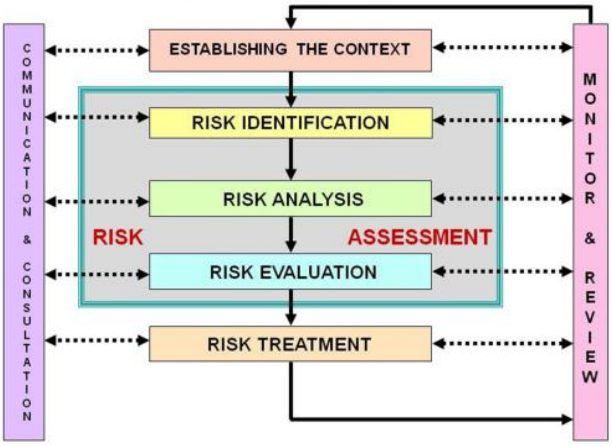

Figure 2 Risk management process

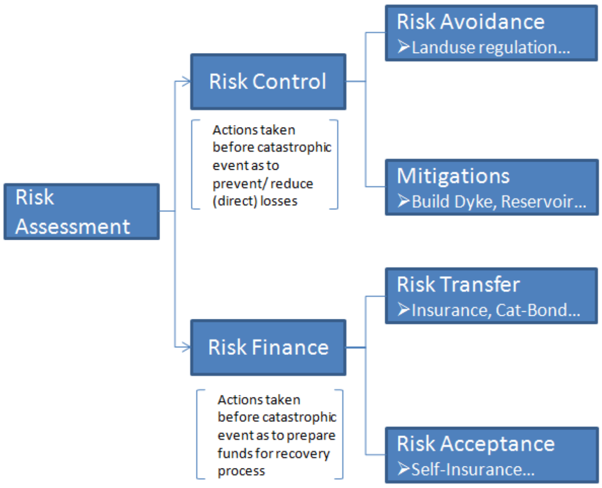

Figure 3 Risk countermeasures

Several methodologies developed to assess flood risk mainly fall into three categories including index-based risk assessment, hazard-based risk assessment, and probability-based flood risk assessment.

1. Index-based flood risk assessment

Based on the understanding that overall risk assessment of earthquake disasters requires a quantitative, systematic index, Davidson in 1997 proposed a composite earthquake disaster risk index (EDRI) for such a purpose [16]. After three years, he extended this concept and methodology to hurricane disaster risk assessment and proposed a hurricane disaster risk index (HDRI) to assess hurricane disaster risk for the United States coast [17]. Zhang in 2005 adapted this methodology to flood risk assessment in the Liao River basin, China, and proposed the flood disaster risk index (FDRI) [18]. Although other indices have been developed for risk assessment, particularly for risk zoning [20][21][22], their basic concepts are similar. All index-based risk assessment includes the following similar steps: (1) Create a conceptual framework of all factors contributing to disaster risk; (2) identify simple measurable indicators to represent each of the factors in the framework; (3) combine the indicators mathematically into composite indices; (4) perform sensitivity analysis; and (5) interpret the numerical findings.

Index-based flood risk assessment has overall advantages of being simple and quantitative. However, the following disadvantages are also obvious: (1) The dependence structure is seldom considered among factors in this method; (2) the combination of indicators is always based on experience and lacks a clear mechanism; (3) weighting factors and indicators play important roles in this method but are sometimes very subjective; and (4) the numerical results of index-based flood risk assessment have only relative significance. Nonetheless, index-based flood risk assessment is still widely used for large-scale flood risk zoning where fine data are not available.

2. Hazard-based risk assessment.

People sometimes confuse hazard maps with risk maps. In Japan, a flood hazard map refers to a map that is prepared primarily to prevent human losses by providing residents with easily understood information on levee braches, flood occurrences, evacuation. A flood hazard map must specify inundation risk areas and contain evacuation information. Moreover, it must be prepared under the responsibility of municipal leaders [23]. As previously mentioned, risk is the combination of hazard and vulnerability. Since hazard maps in Japan must include information on inundation risk areas, evacuation, and preparedness, people may consider them as risk maps. In fact, the hazard map highlights hazard information but shows no information about the consequences of the hazard; thus, it is not a risk map from our perspective. However, some scholars may add information on spatial distribution of property to the hazard map to calculate the risk. Such a method is referred to here as hazard-based risk assessment. The results from this risk assessment method reveal loss according to certain flood events in an area but not the distribution of loss due to a lack of probability analysis. This type of scenario-based risk analysis can be used for flood disaster education and evacuation as well as disaster communication.

3. Probability-based flood risk assessment.

From the perspective of statistics and economics, risk is a probability distribution of potential consequences and cannot be full expressed by a single “risk map.” However, to describe flood risk spatially, numerical characteristics are adopted to represent the probability distribution of potential consequences. Expected losses that imply the probabilities of hazards and the corresponding consequences are often used to create risk maps. To evaluate expected loss, losses according to certain return periods are calculated, and the probability distribution of loss is then calculated. Further, the uncertainty distribution of loss according to certain return periods is also estimated to achieve a more reliable risk curve. Figure 4 illustrates a standard procedure for evaluating the probability distribution of loss caused by flooding [24]. Compared with the last two methods, this method is more probabilistic, theoretical, and objective. It reveals the probabilistic nature of disaster risk and is therefore preferred by economists and insurance companies as well as city planners and administrators. However, it is also the most complex method of the three and requires good resolution data and systemic knowledge such as that of meteorology and hydrology to statistics and economy. In a sense, the first method is that of management, and the second is that of hydrology.

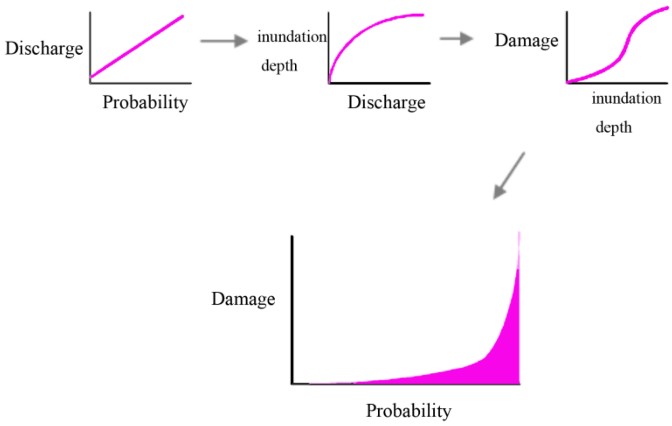

Figure 4 Transformation for traditional expected annual damage computation

1.2 Problem definition and research objectives

1.2.1 Flood risk from multiple sources

If the purpose of flood risk assessment is for designing dams, bridges, or other river management-related hydraulic architectures, it is not necessary to emphasize flood risk from multiple sources because the risk is just from water upstream of the river. However, if we assess spatial flood risk over river basins, multiple flood risk sources should be considered because flooding of the land of the river basin may have multiple flood risk sources such as large and small rivers, local rainfall, and city drainage. To explore this subject, the following actual cases of floods are presented as driving forces that led to my choice of research topic:

Case 1: Toukai heavy rainfall disaster. During September 11–12, 2000, a heavy rainfall event caused by Typhoon No. 14 struck Nagoya city, Toukai district, Japan, which caused 10 deaths, 115 injuries, and more than 270 billion JPY in economic losses [25]. An embankment of about 100 m was destroyed in the Shinkawa River in Nagoya City in which a dyke break led to severe inundation (Fig. 5) [26]. In fact, there are two rivers in this area. The Shinkawa River is a branch of the main river in the area, the Shonaikawa River. Before this disaster, more attention was paid to the main river, which was believed to be the main source of flooding in the city. However, the disaster showed a strong indication that flooding may also originate from the smaller branch. Thus, in areas that include more than one river, flood risk studies should carefully consider multiple rivers.

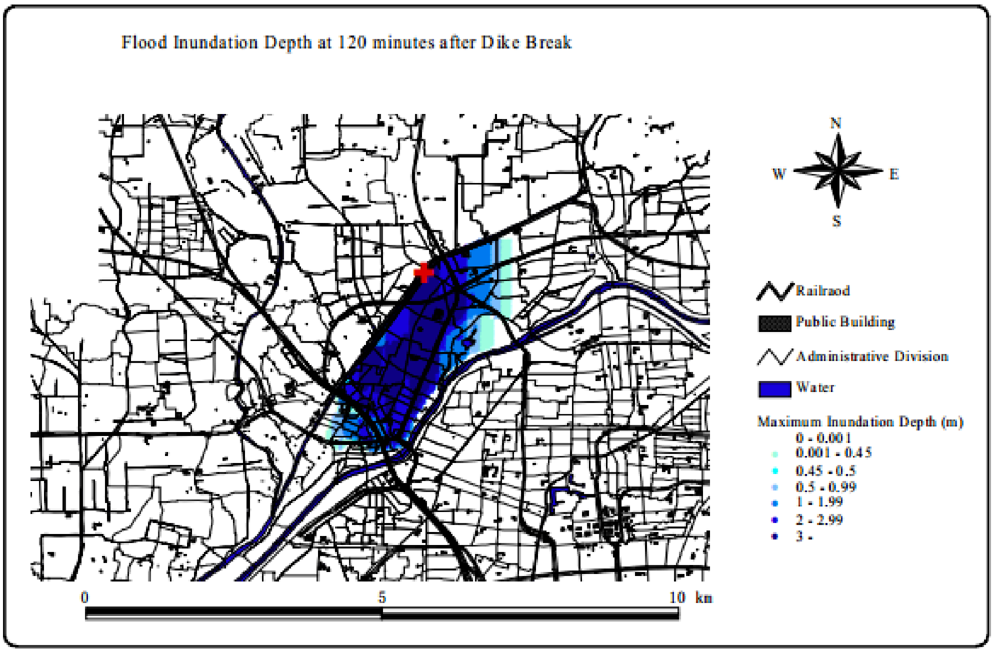

Figure 5 Inundated area of Nagoya city, Toukai district, caused by heavy rainfall from Typhoon No. 14 [26]

Case 2: 2012 Beijing flood disaster. On July 21, 2012, a heavy rainfall event occurred in Beijing, China, and caused flooding throughout the city. Within a day of the flooding, 79 people were killed and at least 10 billion CNY ($1.6 billion USD) in damages was reported including the destruction of at least 8,200 homes [27]. Investigations revealed a phenomenon such that most of the casualties and economic losses were not caused by river flooding but rather by local inundation or the joint effects of flood and inundation, whereby flash flooding carried people into rivers. However, in many places in China, flooding and inundation are managed by different departments, with the former managed by the Hydrology Department and the latter managed by the Urban Infrastructure Department. Officials in both departments believed they had already considered the risks. The Infrastructure Department considered risk from inundation to design of the drainage, and the Hydrology Department considered the flood risk in building dykes. However, neither considered the risk from both flood and inundation, which led to underestimation of flood risk for the city. An important lesson from the 2012 Beijing flood disaster is that the risk from flood and inundation should be considered together. Figure 6 shows several images of the Beijing flood disaster.

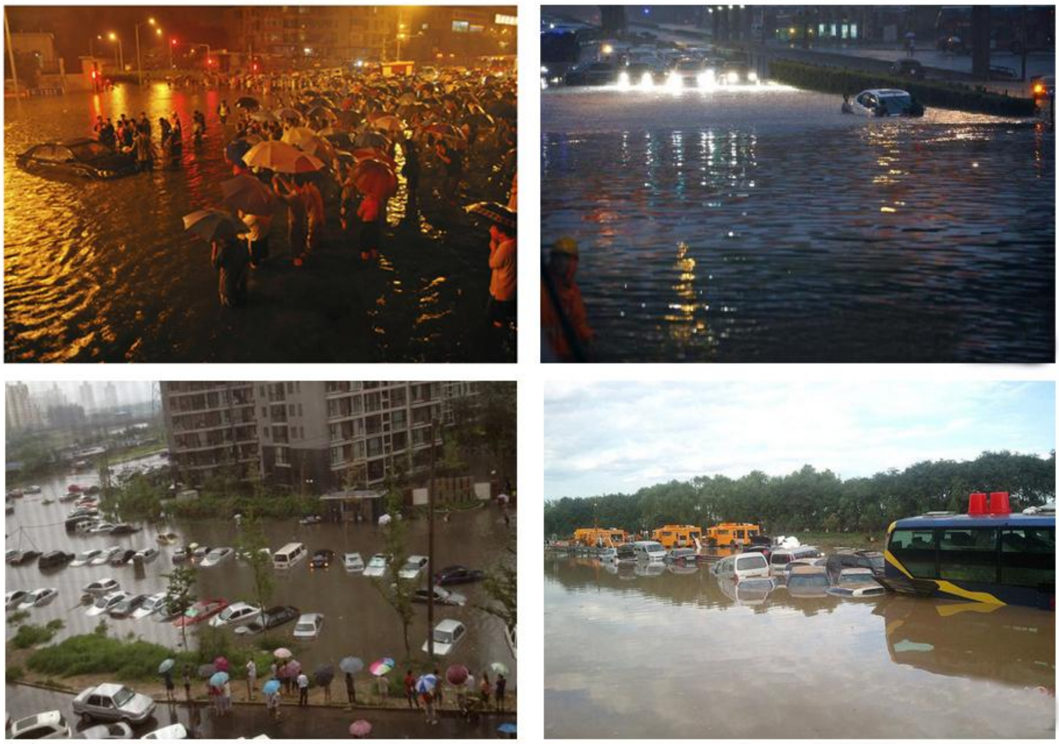

Figure 6 Flooding in Beijing, China, caused by a heavy rain event on July 21, 2012. Top left: people and cars affected by the water. Top right: people attempting to rescue submerged cars. Bottom left: residential areas surrounded by water. Bottom right: cars flushed into drainage area near a road [28]

Case 3: 2013 Yuyao flood disaster. During October 7–8, 2013, a heavy rainfall caused by Typhoon Fitow lashed Yuyao city in East China’s Zhejiang Province. Seventy percent of the downtown area was submerged, and 832,870 people in Yuyao were affected. The typhoon caused direct economic damage of 7 billion CNY (about 1.1 billion USD) [29]. Investigation revealed many flood scenarios occurring simultaneously such as local inundation, river dike breaches and overtopping as well as storm surge. The former flood risk map created by the Hydrology Department that considered only river flooding was grossly underestimated. This flood disaster event also proved the necessity of studying flood risk from multiple sources. Figure 7 shows several images of the Yuyao flood disaster.

Figure 7 Flooding in Yuyao city, Zhejiang Province, East China, caused by Typhoon Fitow on October 7–8, 2013. Top left: downtown area with 70% submersion. Top right: flood flash through the residential area. Bottom left: people boating on a flooded street. Bottom right: damage from river flooding [30]

In these three flood disaster cases, the fact that flood may originate from multiple sources is clearly shown. By increasing the considered factors in these cases, more complex flood sources can be shown. In figure 8, other sources of flooding that may affect an area are plotted. The direct cause of flood risk is the sudden occurrence of a large amount of water. By tracing the sources of this water, flood risk sources are clarified. The water may come from river flows controlled by basin rainfall; inundation directly generated by local rainfall; overflows of lakes, whether ordinary lakes or temporary barrier lakes caused by earthquakes; and runoff from a nearby mountain slope. Moreover, if the area is located near the sea, water may also originate from coastal flooding caused by tsunamis or storm surges. Such sources can cause flood disasters independently or simultaneously. Therefore, to properly assess the flood risk of an area, it is necessary to consider multiple flood sources that may affect the area.

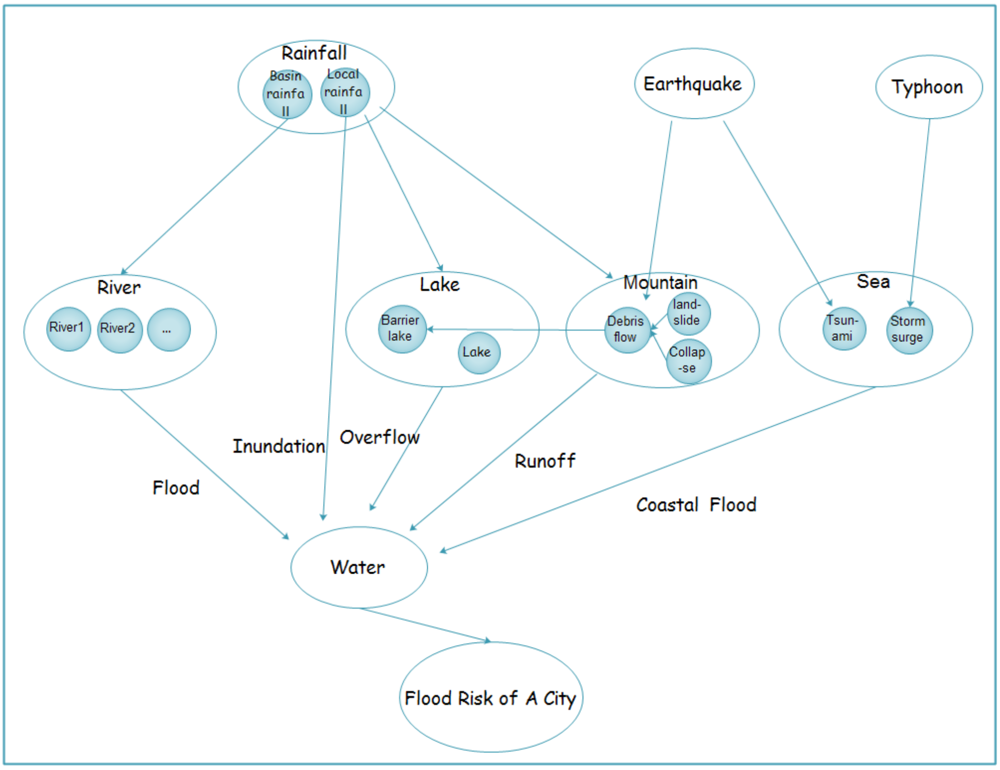

Figure 8 Flood risk from multiple sources

1.2.1 Research objectives

The primary point of this research is spatial flood risk assessment, and the crucial point of this study is consideration of multiple flood sources. As is shown by three cases above, it is necessary to include multiple flood sources in spatial flood risk assessment and evaluate the joint effects of multiple flood sources on the flood-affected area such as those due to river flooding and inundation. Ignoring the joint effects may lead to underestimation of flood risk in an area. Traditional methods of flood risk assessment for the purpose of river management focus mainly on the flood risk of one river and are not proper for spatial flood risk assessment considering all flood sources. Therefore, the research objective of this study is to develop a methodology for assessment of spatial distribution of flood risk considering multiple flood risk sources.

To achieve this objective, in this thesis, river flooding and local inundation, which may include flooding from multiple rivers, excess runoff from slopes near cities, and local inundation directly from rainfall, are considered as main flood sources. These flood risk sources are chosen for two reasons. Compared with other flood sources, river flooding and local inundation are the main causes of flood disasters in most cities. In addition, both river flooding and local inundation are rooted in rainfall. River discharge is controlled mainly by rainfall in corresponding river basins and discharge from slopes, and local inundation is controlled mainly by local rainfall. Studying these flood risk sources is in essence studying the spatial correlation of rainfall and simulation of the rainfall–runoff–inundation process, which connects this study to existing studies. The methodology is developed based on consideration of these flood sources and can be generalized to all flood sources in the future.

Figure 9 visually depicts the research problem and objective. The upper part is a plane figure that shows the spatial relationship between the flood risk assessment area and flood sources. Taking the red point for example, this area may incur flood risk from two rivers in addition to local inundation and mountains near the city. River floods are controlled by rainfall in the upper basin of rivers, and inundation from urban drainage and excess flow from slopes are controlled by local rainfall.

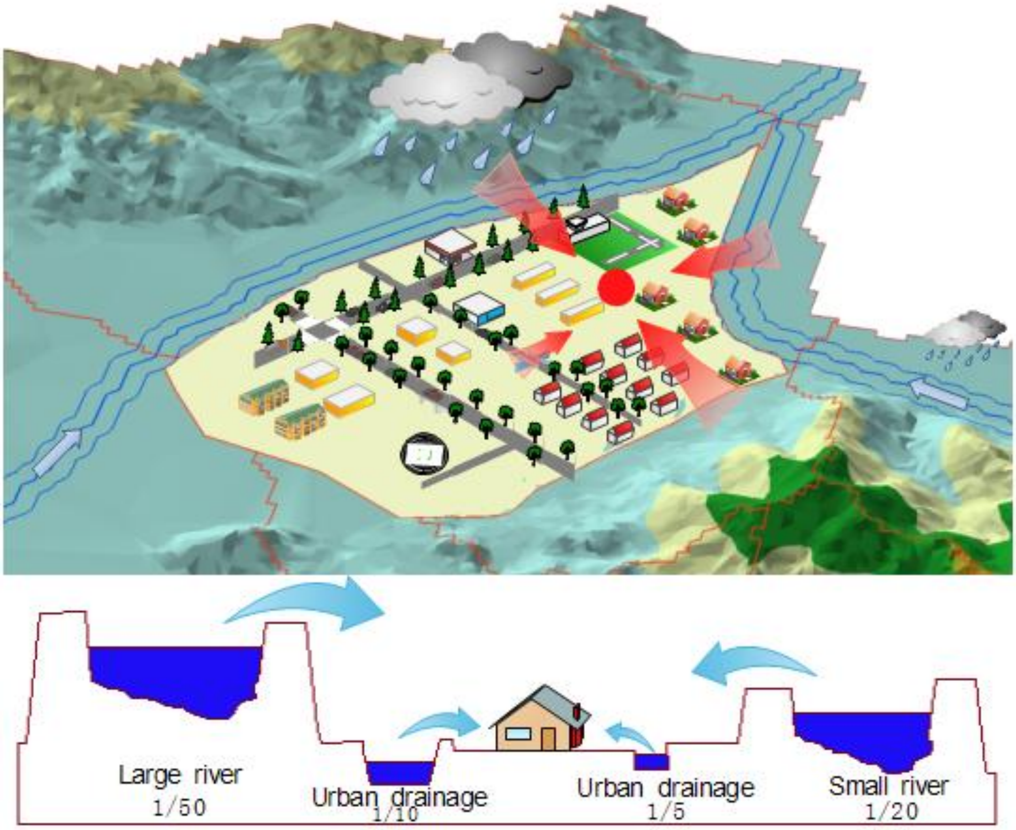

Figure 9 Flood risk from rivers, excess runoff from slopes, and urban drainage

The lower part is a profile map corresponding to the red point in the upper plane figure. The house in the focus area is subject to flooding caused by different sources. Because the characteristics of flood sources differ, their flood risks also differ. For the large river, only flooding in which the return period is smaller than once every 50 years will affect the house. If the small river has a flood return period smaller than once every 20 years, it will also affect the house. However, if the design level of the urban drainage is once every five years, and if the rainfall return period smaller than 1/5, flooding will occur and affect the house. Our challenge is to define the flood risk at the house and assess the flood risk considering the multiple flood risk sources. Thus, the objective of this research is to develop a methodology for solving this problem.

1.3 Outline of thesis

This thesis will be written into six chapters, as shown in figure 10. Chapter 1 is an introduction to the research including the background, problems, objective, and outline of the thesis. Chapter 2 is an overview of the thesis, which presents a large map of the systematic approach for spatial flood risk assessment. In addition, a methodological framework for assessment of the spatial distribution of flood risk will be proposed. From chapter 3 to chapter 5, concrete discussion on technologies and models related to realization of the proposed methodological framework is presented with a case study. In chapter 3, the case study area is introduced, and flood risk identification in this area is conducted. In chapter 4, the methods used to evaluate the joint probability of flood occurrence from multiple sources is discussed. A relatively new technique, the copula method, is introduced for spatial flood risk assessment to capture the spatial dependence of rainfall events in different sub-basins and generate random spatial rainfall events. In chapter 5, an integrated rainfall–runoff–inundation model for spatial flood risk assessment is developed to simulate the consequences of flood events caused by multiple flood sources. In chapter 6, assessment of the spatial distribution of flood risk under the proposed methodological framework is discussed. This thesis ends with a summary of the research findings and a discussion of the remaining works and future research.

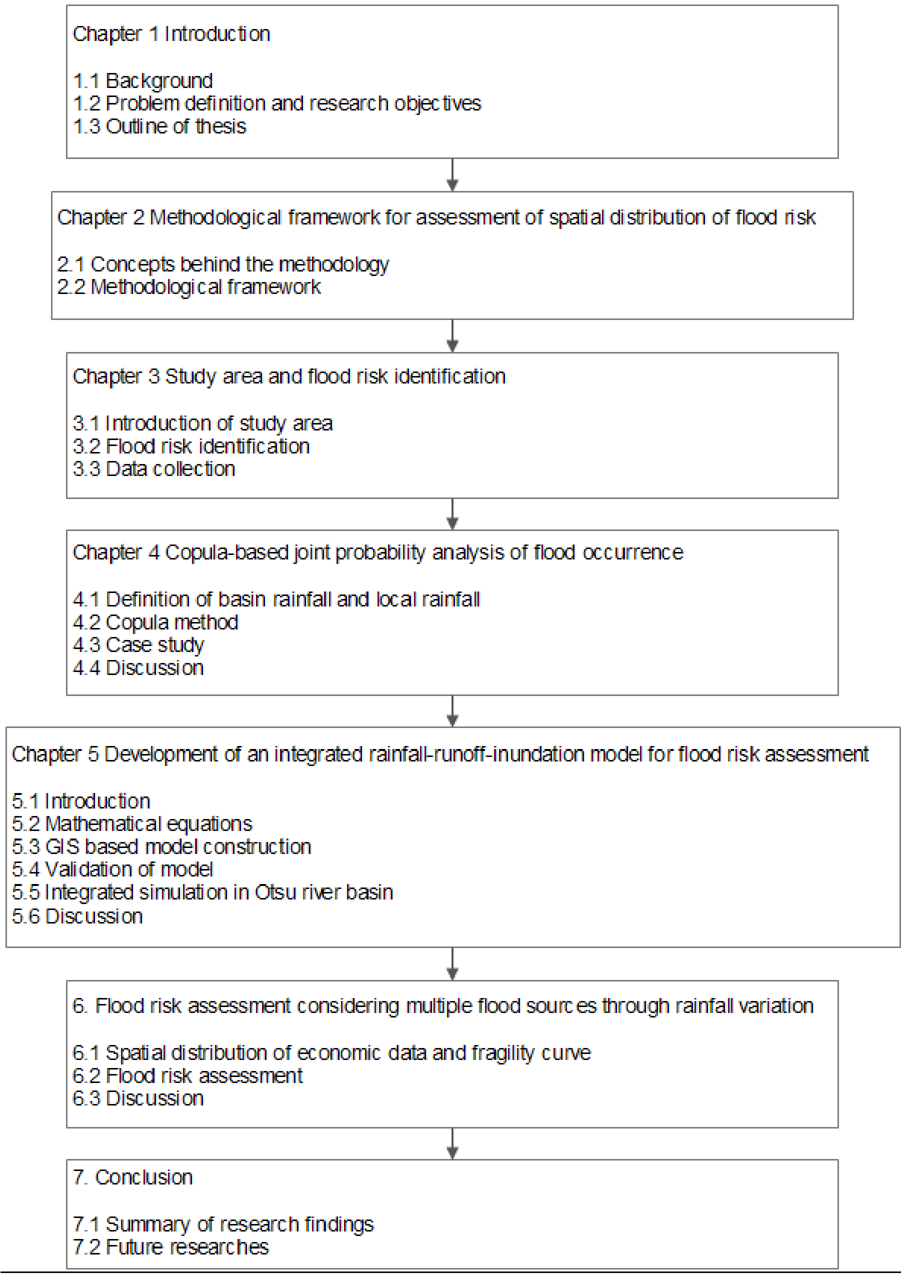

Figure 10 Structure of doctoral thesis

References

[1] WMO-UNESCO Joint-Task Team, UNU and IAHS, 2007. International Flood Initiative: Concept Paper.

[2] Min S K, Zhang X, Zwiers F W, et al. 2011. Human contribution to more-intense precipitation extremes. Nature, 470(7334): 378-381.

[3] Pall P, Aina T, Stone D A, et al. 2011. Anthropogenic greenhouse gas contribution to flood risk in England and Wales in autumn 2000. Nature, 470(7334): 382-385.

[4] Webb P. 2005. Water and Food Insecurity in Developing Countries: Major Challenges for the 21st Century. Water: Global Common and Global Problems

[5] Berga L. 2000. Dams and Floods . Paris: ICOLD.

[6] Conrow E H. 2003. Effective risk management: Some keys to success[M]. Aiaa.

[7] Blaikie P, Cannon T, Davis I, Wisner, B. 1994. At Risk: Natural Hazards, People's Vulnerability and Disasters.

[8] Wisner B, Blaikie P, Cannon T and Davis I. 2004. At Risk: Natural Hazards, People's Vulnerability and Disasters. London, Routledge. 2nd edition.

[9] Dha U N. 1992. Internationally agreed glossary of basic terms related to disaster management . UN DHA (United Nations Department of Humanitarian Affairs), Geneva.

[10] Zhou C, Wan Q, Huang S, Chen D. 2000. A GIS-based Approach to Flood Risk Zonation . Acta Geographica Sinica, 55(1):15-24. (in Chinese)

[11] Du J, He F, Shi P. 2006. Integrated flood risk assessment of Xiangjiang River Basin in China . 06:38-44. (in Chinese)

[12] Tian G, 2006. Flood risk zoning and causal analysis in China. Journal of Catastrophology.

21(2):1-6. (in Chinese)

[13] Okada N. 2004. Urban diagnosis and integrated disaster risk management. Journal of Natural Disaster Science, 26(2): 49-54.

[14] Okada N, Tatano H, Hagihara Y, et al. 2004. Integrated research on methodological development of urban diagnosis for disaster risk and its applications. Annuals of Disaster Prevention Research Institute, Kyoto University, 1-8.

[15] Hori T, Zhang J, Tatano H, et al. 2002. Micro-zonation-based flood risk assessment in urbanized floodplain. Second Annual IIASA-DPRI Meeting Integrated Disaster Risk Management Megacity Vulnerability and Resilience. Laxenburg, Austria: 29-31.

[16] Davidson R A, Gupta A, Kakhandiki A, et al. 1999. Urban Earthquake Disaster Risk Assessment and Management, Vrancea Earthquakes: Tectonics, Hazard and Risk Mitigation. Springer Netherlands: 287-307.

[17] Davidson R A, Lambert K B. 2001. Comparing the hurricane disaster risk of US coastal counties . Natural Hazards Review, 2(3): 132-142.

[18] Zhang H, Zhang J, Han J. 2005. GIS-based assessment and zoning of flood/waterlogging disaster risk: a case study on middle and lower reaches of Liaohe River . Journal of Natural Disasters, 14(6), 141-146. (in Chinese)

[19] Purdy G. 2010. ISO 31000: 2009.setting a new standard for risk management . Risk Analysis, 30(6): 881-886.

[20] Wang Y, Li Z, Tang Z, Zeng G. 2011. A GIS-based spatial multi-criteria approach for flood risk assessment in the Dongting Lake Region, Hunan, Central China. Water Resources Management, 25(13), 3465-3484.

[21] Liu J F, Li J, Liu J, et al. 2008. Integrated GIS/AHP-based flood risk assessment: a case study of Huaihe River Basin in China . Journal of Natural Disasters, 17(6): 110-114. (in Chinese)

[22] Raaijmakers R, Krywkow J, van der Veen A. 2008. Flood risk perceptions and spatial multi-criteria analysis: an exploratory research for hazard mitigation. Natural Hazards, 46(3): 307-322.

[23] Flood Control Division, River Bureau, Ministry of Land, Infrastructure and Transport (MLIT). 2005. Japan, Flood Hazard Mapping Manual in Japan.

[24] Pistrika A, Tsakiris G. 2007. Flood risk assessment: A methodological framework . Water Resources Management: New Approaches and Technologies. European Water Resources Association, Chania, Crete, Greece.

[25] Toukai heavy rain, http://ja.wikipedia.org/wiki/Tokai heavy rain.

[26] Zhang J, Hori T, Tatano H, et al. 2003. GIS and flood inundation model-based flood risk assessment in urbanized floodplain, Proceedings of the International Conference of GIS and Remote Sensing in Hydrology: 16-19.

[27] July 2012 Beijing flood, http://en.wikipedia.org/wiki/July_2012_Beijing_flood.

[28] Special news: 2012 Beijing flood, http://society.people.com.cn/GB/8217/346821/.

[29] Typhoon Fitow, http://en.wikipedia.org/wiki/Typhoon_Fitow.

[30] Special news: 2013 Yuyao flood, http://www.xinhuanet.com/politics/gdzt/yuyaoshuizai.htm.

Chapter 2 Methodological framework for assessment of spatial distribution of flood risk

2.1 Concepts behind the methodology

2.1.1 Concepts of disaster risk

The purpose of this thesis is to develop a methodology for spatial flood risk assessment considering multiple flood sources based on probabilistic methods. Two concepts of disaster risk are implied in the purpose. The first is

Risk = f (probability of inundation and associated consequences).

This concept of risk forms the basis for all probabilistic risk models. As is emphasized, to determine the flood risk, the two components that should be surveyed are the probability of flood events and the associated consequences of the events. The flood risk therefore could be expressed as the probability distribution of flood consequences. In order to map flood risk, the spatial distribution of flood risk is usually expressed as expected loss caused by flood events.

The second concept of disaster risk is

Risk = f (hazard, exposure, and vulnerability).

This concept divides risk into three parts: hazard, exposure, and vulnerability. The formation mechanism of this disaster risk is such that a disaster will occur only if all three conditions are satisfied; there is no risk without exposure or vulnerability. This concept is well explained by reference [1]. As is shown in figure 11, population and assets over the city space are expressed in the orange circle, flood hazard is expressed as the green circle, and the population and assets exposed to the threat of flooding is expressed at the intersection of these two circles. The degree of resistance of the assets and population against flooding is expressed as pillars above the exposure. The colors and heights of the pillars the indicate level of vulnerability. To assess the spatial distribution of flood risk, according to this concept, the spatial distribution of the flood hazard should be clarified. It should then by overlain by the spatial distribution of the population and assets, and exposure can be analyzed. In addition, vulnerability should be evaluated according to exposure. Finally, the spatial distribution of flood risk over an area can be assessed.

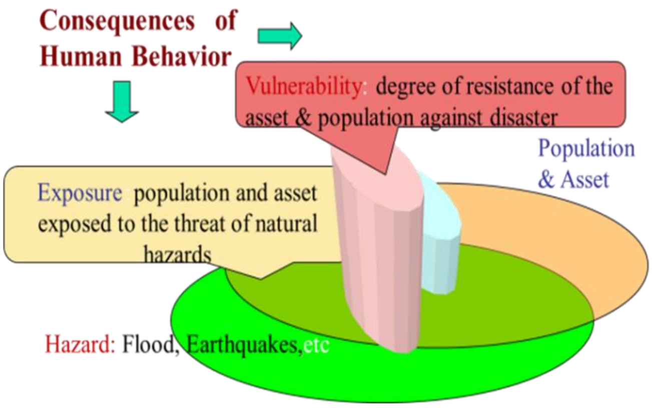

Figure 11 Disaster risk shown as the interaction of hazard, exposure, and vulnerability

In this thesis, a hazard is considered as the spatial distribution of floodwater depth; exposure is considered as assets exposed to the threat of flooding (population is not considered in this thesis); and vulnerability is described as the fragility curve that reflects the relationship between water depth and corresponds with the type of asset. To numerically model flood risk, the following steps should be followed:

(1) Probability of occurrence of inundation should be calculated (hazard).

(2) Associated consequences corresponding with probability of inundation should be calculated (exposure, vulnerability).

(3) Flood risk can then be represented as loss distribution or expected loss calculated from the probability of flood hazard corresponding to exposure and vulnerability.

2.1.2 Integrated disaster risk management

Integrated disaster risk management (IDRiM) is a process for comprehensively and credibly estimating and managing risks from multiple synergistic sources and as such presents a challenge to science and policy communities [2]. It is labeled by systematically thinking and solving disaster risk problems. In this thesis, risk is assessed from multiple synergistic sources to fulfill the requirement of integrated disaster risk management by using the systematic approach.

Flood risk assessment is a systematic problem that includes knowledge of the atmosphere, geography, hydrology, economics, and statistics. Scholars from different field may focus on different parts of the flood risk process. For example, meteorologist are concerned with the role of rainfall in flood risk assessment, and some of prefer to use a single rainfall index to assess flood risk [3]. Hydrologists are concerned with the behavior of rivers, and their concepts of flood risk often relate to hydraulic structures such as dam and bridge design rather than flood risk for the city area [4]. Economists are concerned about the risk in city areas. However, due to a lack knowledge of flooding parameters, some uncertainties are included in rainfall, and flood simulation is not effective. Thus, to solve the systematic problem, systematic methods should be used. The entire process, from rainfall to loss, should be integrated.

The original concept of flood risk assessment is from hazard sources to the hazard-affected sector. People will first consider the return period of a flood and will then analyze the hazard-affected area. This type of hazard-centered risk assessment leads to the problem of people seldom considering flood risk from multiple sources. The systematic approach offers an additional concept that first considers the hazard-affected sector such as a city area, and then traces the hazard sources. This type is known as city centered flood risk assessment. A direct advantage of this type of assessment is that assessing flood risk from multiple sources to an area is naturally highlighted.

In fact, IDRiM is an effective framework for addressing disaster issues including problems from both nature and social systems and is a scheme of system solutions. Our research, located in a segment of the entire framework, focused on a small problem of flood risk assessment. Nonetheless, we have attempted to adapt our method to format a systematical methodological framework, which may helpful for a more thorough understanding of the problem of flood risk from multiple sources.

2.1.3 Spatial correlation of disaster

If a disaster occurs in one area, what will happen in another area? Such a concern is important in flood risk management and refers to spatial correlation of disaster. The spatial correlation of disaster includes two aspects. The first is the spatial correlation of consequence, which indicates how a disaster causing loss in one area will influence other areas. For example, if a flood destroys an auto parts plant in one area, an automobile factory in another area could also incur loss even if the disaster does not affect that area. Such a type of spatial correlation of disaster consequence is analyzed by the Computable General Equilibrium (CGE) model or other economic geography models [5][6][7].

The other, more fundamental, aspect is spatial correlation of the hazard in which a severe event may trigger hazards in many areas. For example, the big earthquake on March 11, 2011, caused a tsunami that affected most of Japan’s east coast [8]. Alternatively, one area may be affected by many hazard sources, as is discussed in this thesis. The spatial correlation of a hazard is usually included in physical hazard simulation models. For example, a tsunami simulation model can a reveal spatial correlation of tsunami inundation in coastal areas, and a flood routing model can reveal the spatial correlation of flooding in upper and lower streams. However, such spatial correlation included in physical simulation models is scenario based and should be statistically studied. The concern of this thesis is the statistical spatial correlation of multiple hazards that may affect same area. Only when the spatial correlation of multiple hazards is understood will flood risk assessment in this area be accurate.

2.2 Methodological framework

2.2.1 General procedure for integrated assessment of flood risk from multiple sources

With an understanding of the above concepts, a general procedure for integrated assessing flood risk from multiple sources is developed by expanding traditional flood risk assessment procedures to multiple sources (Fig. 12). The procedure includes the following four steps: 1. Identify risk sources that affect the study area; 2. Evaluate the joint probability of occurrence of flooding from multiple sources; 3. Simulate flood events caused by multiple sources; 4. Calculate risk. Compared with traditional flood risk assessment procedures, this procedure emphasizes two points. The first is estimation of the joint probability of flood occurrence from multiple sources, and the second is the requirement of integrated simulation of processes from multiple hazards to water inundation depth.

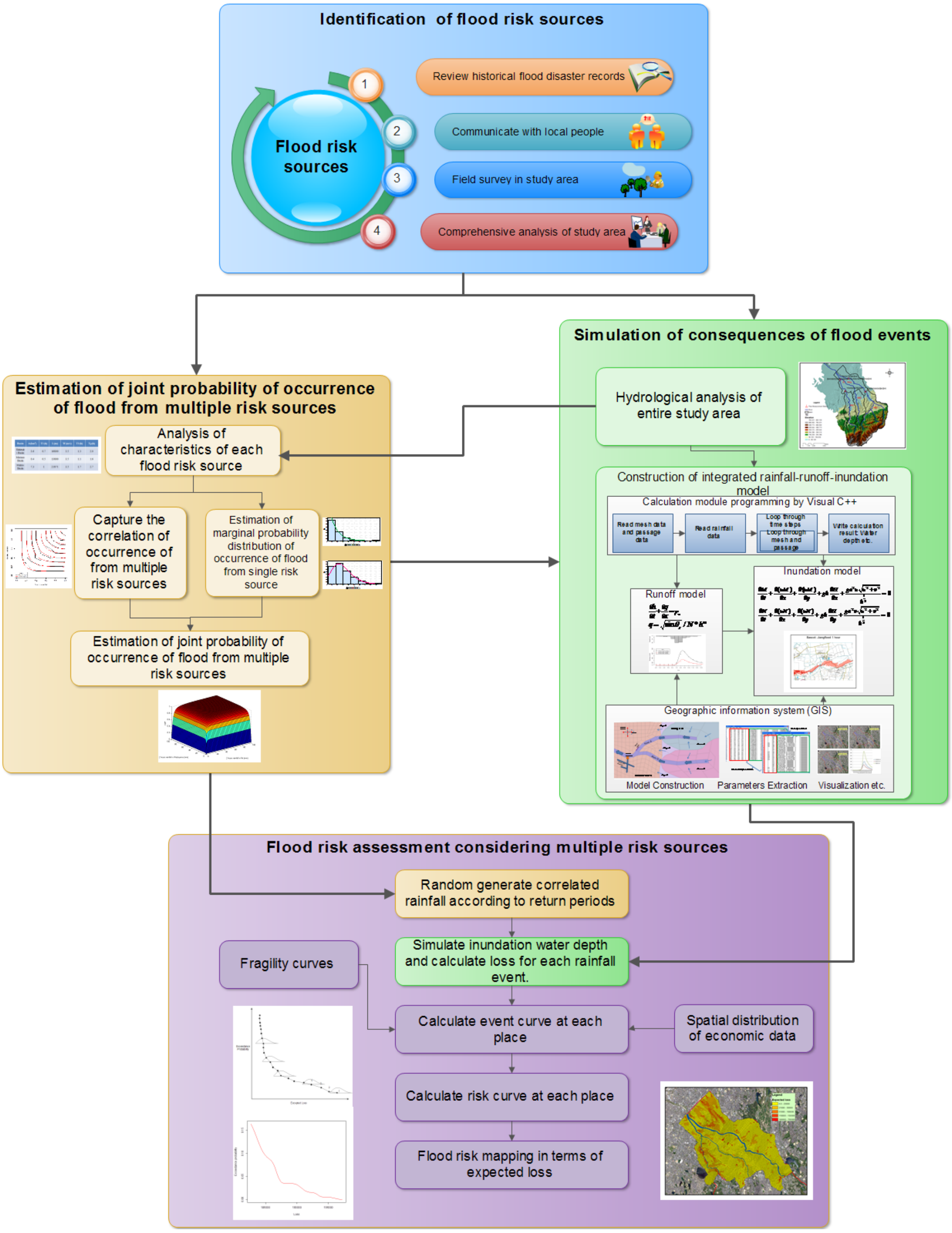

Figure 12 Procedure for evaluating flood risk distribution in an area considering multiple flood sources

Step 1: Identify risk sources that affect the study area.

Following the concept of city-centered flood risk assessment, the area affected by the hazard is considered first. Then, risk sources that may affect the hazard-affected body can be traced. If we focus on entire river basins, we must first assign a risk assessment area. In a river basin, not all areas incur flood disasters from multiple sources, and flood simulation will not include all areas. Therefore, empirical and qualitative analysis should be conducted to define the center area that may incur flood disasters from multiple sources. Identification of flood risk sources can be achieved through reviewing historical flood disaster records, communication with local people and local government, field survey or comprehensive analysis of the natural conditional of the study area. Technologies such as spatial analysis and hydrology analysis can be used for this purpose.

Step 2: Evaluate the joint probability of flood occurrence from multiple sources.

After identifying risk sources, those that may affect the study area are revealed. The next step is evaluation of the joint probability of flood occurrence from these sources. The characteristics of each source should be analyzed firstly. Synchronous data from multiple sources should be collected to evaluate the dependence structure among them. Then, the joint probability of flood occurrence from multiple sources can be determined by fitting of marginal and multivariable distributions. In addition, extreme events are the main concern in flood risk assessment but are rare in reality. Therefore, generation of extreme events under the dependence structure among sources is also necessary for risk assessment.

Step 3: Simulation of consequence of flood events.

To assess the spatial distribution of flood risk, it is necessary to simulate the spatial distribution of the flood hazard indices such as water depth and flow velocity etc. Since the flood may come from multiple sources, the simulation model should be able to consider various situations. Many models developed to simulate various hydrological phenomena include evaporation models, runoff models, and inundation models. Most of them are designed for a specific purpose and work individually. To consider flood risk from multiple sources, it is necessary to develop an integrated model to simulate the overall process of flood formation. An ambitious blueprint, for example, to consider flood risk caused by overtopping or breaking of Barrier Lake, which was created by an earthquake, should include models that are able to simulate the formation of Barrier Lake after the earthquake.

Step 4: Flood risk assessment considering multiple risk sources.

As previously mentioned, flood risk can be expressed as the probability distribution of loss at a location. After simulating the flood events, spatial distribution of the water depth, flow velocity, and other hazard indices can be quantified. Along with the spatial distributed asset data and fragility curve, the loss can be calculated. A flood event curve can then be created as a result of Monte Caro simulation of loss attributed to flood events. Finally, the risk curve can be calculated considering the probability distribution of uncertainty in the loss evaluation.

2.2.2 Methodological framework for integrated assessment of flood risk from river floods and local inundation

As explained in the research objective, river flooding and local inundation are considered in this thesis as main flood sources. The methodology is developed based on consideration of these flood sources and can be generalized to all flood sources. Therefore, based on the proposed general procedure, this section will introduce a methodological framework for integrated assessment of flood risk from river flooding and local inundation, which may include flooding from multiple rivers, excess runoff from slopes near cities, and local inundation directly from rainfall. Rainfall is the root cause of river flooding and local inundation. Discharges of rivers that cause river flooding are mainly controlled by basin rainfall, and discharges from slopes as well as local inundation are mainly controlled by local rainfall. The fault tree of river floods and local inundations is shown in figure 13.

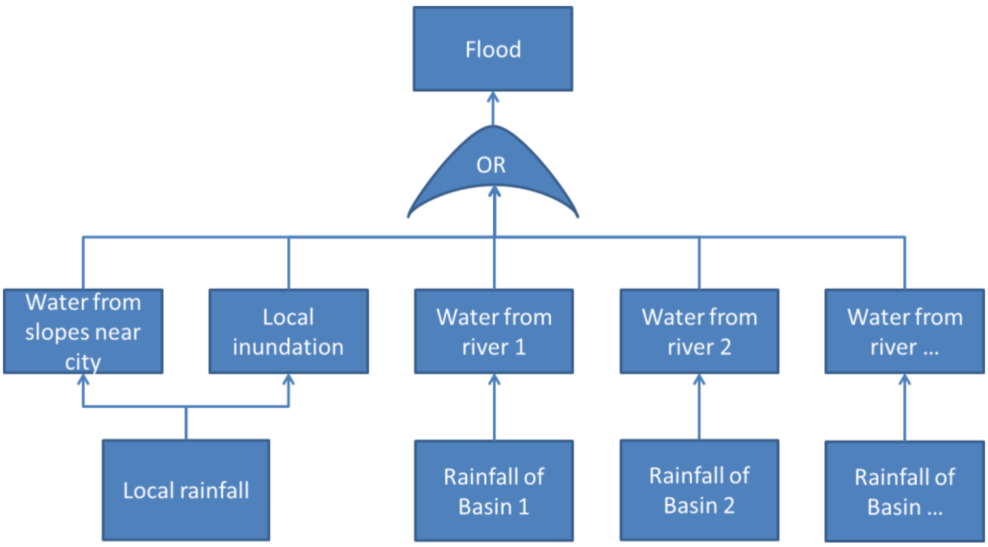

Figure 13 Fault tree of river flooding and local inundation

In this sense, the core parts of assessing flood risk from river flooding and local inundation are included in the study of the correlation of local rainfall and basin rainfall with simulation of the rainfall–runoff–inundation process in an area. By following the proposed general procedure for the concrete method and implementation step, the methodological framework for integrated assessment of flood risk from multiple rivers, excess runoff from slopes, and local inundation can be achieved (Fig. 14).

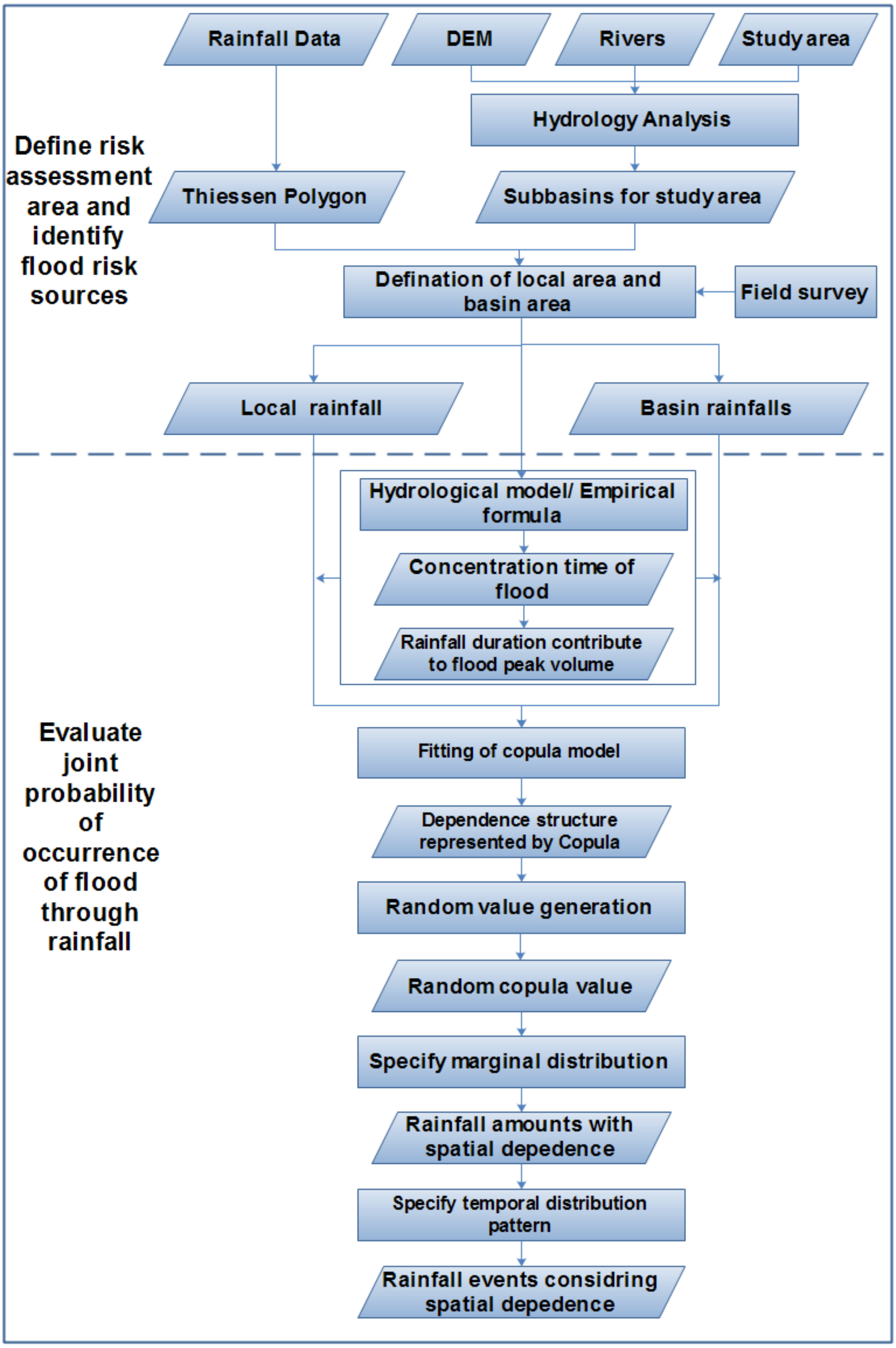

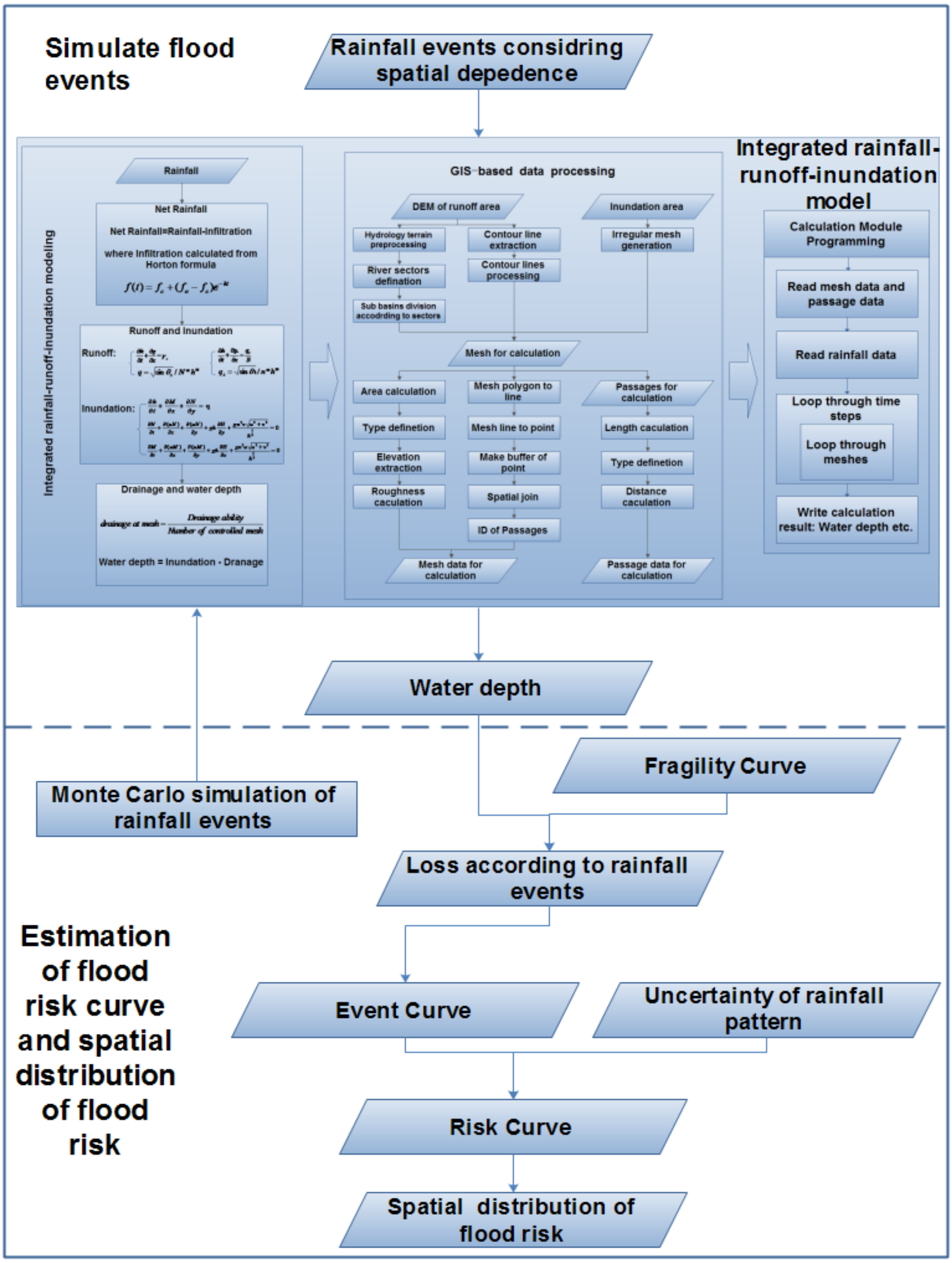

Figure 14 Methodological framework for integrated assessment of flood risk from multiple rivers and local inundation

In the first step, the center flood risk assessment area is defined, and multiple sources that may affect the flood risk assessment area are identified. As previously stated, the cause of river flooding, local inundation, and excess runoff from slopes are local rainfall and basin rainfall. The purpose of this step is to identify the local and basin rainfall for an area. This identification is based on the rainfall characteristics and the geographic features of the study area. If the variation of rainfall within the study area is not large and the rainfall characteristics can be expressed as reprehensive rainfall, the local rainfall and basin rainfall can be the same. If the variation of rainfall within the study area is large and the rainfall characteristics can be expressed as reprehensive rainfall, more detailed analysis based on geographical features should be conducted.

In the second step, the hydrology model or empirical formula is used to calculate the time-of-arrival of flooding in each river sub-basin. In particular, the rainfall duration contribution to flood peak volume is evaluated. Then, the local rainfall and basin rainfall are rearranged according to the contribution of their duration to flood peak volume. The rearranged rainfall data include potential descriptions of the statistical characteristics of flooding from rivers, local inundation, and excess runoff from slopes. Then, taking the rearranged local rainfall and basin rainfall data as input, a proper copula function is selected to model the joint distribution of rainfall. The random correlated rainfall amount can be generated according to the copula model. With the specified temporal pattern, rainfall events considering the spatial dependence structure among local rainfall and basin rainfall can be generated. The detailed process of this step is described in chapter 4.

The generated spatial correlated rainfall is then put into the integrated rainfall–runoff–inundation model developed in step 3 to simulate flooding from rivers, local inundation, and excess runoff from slopes caused by local and basin rainfall. The theoretical framework of this integrated model consists of kinematic wave equations and simplified shallow water equations. Model construction and data preparation is conducted through hydrology analysis and spatial analysis of the geographical information system (GIS), and the calculation module is programmed on the platform of visual c++. The output of the model is spatial distribution of water depth. Details of the model are provided in chapter 5.

The last step estimates the flood risk curve and spatial distribution of the flood risk. First, the losses according to rainfall events are calculated by using simulated water depth and the fragility curve, which reflect the relationship between water depth and correspond to the type of asset. After Mont Caro simulation of rainfall events, a set of loss data corresponding to the return period of rainfall can be obtained, and the event curve can be drawn. Finally, the risk curve can be calculated considering the probability distribution of the uncertainty of loss evaluation.

References:

[1] Hagihara Y, Okada N, Tatano H. Introduction to Integrated Disaster Risk Management, Kyoto University Academic Press, pp. 141-143. (in Japanese)

[2] Amendola A, Linnerooth-Bayer J, Okada N, et al. 2008. Towards integrated disaster risk management: case studies and trends from Asia . Natural Hazards, 44(2): 163-168.

[3] Bocchiola D, Michele C D, Rosso R. 1999. Review of recent advances in index flood estimation . Hydrology and Earth System Sciences, 7(3): 283-296.

[4] Plate E J. 2002. Flood risk and flood management . Journal of Hydrology, 267(1): 2-11.

[5] Tatano H, Tsuchiya S. 2008. A framework for economic loss estimation due to seismic transportation network disruption: a spatial computable general equilibrium approach . Natural Hazards, 44(2): 253-265.

[6] Tsuchiya S, Tatano H, Okada N. 2007. Economic loss assessment due to railroad and highway disruptions . Economic Systems Research, 19(2): 147-162.

[7] Okuyama Y, Chang S. 2004. Modeling spatial and economic impacts of disasters. Springer.

[8] 2011 Tohoku earthquake and tsunami,
http://en.wikipedia.org/wiki/2011_Tohoku_earthquake_and_tsunami.

Chapter 3 Study area and flood risk identification

3.1 Introduction of study area

3.1.1 Natural conditions

The study area is located in the southern part of Osaka prefecture, Japan. Otsu River is a river of Osaka prefecture rising along Katuragi Mountain and flowing about 68 km westward to Osaka Bay. It consists of five branches include the Chichioni, Higashimakio, Makio, Matsuo, and Ushitaki rivers. The river basin extends from 34°20′N to 34°30′N and 135°23′E to 135°21′E. The area of the river basin is 102.2 km^2 and includes the cities of Izumi, Kishiwada, Izumiotsu and the town of Tadaoka and is the largest secondary drainage in Osaka prefecture. The upstream of the basin is a mountainous area covered by natural landscape; the middle part of the basin is hilly and partly developed; and the downstream of the basin is a well-developed urban area [1]. A sketch map of Otsu River basin is shown in figure 15.

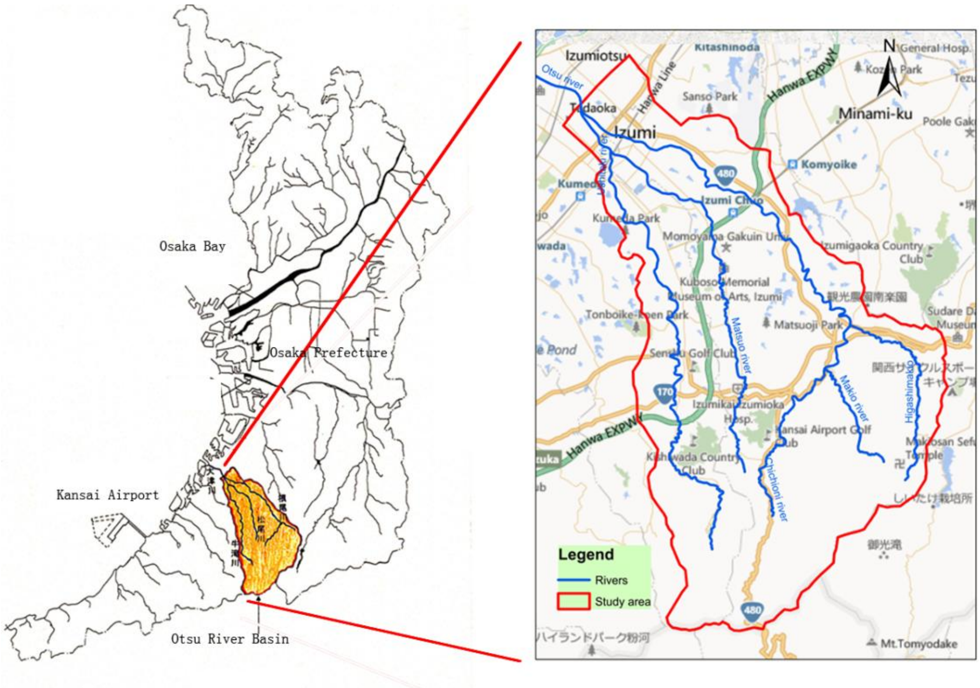

Figure 15 Sketch map of study area

In this area, the average annual temperature is 16 ℃, and the average annual rainfall is about 1200 mm, the active rain season in June and the typhoon season in September account for most rainfall amounts. Figure 16 show the trends in annual rainfall and temperature, and figure 17 shows those in monthly rainfall and temperature.

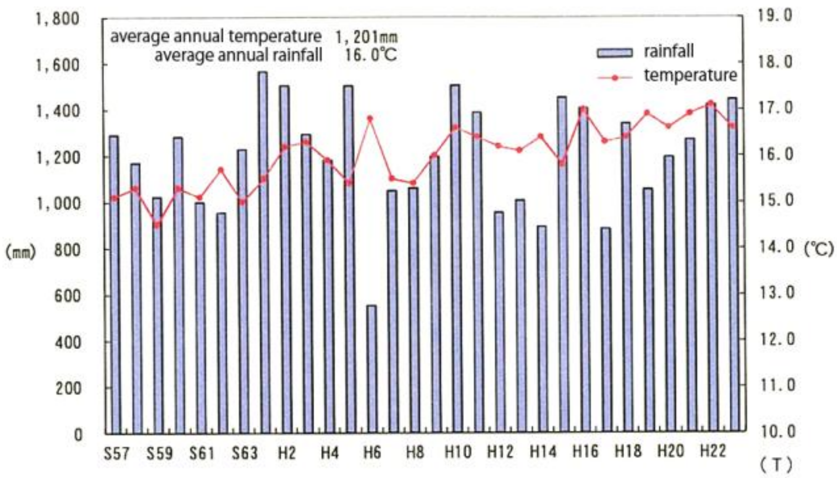

Figure 16 Trends of annual rainfall and temperature

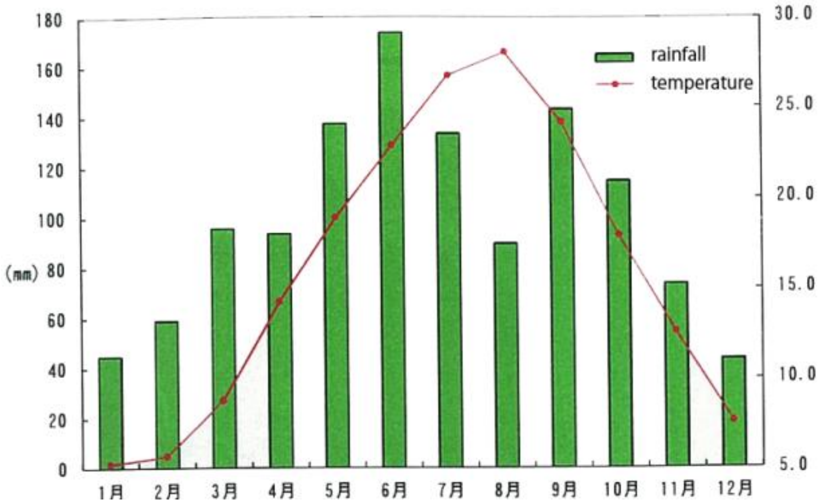

Figure 17 Trends of monthly rainfall and temperature

3.1.2 Historical flood disasters

Flooding is the main type of disaster in this area. From 1950 to 2011, 14 flood disaster events were recorded. For example, in 1961, a typhoon and heavy rainfall (44.2 mm/h) caused inundation of more than 145,959 houses the deaths of 35 people. In 1982, a typhoon and heavy rainfall (37 mm/hr) caused inundation of more than 5700 houses and economic losses of civil infrastructure totaling about 1,083 JPY. In addition, three parts of the dyke of the Makio River totaling 250 m broke. In 1989, two flood events were recorded. On September 2, heavy rainfall (32 mm/hr) caused inundation of more than 200 houses and civil infrastructure losses of 40 million JPY. On September 19, a typhoon and heavy rainfall (38 mm/hr) caused inundation of more than 800 houses and civil infrastructure losses of 26.4 million JPY. The latest flood disaster occurred in 2011, when heavy rainfall (32 mm/hr) caused some loses in civil infrastructure but no inundation of houses.

The Otsu River basin is the representative area for our study for the following reasons. This area incurs severe damages from flood disasters, and local inundation accounts for a large number of these losses. In addition, multiple rivers are located in this area. Thus, some parts of this area may be affected by multiple rivers, particularly the confluence area. Therefore, Otsu River basin was selected as the main case in the study area for integrated assessment of flood risk from multiple rivers, excess runoff from slopes, and local inundation.

3.2 Flood risk identification

3.2.1 Definition of flood risk assessment area

The study area is the entire basin of Otsu River, which includes three sub-basins of Makio, Matsuo, and Ushitaki rivers. To study the flood risk from multiple sources, it is not necessary to consider the enter basin at the same time. In the proposed methodology, the study area is considered as two parts including the center area in which the flood risk assessment is conducted and the outside area, which is treated as the input condition of the flood risk assessment area.

In fact, definition of the flood risk assessment area from the study area is relatively subjective work; all areas can be defined as flood risk assessment areas. In this thesis, the area potentially affected by multiple flood sources is the focus. Therefore, the downstream of the basin in which three river flows are concentrated is the first area to be considered. As shown in figure 18, the downstream of the basin is flat, which gives it a better chance of flooding by multiple rivers and local inundation. In addition, the population and properties are concentrated in this area; therefore, it is meaningful to consider this area first as a risk assessment area. Five flow gauge stations are located in the downstream of the basin. In order to validate the rainfall–runoff–inundation model, the boundaries of the risk assessment area are determined by these flow gauge stations.

The Yamadaibashi and Kawanakabashi flow gauge stations were used as outlets for hydrological analysis in the GIS is conducted. The procedure for basin division based on the digital elevation model (DEM) is modularized and integrated in the Arc Hydro program [2]. The procedure includes DEM reconditioning, which modifies the DEM by imposing linear features; fill sinks, which modify the elevation value to eliminate problems that occur when a cell is surrounded by higher elevation cells, trapping water in that cell and impeding flow; flow direction calculation, which computes the flow direction grid; flow accumulation calculation, which computes the accumulated number of cells upstream of a cell; stream definition; stream segmentation; catchment grid delineation; and catchment polygon processing. Figure 18 shows the division of the study area. The upper part is the downstream area, defined as the risk assessment area, and the lower part is the upstream area, defined as the outside area.

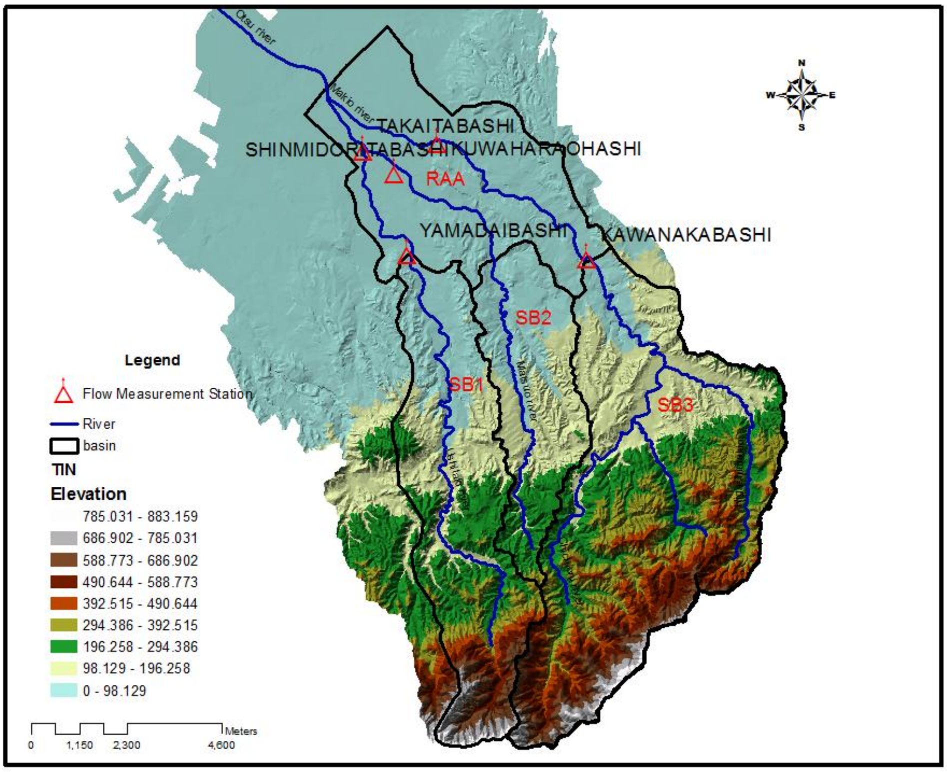

Figure 18 Definition of flood risk assessment area

3.2.2 Risk identification

The purpose of risk identification is to identify risk sources that may affect the risk assessment area. For the risk assessment area defined in this paper, flood sources include river flooding from Ushitaki River, which is controlled by rainfall in the upper part of Ushitaki sub-basin (SB1); flooding from Matsuo River, which is controlled by rainfall in the upper part of Matsuo sub-basin (SB2); flooding from Makio River, which is controlled by rainfall in upper part of Makio sub-basin (SB3); and local inundation from urban drainage or slope flow, which controlled by rainfall in the flood risk assessment area (RAA). The spatial relationship of these flood risk sources is shown in figure 18. The fault tree of the flood disaster is shown in figure 19.

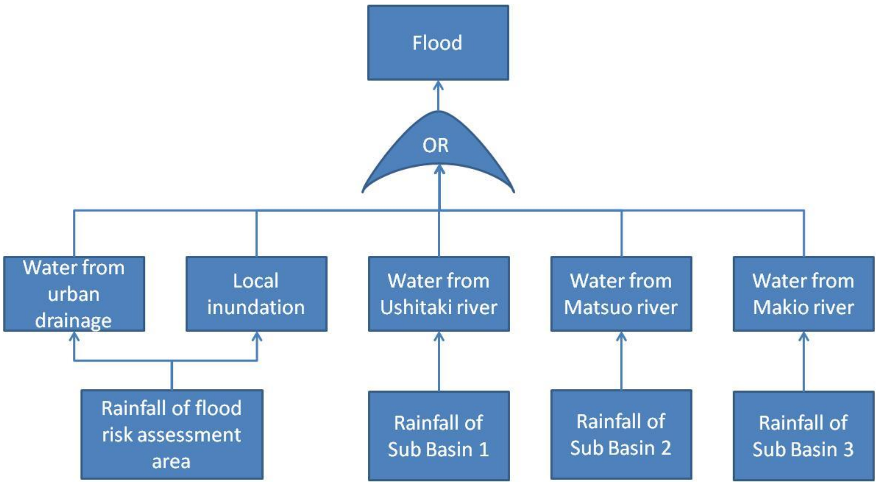

Figure 19 Fault tree of flood disaster in risk assessment area

As shown in figure 19, in order to assess flood risk of the area considering multiple flood sources, it is necessary to study the joint distribution of rainfall in RAA, SB1, SB2, and SB3. However, the significant rainfall duration for causing floods differs among sub-basins. For example, although a 3 h rainfall event may be significant for a larger river to produce a flood peak in risk assessment area, only 2 h may be enough for a small river to produce a flood peak in the risk assessment area. In risk identification, the significant rainfall duration in each sub basin also should be pointed out.

The concentration time of flooding, a concept used in hydrology to measure the response of a watershed to a rain event, was adopted to identify significant rainfall duration in each sub basin. It is defined the time required for disturbance of rainwater to propagate from the top of a slope at the most remote portion of the basin in the sense of dynamics to the outlet [3]. Based on this definition, the concentration time of flooding can be thought as the duration that contributes to flood peak volume. The concentration time could be either simulated by a hydrology model or calculated by an empirical formula. Many previous studies on concentration time have been reported. In this paper, commonly used formulas include Kraven, uniform flow velocity, Public Works Research Institute, and Kadoya formulas are summarized (table 1) [4].

Table 1 Empirical formulas for evaluation of concentration time of flood

	T_1 flow time (hr)	T_2 inlet time (hr)	T_p concentration time (hr)	Parameters
Kraven formula	$T_1 = \frac{\sqrt{A}}{\sqrt{2}} \cdot T'$	$T_2 = \frac{1}{3600} \cdot \frac{L}{W}$	$T_p=T_1+T_2$	A: area of watershed up on the river; (km^2) T': maintain area 1/2; Steep slope area 1/3 (hr) L: river length (m) W: flood speed (m/s). 3.5m/s if the slope larger than 1/100; 3.0m/s if the slope smaller than 1/100 and larger than 1/200; 2.1m/s if the slope larger than 1/200;
Uniform flow velocity formula	Same to Kraven formula	Same to Kraven formula, however the W is calculated by the following formula: $W = \frac{1}{n} \cdot R^{2/3} \cdot I^{1/2}$	$T_p=T_1+T_2$	W: flood speed (m/s) n: roughness coefficient R: hydraulic radius (m) I: river slope
Kadoya formula			$T_p = CA^{0.22} r_e^{-0.35}$	C: coefficient determined by land use A: area of river basin (km^2) r_e: efficient rainfall (mm/hr)
PWRI formula (Public Works Research Institute)			Urban basin: $T_p = 2.4 \times 10^{-4} \left(\frac{L}{\sqrt{S}} \right)^{0.7}$ Nature basin: $T_p = 1.67 \times 10^{-4} \left(\frac{L}{\sqrt{S}} \right)^{0.7}$	L: longest path of river basin (m) S: slope of the longest path

In this thesis, the flood concentration times of the study area were calculated by the empirical Kraven formula. The parameters and calculation results are shown in table 2. The flood concentration time of Ushitaki Basin is 2 h; that of Matsuo Basin is 1.6 h; and that of Makio Basin is 2.7 h. Thus, rainfall events of 2 h, 1.6 h, and 2.7 h in Ushitaki, Matsuo, and Makio will contribute to the peak discharge at the outlet. Moreover, at any point in the study area, the peak discharge including peak rainfall can be fully explained by the rainfall amount within 3 h. Inundation is explained by hourly rainfall; river flooding is explained by 2 h and 3 h rainfall amounts. Thus, we have reason to assert that the analysis of joint probability of rainfall amounts of 1 h, 2 h, and 3 h will reflect the relationship of local rainfall and basin rainfall, which further reveals the joint probability of flooding from multiple sources.

Table 2 Parameters and calculation results for the concentration times of flood

Basin	A (km^2)	T′ (h)	T1 (h)	L (m)	W (m/s)	T2 (h)	Tp (h)

Ushitaki Basin	3.6	0.5	0.7	16800	3.5	1.3	2.0
Matsuo Basin	0.4	0.5	0.5	13800	3.5	1.1	1.6
Makio Basin	7.3	0.5	1	21871	3.5	1.7	2.7

3.3 Data collection

In order to implement the case study in the Otsu River Basin, relevant data were collected including rainfall gauge, river flow gauge, geographical, historical, and other data. The data, usage, and sources are list in table 3.

Table 3 Data collection

Catalog	Data	Usage	Source
Rainfall gauge data	Length of rainfall data at Kuki, Wakakashi, Ohno, Futsunami, Zensyoh, Makiosan, Harukigawa, Kitatanaka, Chichioni, Matsuoji, Ushitaki, Ohsawachoh stations (2005–2012) Length of rainfall data at Kishiwada, Yamataki, Ohtori, Yokoyama stations (1963–2012)	Rainfall analysis to further reveal the joint probability of floods from multiple sources.	River Management Department of Osaka prefecture
River flow and water stage gauge data	Kawanakabashi, Takaitabashi, Kuwaharaohashi, Shimidoriihashi, (1994–2012)	Validation of rainfall–runoff model	River Management Department of Osaka prefecture
Geographical data	Digital Elevation Model (DEM)	Hydrological analysis	Reference [5]
	Location of rain gauge station (x,y)	Analysis of spatial distribution of rainfall	River Management Department of Osaka prefecture
	Location of flow gauge station (x,y)	Validation of rainfall–runoff model	
	River information (river section, etc.)	Flood simulation	Reference [6]
	Land use information	Analysis of roughness	
Historical data	Area survey data	For reference	River Management Department of Osaka
	Historical flood disaster records	For reference	

			prefecture
Economy related data	Population	Risk assessment	Reference [7] [8] [9]
	Assets	Risk assessment	
Other data	Reports of river and basin planning of Otsu River area	For reference	River Management Department of Osaka prefecture

References:

[1] Osaka prefecture, basic policy for river improvement, http://www.pref.osaka.lg.jp/kasenseibi/keikaku/ootsukihon.html.

[2] Maidment, D R (Ed.). 2002. ArcHydro: GIS for water resources. ESRI, Inc.

[3] Kadoya, M, Fukushima, A. 1976. Concentration Time of Flood In Small or Medium River Basin. Disaster Prevention Research Institute Annuals, 19: 143-152.

[4] Japan Society of Civil Engineers. 1986. The Collection of Hydraulic Formulae. (in Japanese)

[5] Geospatial Information Authority of Japan. http://www.gsi.go.jp/.

[6] Geographical Information System, Ministry of Land, Infrastructure, and Transport of Japan. http://nlftp.mlit.go.jp/ksj/gml/datalist/KsjTmplt-W05.html.

[7] Sinfonica. 2010. Areal mesh-based census of Japan. (in Japanese)

[8] Sinfonica. 2009. Areal mesh based economy census of Japan. (in Japanese)

[9] Sinfonica. 2006. Establishment and enterprise census of Japan. (in Japanese)

Chapter 4 Copula-based joint probability analysis of flood occurrence

4.1 Definition of basin rainfall and local rainfall

After risk identification, the risk sources that may affect the study area can be understood. The next step is evaluating the joint probability of flood occurrence from these sources. The joint probability of flood occurrence from multiple sources can be determined by fitting of marginal distributions and multivariable distributions through the copula method. As was analyzed in chapter 3, the root cause of both river flooding and inundation in the study area is rainfall. The rainfall data was adopted to analyze the joint probability of flood occurrence from multiple sources. As described in the preceding chapter, according to the spatial relationship of the risk assessment area and flood risk source, rainfall is divided into basin rainfall and local rainfall, and the joint probability of flood occurrence from river floods and local inundation was analyzed through the joint probability of the occurrence of basin rainfall and local rainfall.

Two methods are used to define basin rainfall and local rainfall. An intuitive method is to correlate a representative rainfall for each basin and risk assessment. For example, in the study area, for the upper parts of Ushitaki (SB1), Matsuo (SB2), and Makio sub-basins (SB3) and the flood risk assessment area, representative rainfall is given. All of these representative rainfall amounts are calculated through interpolation of rainfall data of rain gauge stations. However, this method has two limitations.

The first problem relates to data collection. The rain gauge stations are not always well distributed in river basins, and the interpolated representative rainfall for each sub-basin and risk assessment area is not always reliable. For instance, for a sub-basin that has no rain gauge stations and few in the surrounding area, the interpolated rainfall will not effectively represent the basin. Therefore, in such extreme situations of only one rain gauge station in the overall basin, this method would obviously fail.

The second problem relates to the difficulty of implementation. Even if the representative rainfall of each sub-basin could be calculated from enough rain gauge stations, the complexity of the joint spatio–temporal correlation of rainfall will make risk analysis difficult to implement. For instance, in our case, we should build at least four-dimensional (4D) joint distribution to express spatial correlation and three-dimensional (3D) joint distribution to express temporal correlation of sub-basin 3, two-dimensional (2D) joint distribution to express temporal correlation of sub-basin 1 and sub-basin 2, and temporal correlation between sub-basins. All of these correlations should be integrated into one large joint distribution, which is difficult to implement.

In such cases, an additional method is adopted. If the study area is not very large, assuming rainfall in the overall study area can be represented by one representative rainfall, the hourly rainfall can be treated as local rainfall, which causes local inundation. The rainfall amount in the duration of concentration time can be treated as basin rainfall, which causes river flooding. In the study area, the flood concentration time of Ushitaki Basin is 2 h, that of Matsuo Basin is 1.6 h, and that of Makio Basin is 2.7 h. It implied that 1h rainfall amount could represent basin rainfall in the risk assessment area; 2 h rainfall could represent basin rainfall in Ushitaki and Matsuo basins, and 3 h rainfall could represent that in Makio Basin. Thus, analysis of joint probability of local rainfall and basin rainfall become analysis of rainfall amounts of 1 h, 2 h, and 3 h rainfall as overall representative rainfall. The joint probability of flood occurrence from multiple sources becomes the joint probability of rainfall amount for different durations.

In this chapter, the copula method is adopted to model the joint probability of basin rainfall and local rainfall.

4.2 Copula method

4.2.1 Brief description of copula

Copulas are functions that join, or couple, multivariate distribution functions to their one-dimensional (1D) marginal distribution functions [1]. Copulas are applied primarily in actuarial and financial fields, particularly for calculating value at risk (VaR) [2]; however, they have also been applied to the hydrological research of Salvadori et al. [3], Zhang et al. [4], and Ghosh [5]. Moreover, basic information on copula theory and practice in hydrology has been reported by hydrologists Salvadori et al [6]. and Genest and Favre in research on the pairwise dependence among the depth, volume, and peak duration of flow or the duration intensity of rainfall [7]. Moreover, the copula method has been used by Serinaldi to address non-Gaussian temporal structures in the development of a multisite daily rainfall generator [8].

In the bivariate case, according to Sklar’s theory [9], the joint cumulative distribution function *H(x,y)* of any pair *(x,y)* of continuous random variables may be written in the form

$$H(x,y) = C(F(x), G(y)) \;\; x, y \in \mathrm{R},$$

where *F(x)* and *G(y)* are continuous marginal distributions, so that *C:*$[0,1]^2 \rightarrow [0,1]$ for all copulas.

Sklar's theory offered an intuitionistic way of constructing a copula, in which joint distribution functions can be expressed in terms of a copula and univariate distribution functions. It also can be inverted to express copulas in terms of a joint distribution function and the inverses of the margins:

$$C(x,y) = H(F^{-1}(x), G^{-1}(y)),$$

Where $F^{-1}(x)$ and $G^{-1}(y)$ are defined as quasi-inverses of *F(x)* and *G(y)*. Thus, given a bivariate distribution function *H* with continuous margins *F(x)* and *G(y)* with a probability integral transform, a copula can be obtained. Then, the obtained copula can be used for a new distribution function:

$$H'(x,y) = C(F'(x), G'(y)).$$

Other methods have also been used for copula construction such as geometric and algebraic methods. Monographs by Joe and Nelsen offer details of these methods [1][10]. A copula offers a method for measuring scale-free dependence and for constructing families of joint distribution. One of the main advantages provided by a copula is that the selection of an appropriate model for the dependence between varieties, represented by the copula, can then proceed independently from the choice of marginal distributions [7].

Table 4 lists some copulas that frequently appear in economic and hydrological studies including three Archimedean copulas such as Gumbel, Frank, and Clayton copulas, and two elliptical copulas such as Normal Copula and t-Copula.

Table 4 Copulas that frequently appear in economic and hydrological studies

Copula	Equation
Gumbel–Hoggard	$C_\theta(u,v) = \exp\{-[(-\ln u)^\theta + (-\ln v)^\theta]^{1/\theta}\}$
Frank	$C_\theta(u,v) = \frac{1}{\theta}\ln[1 + \frac{[\exp(\theta u)-1][\exp(\theta v)-1]}{\exp(\theta)-1}]$

Clayton	$C_\theta(u,v) = [u^{-\theta} + v^{-\theta} - 1]^{-\frac{1}{\theta}}$
Normal Copula	$C(u,v;\theta) = \int_{-\infty}^{\Phi^{-1}(u)} \int_{-\infty}^{\Phi^{-1}(v)} \frac{1}{2\pi(1-\theta^2)^{1/2}} \times \{\frac{-(s^2 - 2\theta st + t^2)}{2(1-\theta^2)}\} dsdt$
t-Copula	$C(u,v;\theta_1,\theta_2) = \int_{-\infty}^{t_{\theta_1}^{-1}(u)} \int_{-\infty}^{t_{\theta_2}^{-1}(v)} \frac{1}{2\pi(1-\theta_2^{\,2})^{1/2}} \times \{1 + \frac{-(s^2 - 2\theta_2 st + t^2)}{\theta_1(1-\theta_2^{\,2})}\}^{-(\theta_1+2)/2} dsdt$

4.2.2 High-dimension copula

Most of copulas adopted in applications are bivariate cases. In actual cases, higher dimension copulas are often required. In our case study, multivariate copulas are required to analyze the joint distribution of flood risk sources.

Sklar's theory can easily extend to multivariate versions. Let H be any dimension of distribution function with margins F_1, F_2, …, F_n. Then, there exists an n-copula C:$[0,1]^n \rightarrow [0,1]$ such that for all x in R^n,

$$H(x_1, x_2, ..., x_n) = C(F_1(x_1), F_2(x_2), ..., F_n(x_n)) \quad x \in \mathrm{R}^n .$$

If F_1, F_2, …, F_n are all continuous, then C is unique; otherwise, C is uniquely determined for Ran$F1$ × Ran$F2$ × … × RanFn. Conversely, if C is an n-copula and F_1, F_2, …, F_n are distribution functions, then the function H is defined as an n-dimensional distribution function with margins $F1$, $F2$, …, Fn.

However, some properties can extend from bivariate copula to multivariate copula. Compared with research on bivariate copulas, those on multivariate copulas are few. Moreover, building a high-dimension copula is not an easy task. Our case study required a high-dimensional copula to analyze the joint behaviors among different duration of rainfalls. The methods of construction of the high-dimension copula are reviewed.

4.2.1.1 Nested Archimedean constructions (NACs)

Archimedean copulas are an important class of copulas with a wide range of applications owing to their ease of construction, large variety of families, and some favorable properties [1]. The definition of an Archimedean copula is given below:

Let φ be a continuous, strictly decreasing function from [0,1] to $[0,\infty)$ such that $\varphi(1) = 0$, and let $\varphi^{[-1]}$ be the pseudo-inverse of φ. That is,

$$\varphi^{[-1]}(t) = \begin{cases} \varphi^{-1} & 0 \le t \le \varphi(0) \\ 0 & \varphi(0) \le t \le \infty \end{cases}.$$

Then, the function

$$C(u,v) = \varphi^{-1}(\varphi(u), \varphi(v))$$

is a copula if φ is convex. φ is the generator of the copula. With different φ, different families of Archimedean copulas are constructed.

By taking advantage of properties of Archimedean copulas, high-dimension copulas can be constructed. Three methods are used to build multivariate Archimedean copulas including the exchangeable multivariate Archimedean copula (EAC), the fully nested Archimedean construction (FNAC), and the partially nested Archimedean construction (PNAC) [11].

The EAC takes the basic form of an Archimedean copula and allows the specification of only one generator, φ, regardless of dimension. Hence, all k-dimensional marginal distributions (k < d) are identical.

$$C(u_1, u_2 ... u_d) = \varphi^{-1}(\varphi(u_1), \varphi(u_2) ... \varphi(u_d))$$

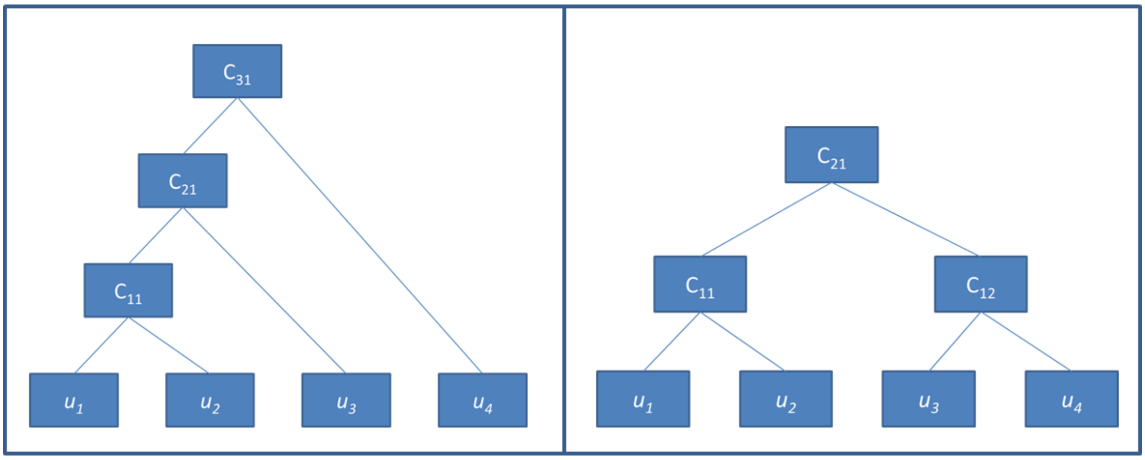

Figure 20 Four-dimensional (4D) fully nested Archimedean construction

The FNAC takes a nesting form to build a multivariate Archimedean copula. The structure of a 4D FNAC is described in the left side of figure 20. As shown in the figure, FNAC simply adds a dimension step by step. Then, the copula formula could be written as

$$C(u_1,u_2,u_3,u_4)=C_{31}(u_4,C_{21}(u_3,C_{11}(u_1,u_2)))$$
$$=\varphi_{31}^{-1}(\varphi_{31}(u_4)+\varphi_{31}(\varphi_{21}^{-1}(\varphi_{21}(u_3)+\varphi_{21}(\varphi_{11}^{-1}(\varphi_{11}(u_1)+\varphi_{11}(u_2))))))\ .$$

The copula for this 4D case requires three bivariate copula, C_{11}, C_{21}, and C_{31}, with corresponding generators of φ_{11}, φ_{21}, and φ_{31}.

The PNAC takes a different nesting form to build a multivariate Archimedean copula. The structure of 4D PNAC is described in the right side of figure 20. As shown in the figure, PNAC is a partially exchangeable structure that can be written as

$$C(u_1,u_2,u_3,u_4)=C_{21}(C_{11}(u_1,u_2),C_{12}(u_3,u_4))$$
$$=\varphi_{21}^{-1}(\varphi_{21}(\varphi_{11}^{-1}(\varphi_{11}(u_1)+\varphi_{11}(u_2)))+\varphi_{21}(\varphi_{12}^{-1}(\varphi_{12}(u_3)+\varphi_{12}(u_4))))\ .$$

The copula for this 4D case requires three bivariate copula, C_{11}, C_{12}, and C_{21}, with corresponding generators of φ_{11}, φ_{12}, and φ_{21}.

More general cases can be constructed by the notation hierarchical Archimedean copula [10-13]. However, some disadvantages limit the application of nested Archimedean copulas. They are less flexible and allow for the free specification of only d – 1 copulas. Moreover, the same Archimedean copula families are required in the nested process; different Archimedean copula families may be used under strict constraints. Further, in order for the resulting d-dimensional distribution to be a proper copula, the degree of dependence, as expressed by the copula parameter, must decrease with the level of nesting.

4.2.1.2 The pair copula construction (PCC)

The pair copula construction (PCC) is a more flexible method for multivariate copula because it adopts a hierarchical idea and takes advantage of density function. The modeling scheme is based on the decomposition of a multivariate density into d(d − 1)/2 bivariate copula densities, of which the first d − 1 are unconditional, and the rest are conditional [14]. The multivariate joint density function can be written as the combination of marginal distribution and conditional distribution:

$$f(x_1,x_2...x_n)=f(x_n)\cdot f(x_{n-1}\,|\,x_n)\cdot f(x_{n-2}\,|\,x_n,x_{n-1})...f(x_1\,|\,x_2,...,x_n)\ .$$

By Sklar’s theorem, which shows

$$F(x_1,x_2...x_d)=\mathrm{C}(F_1(x_1),F_2(x_2)...F_n(x_n))\ ,$$

using the chain rule, we have

$$f(x_1, x_2 \ldots x_n) = c_{1\ldots n}(F_1(x_1), F_2(x_2) \ldots F_n(x_n)) \cdot f_1(x_1) \ldots f_n(x_n),$$

where $c_{1\ldots n}$ denotes the densities of $C_{1\ldots n}$. From these formulas, a general formula that is expressed in each term can be derived:

$$f(x|\mathbf{v}) = c_{xv_j|\mathbf{v}_{-j}}(F(x|\mathbf{v}_{-j}), F(u_j|\mathbf{v}_{-j})) \cdot f(x \mid \mathbf{v}_{-j}),$$

where $\mathbf{v}_{-j}$ denotes the v-vector excluding v_j. Formula therefore can be represented in terms of bivariate copulas. Another crucial question is how to obtain the conditional distribution functions $F(x|\mathbf{v})$. Jeo [10] show that for every *j*,

$$F(x|\mathbf{v}) = \frac{\partial c_{xv_j|\mathbf{v}_{-j}}(F(x|\mathbf{v}_{-j}), F(u_j|\mathbf{v}_{-j}))}{\partial F(u_j|\mathbf{v}_{-j})}.$$

The concept of PCC is highly iterative. To understand it visually, we take 3D joint densities. For example,

$$\begin{aligned} f(x_1, x_2, x_3) &= f(x_1) \cdot f(x_2 \mid x_1) \cdot f(x_3 \mid x_1, x_2) \\ &= f(x_1) \cdot c_{1,2}(F_1(x_1), F_2(x_2)) \cdot f_2(x_2) \cdot f(x_3 \mid x_1, x_2) \\ &= f(x_1) \cdot c_{1,2}(F_1(x_1), F_2(x_2)) \cdot f_2(x_2) \cdot c_{2,3|1}(F(x_2 \mid x_1), F(x_3 \mid x_1)) \cdot c_{1,3}(F_1(x_1), F_3(x_3)) \cdot f_3(x_3) \end{aligned}$$

As is shown above, the 3D joint densities are represented in terms of bivariate copulas $C_{1,2}$, $C_{1,3}$, and $C_{2,3|1}$ with densities $c_{1,2}$ $c_{1,3}$ $c_{2,3|1}$. These so-called pair copulas may be chosen independently of each other. The multivariate copulas can also be expressed as

$$c(x_1, x_2, x_3) = c_{1,2}(F_1(x_1), F_2(x_2)) \cdot c_{1,3}(F_1(x_1), F_3(x_3)) \cdot c_{2,3|1}(F(x_2 \mid x_1), F(x_3 \mid x_1)),$$

where $F(x_2 \mid x_1) = \partial C(x_1, x_2) / \partial x_1$ and $F(x_3 \mid x_1) = \partial C(x_1, x_3) / \partial x_1$.

Since the decomposition is not unique, many different ways can be used for ordering variables. Two main types of PCCs have been proposed in previous research: canonical vines and D-vines [15].

The main concept of canonical vines is that each tree T_j has a unique node connected to n-j edges. Canonical vine trees have a star structure. The multivariate density function of canonical vines can be written in the following form:

$$f(\mathbf{x}) = \prod_{k=1}^{d} f_k(x_k) \times \prod_{i=1}^{d-1} \prod_{j=1}^{d-i} c_{i,i+j|1:(i-1)}(F(x_i \mid x_1 \ldots x_{i-1}), F(x_{i+j} \mid x_1 \ldots x_{i-1}) \mid \theta_{i,i+j|1:(i-1)}),$$

where $\theta_{i,i+j|1:(i-1)}$ is the corresponding parameter of $c_{i,i+j|1:(i-1)}$. Figure 21 shows a canonical vine with four variables.

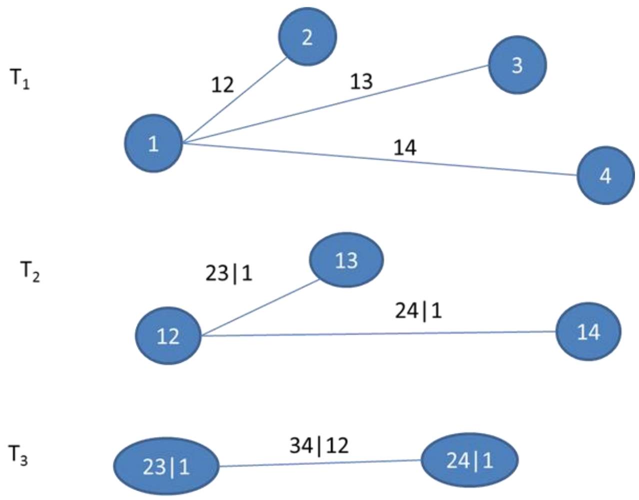

Figure 21 Canonical vine with four variables

The multivariate copula can be expressed as

$$\begin{aligned} c(x_1,x_2,x_3,x_4) = & c_{1,2}(F_1(x_1),F_2(x_2)) \cdot c_{1,3}(F_1(x_1),F_3(x_3)) \cdot c_{1,4}(F_1(x_1),F_4(x_4)) \\ & \cdot c_{2,3|1}(F(x_2 \mid x_1),F(x_3 \mid x_1)) \cdot c_{2,4|1}(F(x_2 \mid x_1),F(x_4 \mid x_1)) \\ & \cdot c_{3,4|12}(F(x_3 \mid x_1,x_2),F(x_4 \mid x_1,x_2)) \end{aligned}$$

In a D-vine, no node in any tree T_j is connected to more than two edges, and the structure is a straight line. The multivariate density function of D-vines can be written in the following form:

$$f(\mathbf{x}) = \prod_{k=1}^{d} f_k(x_k) \times \prod_{i=1}^{d-1} \prod_{j=1}^{d-i} c_{j,i+j|(j+1):(j+i-1)}(F(x_j \mid x_{j+1} \ldots x_{j+i-1}), F(x_{i+j} \mid x_{j+1} \ldots x_{j+i-1}) \mid \theta_{j,i+j|(j+1):(j+i-1)})$$

where $c_{j,i+j|(j+1):(j+i-1)}$ is the corresponding parameter of $\theta_{j,i+j|(j+1):(j+i-1)}$. Figure 22 shows a D-vine with four variables.

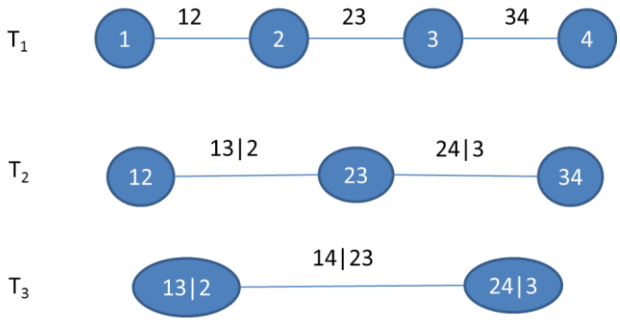

Figure 22 D-vine with four variables

The multivariate copula can be expressed as

$$\begin{aligned} c(x_1,x_2,x_3,x_4) = & c_{1,2}(F_1(x_1),F_2(x_2))\cdot c_{2,3}(F_2(x_2),F_3(x_3))\cdot c_{3,4}(F_3(x_3),F_4(x_4)) \\ & \cdot c_{1,3|2}(F(x_1\mid x_2),F(x_3\mid x_2))\cdot c_{2,4|3}(F(x_2\mid x_3),F(x_4\mid x_3)) \\ & \cdot c_{1,4|23}(F(x_1\mid x_2,x_3),F(x_4\mid x_2,x_3)) \end{aligned}$$

Compared with D-vines, fitting a canonical vine may be advantageous when a particular variable is known to govern interactions in the dataset [16]. In our study, it this method can be used to determine rainfall at the most concerned risk response units, which are the key variables. Thus, the canonical vine pair copula construction is adopted.

4.3 Case study

In this section, the copula method is adopted to model the joint probability of basin rainfall and local rainfall to reveal the joint probability of flood occurrences in the Otsu River Basin from multiple sources, which was introduced in chapter 3. As previously discussed, basin rainfall and local rainfall can be defined by different duration of basin representative rainfall. Therefore, the case of copula analysis based on this definitions of basin rainfall and local rainfall are presented.

4.3.1 Data preprocessing

4.3.1.1 Calculation of representative rainfall for study area

Representative rainfall of the study area can be calculated by using the recorded rainfall data of rain gauge stations in and around the study area. Thiessen polygons and inverse distance interpolation are methods commonly used to calculate basin rainfall. Recently, Kriging interpolation families, which are labeled by considering both location information and observation data, were studied to calculate basin rainfall; however, the precision of these data depend highly on the number of rain gauge stations [17]. In the case study area, the number of rain gauge stations, including those with both long and short records, is only 16. Therefore, the traditional Thiessen polygon method was used to calculate the basin rainfall. The locations of the rainfall stations and the corresponding Thiessen polygon are shown in figure 23.

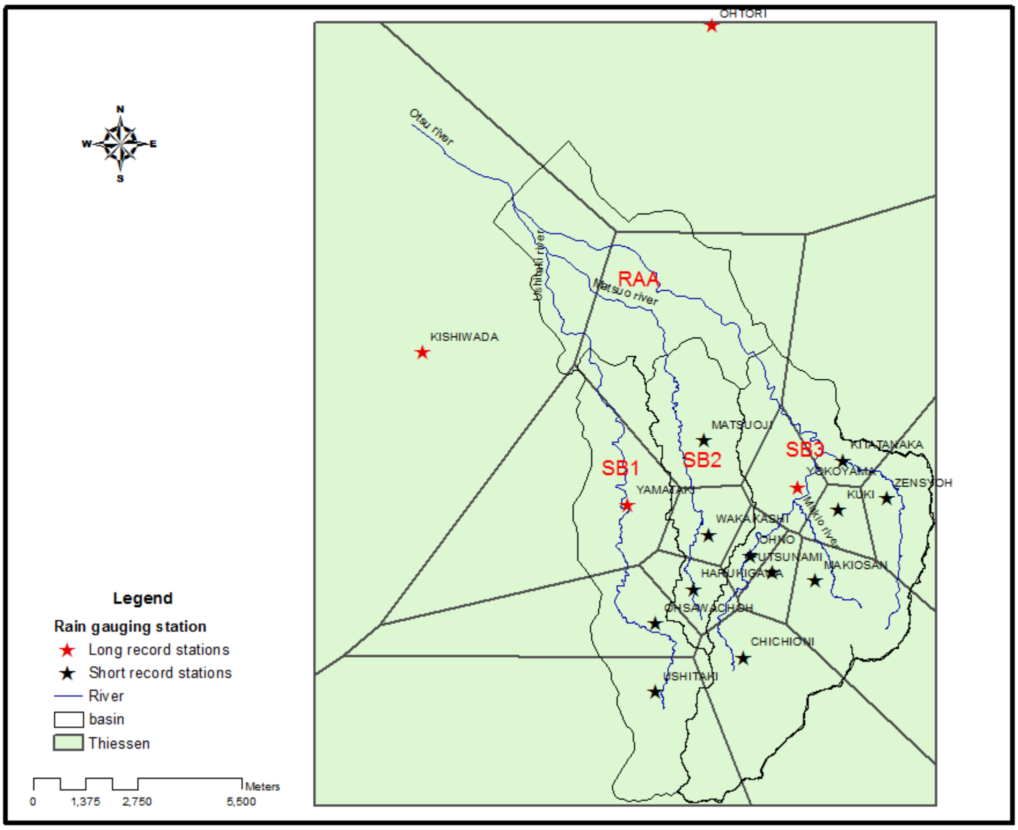

Figure 23 Locations of rainfall stations and corresponding Thiessen polygon

4.3.1.2 Strategy for dealing with rainfall record length

While reviewing the rainfall data of the study area, we determined that only four rain gauge stations (marked by red star in figure 23) have long 58-year records. The other 10 rain gauge stations (marked by black star in figure 23) have short records of only eight years. Obviously, the dependence structure of rainfall cannot be accurately captured simply by the long record data. However, if the short records are used, the long record data have to be cut according to the short records; thus, the rainfall characteristic analysis (i.e. maximum rainfall) will be influenced. Traditional methods may have no resolution for such a problem due to integrated analysis of rainfall characteristic analysis (marginal distribution) and the rainfall spatial dependence structure (joint distribution). However, owing to the advantage provided by the copula such that that the selection of an appropriate model for the dependence between x and y, represented by the copula, can then proceed independently from the choice of the marginal, this problem can be solved through following three steps:

1. Capture rainfall dependence structure through a copula function using all of the rainfall data spread throughout the basin.

2. Analyze rainfall characteristics using the long record data (i.e. maximum rainfall distribution).

3. Study the joint rainfall characteristics based on steps 1 and 2.

4.3.1.3 Definition of rainfall events

In order to investigate the relationship between basin rainfall and local rainfall, the rainfall events should first be defined in which two methods, the interval time method and the mean-time method, can be adopted [18]. In this study, the interval time method was used, and, according to reference [19], 6 h was chose as interval for separating the rainfall time series. That is, a minimum rainfall hiatus of 6 h between non-zero records was selected to define the rainfall events, as shown in figure 24.

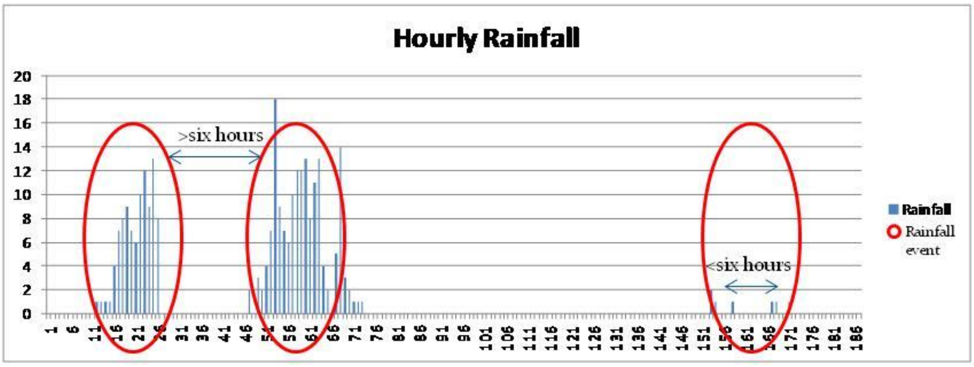

Figure 24 Definition of rainfall events

4.3.1.4 Setting a threshold for convenience in extreme rainfall analysis

Although all rainfall data can be used to evaluate the rainfall dependence structure, flood risk analysis is concerned more with extreme rainfall. In our case, the length of rain gauge records was not very long. For maximum utilization of the rainfall data in extreme rainfall analysis, the concept of peak over threshold (POT) was adopted in which a convenient threshold was set for flood risk analysis, and the numbers of tie values were reduced for copula analysis. We checked the threshold based on the quantitative analysis of rainfall data as well as a review of historical disasters. Mean residual life plotting is a commonly used tool to check the proper threshold [20],which involves plotting the threshold *u* against the 'mean excess' (the mean of the exceedances of *u*, minus *u*), for a range of values of *u*. A mean residual lift plot of a maximum 1 h rainfall is shown in figure 25. From the figure, it appears that a value between 15 mm/h and 20 mm/h can be set as a proper threshold. However, records indicate that the minimum value of rainfall that caused the flood disaster was 17 mm/h, which occurred on May 12, 1999, and caused 50 houses to be inundated. Therefore, 17 mm/h in this area was selected as the threshold for rainfall analysis. Peak rainfall larger than 17 mm/h were treated as dangerous rainfall, and that smaller than 17 mm/h was ignored. The following analysis focuses on dangerous rainfall events that may cause flood disasters.

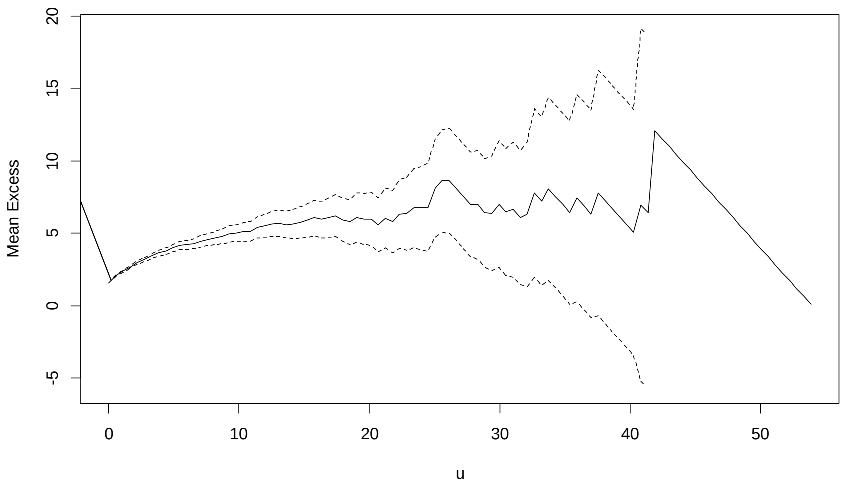

Figure 25 Mean residual life plot for checking rainfall threshold

4.3.2 Rainfall spatial dependence analysis through copula

4.3.2.1 Pair-wise copula construction

A widely used method for estimating the copula parameter is a parametric two-step procedure often referred to as the inference from margins (IFM) method recommended by Joe [10]. This method first requires fitting of marginal distribution and then estimates the parameter of the copula by maxima likelihood using data transferred from marginal distribution. This method usually performs well; however, the estimates of the association parameters derived by the IFM technique clearly depend on the choice of the marginal distributions and thus always run the risk of being unduly affected if the models selected for the margins turn out to be inappropriate [7]. In our research, the copula was used to represent the correlation of *n* hour rainfalls, and different datasets were used to analyze the dependence structure and marginal distribution. Therefore, the IFM method may be not suitable for this study. As the dependence structure captured by a copula has no relationship with the individual behavior of the variables, inference of the copula parameter relies only on the ranks of the observations. Instead of the parametric method, rank-based non-parametric methods such as inversion of Kendall's tau or Spearman's rho and semi-parametric methods such as maximum pseudo-likelihood are available [21]. In this paper, the maximum pseudo-likelihood method was used.

The observed data was first plotted in a 3D space, as shown in figure 26. From this 3D scatter plot, the trend of rainfall data can be primarily understood. Rainfall amounts are clustered at low values, and e scattered at high values. Although these results represent quite normal phenomena in rainfall data, they do not reflect the dependence structure of rainfall.

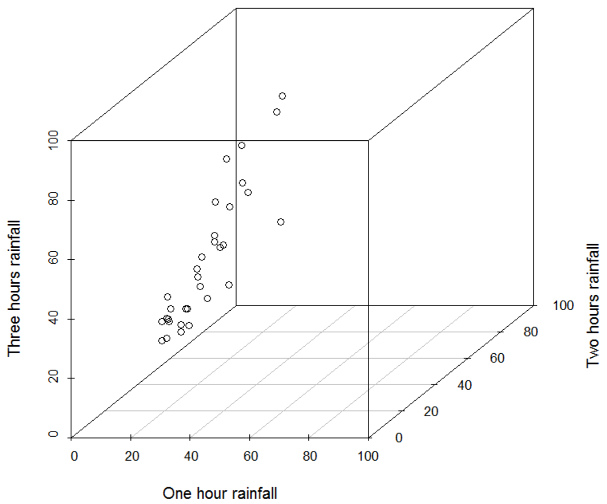

Figure 26 Three-dimensional (3D) plot of observed rainfall data

As previously stated, the rank-based copula is a proper tool for revealing the dependence structure of rainfall data. Therefore, the data was transformed to rank-based pseudo-observations through the following method: Given *n* realizations $x_i = (x_{i1},...x_{id})^T$, $i \in \{1,...n\}$ of a random vector *X*, the pseudo-observations are defined via $u_{ij} = r_{ij}/(n+1)$ for $i \in \{1,...n\}$ and $j \in \{1,...d\}$, where r_{ij} denotes the rank of x_{ij} among all x_{kj}, $k \in \{1,...n\}$.

To visualize the dependence structure clearly, the pseudo-observation data was pair-wise plotted, as shown in figure 27.

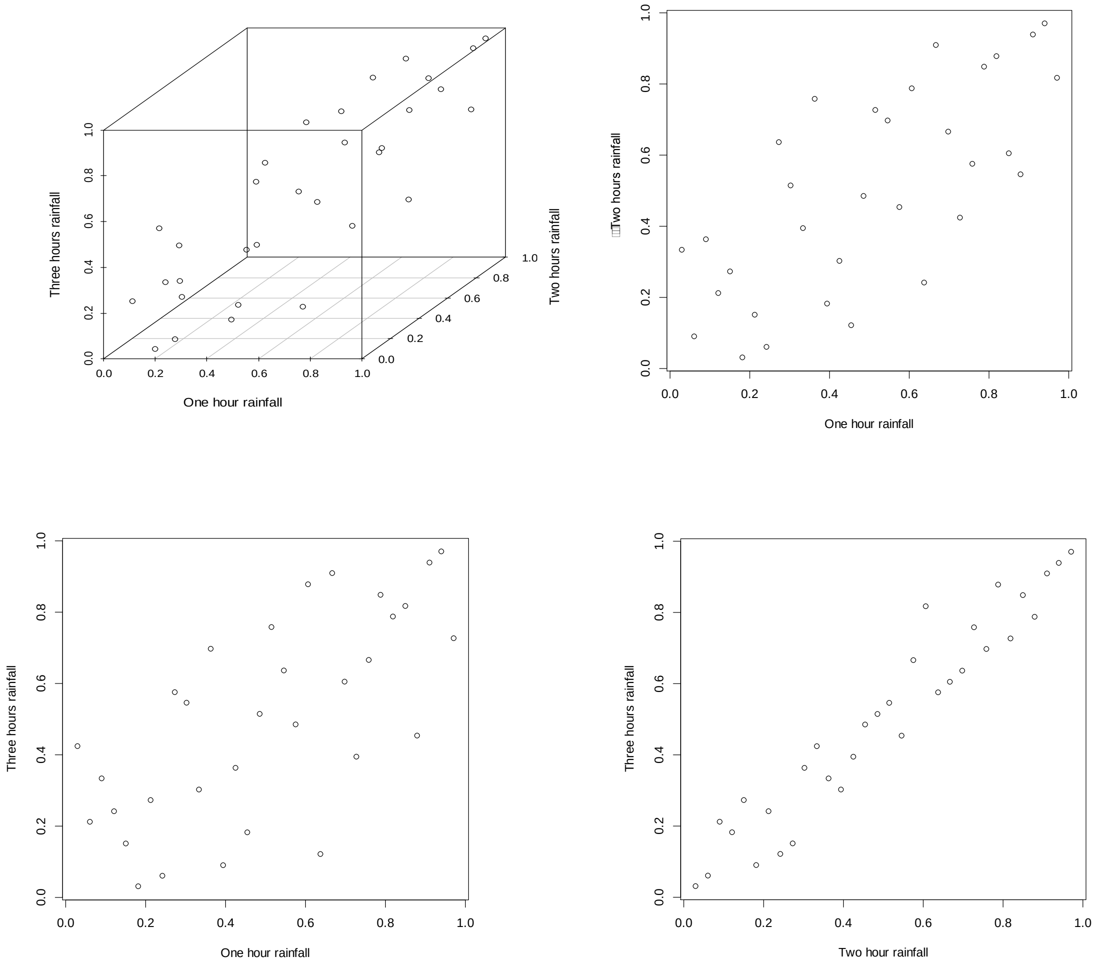

Figure 27 Pseudo-observation data (range in [0,1]) transformed from observed data

To model the multivariate dependence structure among 3 h rainfall events, it is necessary to first evaluate the pair-wise copula. Several types of copulas that frequently appear in the hydrological research were considered, including the normal copula, t copula, Clayton copula, Frank copula, and Gumbel copula.

For the copula selection, the most intuitionistic method is through a graphical diagnostic: either direct comparison of a scatter plot of pair data with artificial datasets generated from copula or comparison of level curves of empirical distribution with level curves of theoretical distribution [7]. Moreover, information criteria such as Akaike information criterion (AIC) and the Bayesian information criterion (BIC) appearing frequent in some research of the application of a copula for quantitative validation of a chosen copula. However, they are not able to provide an understanding of the power of the decision rule employed [22]. Another method for quantitative validation is goodness of fit (GOF). Genest, Remillard, and Beaudoin reviewed GOF tests for copulas concentrating on blanket tests, in which implementation requires neither an arbitrary categorization of the data nor an strategic choice of smoothing parameter, weight function, kernel, or window. Several Cramer-von Mises statistics such as sentinel node (Sn), sentinel node biopsy (SnB), sentinel node concept (SnC), and Das Sentinel-Node-Konzept (SnK) are therefore recommended [23]. In the present study, Sn was selected for GOF, and AIC is also presented as a reference. Table 5 shows the parameters and GOF for each type of copula.

Table 5 Parameters and goodness of fit (GOF) for each type of copula

	1 h rainfall amount versus 2 h rainfall amount			1 h rainfall amount versus 3 h rainfall amount			2 h rainfall amount versus 3 h rainfall amount		
Copula	Parameter	Sn/P-Value	AIC	Parameter	Sn/P-Value	AIC	Parameter	Sn/P-Value	AIC
Gumbel	2.003	0.020/0.785	-22.12	1.913	0.027/0.459	-16.13	5.745	0.023/0.386	-78.24
Frank	5.812	0.026/0.066	-18.52	5.375	0.031/0.436	-18.78	20.474	0.026/0.351	-73.17
Clayton	1.227	0.076/0.017	-11.55	0.994	0.099/0.006	-7.76	5.284	0.075/0.008	-57.51
Normal Copula	0.748	0.022/0.758	-20.63	0.648	0.039/0.115	-15.60	0.964	0.025/0.321	-77.06
t-Copula (4)	0.683	0.309/0.492	-16.81	0.699	0.029/0.303	-13.11	0.960	0.027/0.191	-76.33

Both Sn with p-value and AIC in table 5 indicate that the Gumbel–Hoggard copula is the best fit for the study area. Figure 28 plots empirical copula estimated from the ranked rainfall data (pseudo-observations) and best fitted copula. The GOF test and plotted values indicate that the rainfall spatial dependence structure has been captured. Moreover, the rainfall data used is extreme rainfall selected from rain gauge records; thus, it is reasonable to say that the captured rainfall spatial dependence structure can represent extreme rainfall dependence. This finding is significant for flood risk assessment.

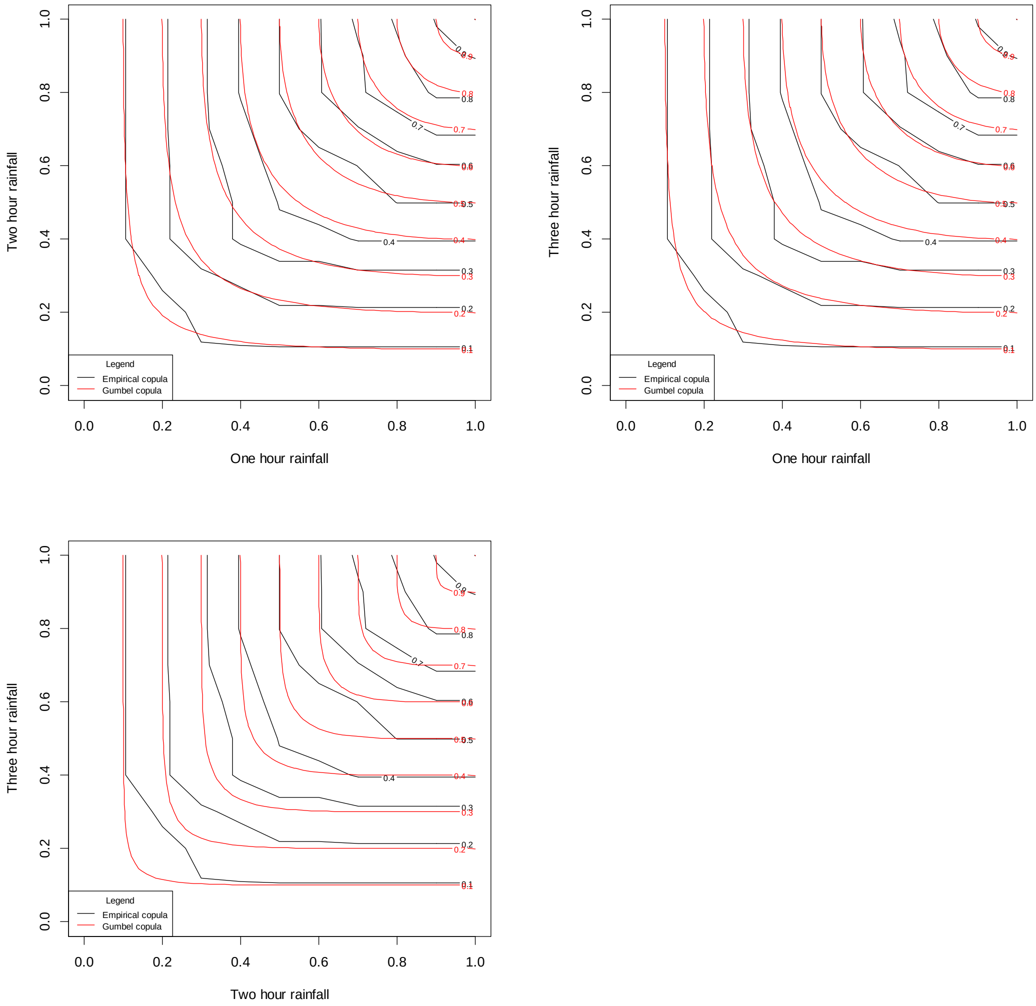

Figure 28 Comparison of empirical copula with best-fitted copula

4.3.2.2 Multivariate copula construction

After selection of pair-wise copulas, the multivariate copula can be constructed. In this study, canonical vine trees were used to construct the multivariate copula. Even if the correlation of 2 h and 3 h rainfall is stronger than the relationship between 1 h and 2 h rainfall or that between 1 h and 3 h rainfall, 1 h rainfall should be chosen as the root node because in flood risk assessment, the relationship between 1 h and 2 h rainfall or that between 1 h and 3 h rainfall is more important than that between 2 h and 3 h rainfall. The canonical vine trees were established following the method introduced in section 4.2.1.2, as shown in figure 29.

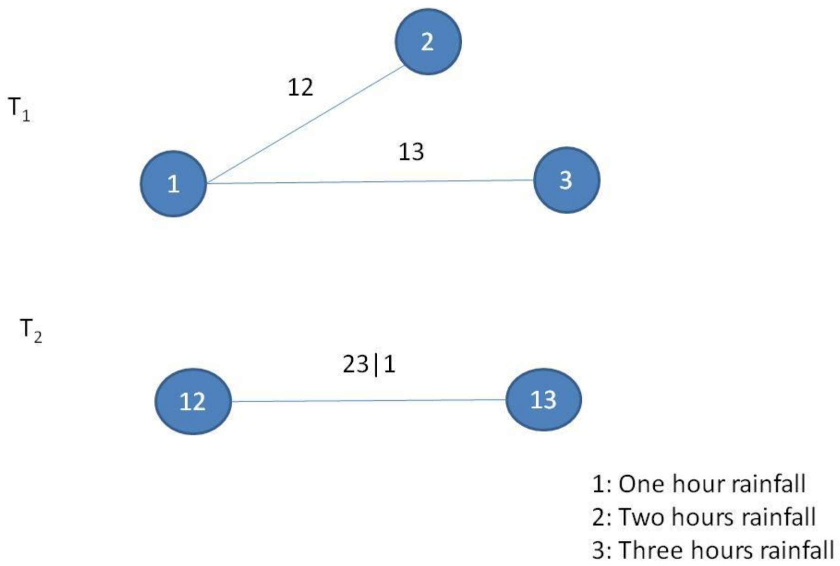

Figure 29 Canonical vine trees of study area

Then, the multivariate copula can be estimated by the pair-wise copula $C_{1,2}$, $C_{1,3}$, $C_{2,3|1}$ with densities $c_{1,2}$ $c_{1,3}$ $c_{2,3|1}$ in the following formula:

$$c(x_1, x_2, x_3) = c_{1,2}(F_1(x_1), F_2(x_2)) \cdot c_{1,3}(F_1(x_1), F_3(x_3)) \cdot c_{2,3|1}(F(x_2 | x_1), F(x_3 | x_1)),$$

where $F(x_2 | x_1) = \partial C(x_1, x_2) / \partial x_1$ and $F(x_3 | x_1) = \partial C(x_1, x_3) / \partial x_1$. It should be noted that here, $C_{2,3|1}$ is not the $C_{2,3}$ presented in section 4.3.2.2; it is a conditional copula. The procedures of integrated estimation of parameters can be found in reference [24]. The parameters $C_{1,2}$, $C_{1,3}$, $C_{2,3|1}$ are 2.003, 1.913, 4.133 respectively.

4.3.3 Application of copula-based dependence structure to rainfall analysis

As shown in $f(x_1, x_2 ... x_n) = c_{1...n}(F_1(x_1), F_2(x_2) ... F_n(x_n)) \cdot f_1(x_1) ... f_n(x_n)$, once the copula-based dependence structure is determined, it is easy to construct multivariate distribution from marginal distributions. In this section, the estimated copula-based dependence structure is applied to extreme rainfall analysis, which is used in flood risk assessment. The purpose of rainfall modeling can be classified into three main areas: (1) stochastic models of rainfall related to global climate change, (2) stochastic rainfall models describing the generation of the sequence of dry and wet spells, and (3) models of frequency analysis of rainfall [25]. Extreme rainfall analysis presented in this section falls in the third category. The purpose of this section is to study the joint behavior of extreme rainfall and randomly generate correlated extreme rainfall for flood risk analysis. We followed three steps to realize the purpose:

1. Fit marginal extreme value distribution for each rainfall duration independently. Pair-wise values are not necessary because the dependence structure has been previously captured.

2. Randomly generate the correlation value from the copula model.

3. Transform the correlated extreme rainfall values from the copula model and marginal distribution.

4.3.3.1 Analysis of marginal distribution

Many previous studies on fitting extreme rainfall distribution have been conducted, and several types of distribution have been found to fit rainfall data well. However, no distribution is universally fitted to all rainfall data owing to the varied natures of rainfall, purpose of study, and location. For example, although De Michele and Salvadori reported that generalized Pareto (GP) distribution is the best fitted [26] this distribution was reported by Kao and Govindaraju to be the weakest distribution [27]. Therefore, a set of distributions including GP, exponential distribution (EXP), gamma distribution (GM), and Weibull distribution were selected as candidates and were tested by GOF.

Table 6 Parameters and goodness of fit (GOF) for marginal extreme distribution

	1 h rainfall		2 h rainfall		3 h rainfall	
Distribution	Parameters	K-S test	Parameters	K-S test	Parameters	K-S test
Generalized Pareto distribution	$k = 0.12$ $\sigma = 5.23$ $\mu = 17.41$	0.074	$k = -0.1024$ $\sigma = 13.38$ $\mu = 20.74$	0.119	$k = -0.235$ $\sigma = 21.38$ $\mu = 21.48$	0.069
Exponential distribution	$\lambda=0.043$	0.518	$\lambda = 0.031$	0.428	$\lambda = 0.026$	0.383
Gamma distribution	$\alpha = 12.59$ $\beta = 1.85$	0.167	$\alpha = 8.46$ $\beta = 3.89$	0.105	$\alpha = 7.13$ $\beta = 5.44$	0.061
Weibull distribution	$\alpha = 4.97$ $\beta = 24.98$	0.171	$\alpha = 3.9834$ $\beta = 35.522$	0.134	$\alpha = 3.53$ $\beta = 42.11$	0.095

From the Kolmogorov–Smirnov test in table 6, it is obvious that GP distribution is best for describing 1 h rainfall and that GM is the best distribution for 2 h and 3 h rainfall. A histogram with the best fit probability density function is plotted in figures 30, 31, and 32. It is interesting to note that the distribution differs for maximum 1 h, 2 h, and 3 h rainfall amounts.

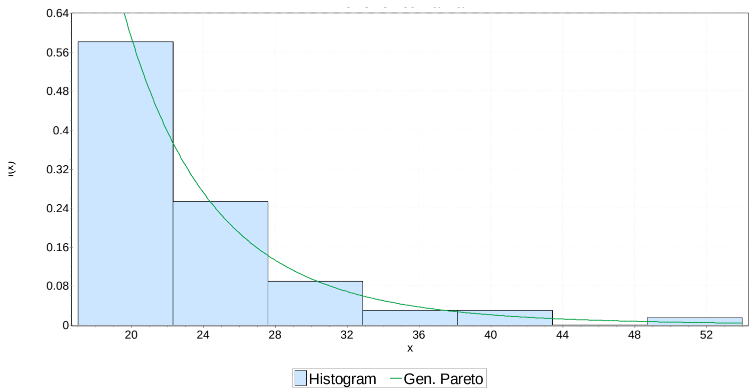

Figure 30 Probability density function (PDF) of 1 h rainfall

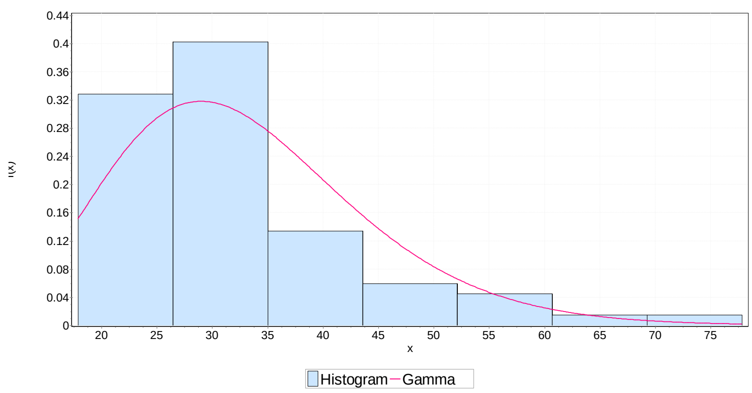

Figure 31 Probability density function (PDF) of 2 h rainfall

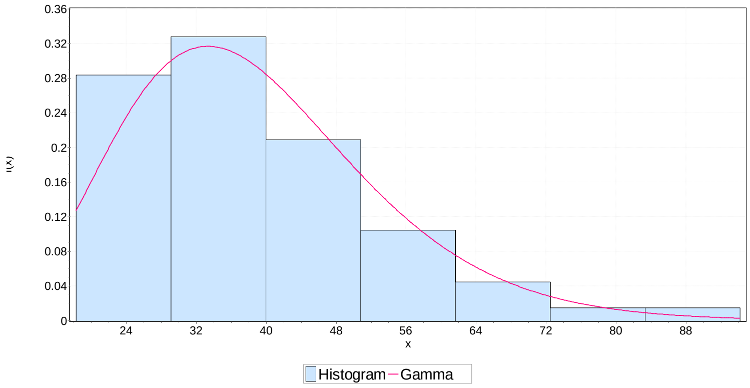

Figure 32 Probability density function (PDF) of 3 h rainfall

4.3.3.2 Correlated rainfall generation

Based on the copula model and marginal distributions, the joint distribution of 1 h, 2 h, and 3 h rainfall could be obtained. Because they are the main causes of flood disasters, they should be treated preferentially. Then, the correlated maximum 1 h, 2 h, and 3 h rainfall could be simulated. Figure 33 shows 1000 randomly generated rainfall from the copula model and marginal distributions. Compared with observed rainfall data, the correlation of different durations of rainfall events were captured; thus, simulated rainfall can be used in this study area.

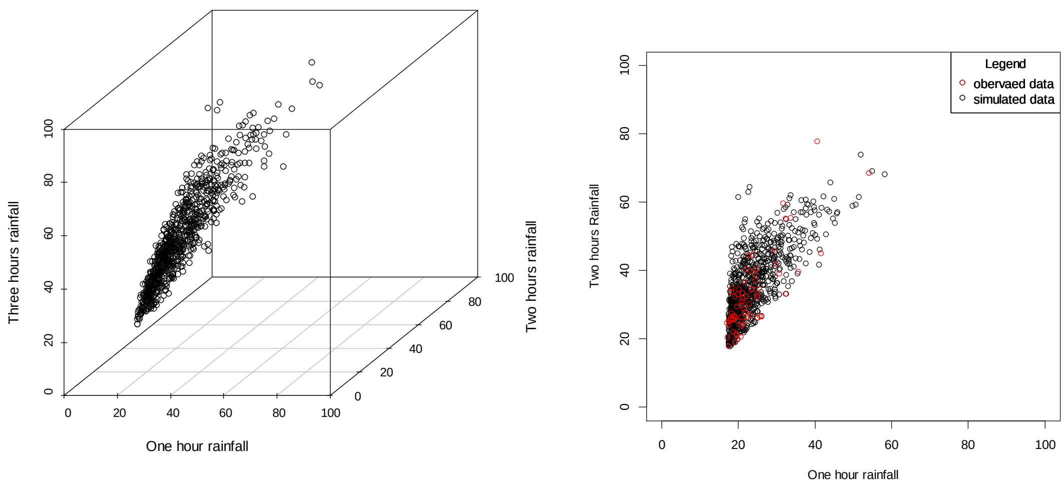

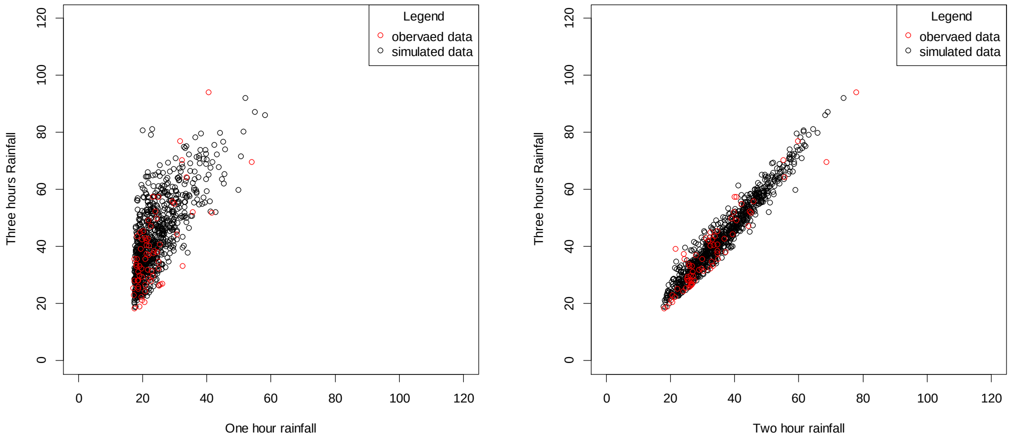

Figure 33 1000 randomly generated rainfall from the copula model and marginal distributions. Upper left: three-dimensional (3D) plot of random value; upper right: comparison of simulated value with observed value for 1 h and 2 h rainfall events; bottom left: comparison of simulated value with observed value for 1 h and 3 h rainfall events; bottom right: comparison of simulated value with observed value for 2 h and 3 h rainfall events

4.3.4 Rainfall event simulation

In the previous sections, rainfall events of significant durations were analyzed including maximum 1 h, 2 h, and 3 h events. To complete the rainfall event simulation, two remaining problems must be addressed. The first is determination of the position of the rainfall peak, and the second is determination of other parts of rainfall in addition to significant rainfall.

In fact, these two problems can be summarized as a rainfall pattern problems, which have been discussed in previous research. In the 1940s, scholars studied rainfall data in the Ukraine and proposed seven rainfall patterns. They found that uniform rainfall patterns were quite few [28]. After that, Yen and Chow proposed a non-uniform rainfall pattern that considered the position of maximum rainfall [29]. Keifer and Chu proposed a Chicago rainfall pattern directly related to a rainfall intensity formula [30]. Pilgrim and Cordery also proposed a method for determining rainfall pattern that adopted the average percentile of all recorded rainfall in each time interval [31]. Several agencies also proposed method for entire countries, such as that proposed by the U.S. Soil Conservation Service [32]. In Japan, two main methods are adopted. The first directly uses an actual rainfall pattern typically chosen from rainfall datasets of flood disasters. All of the rainfall designs are based on this typical rainfall pattern. The second assumes a rainfall pattern (center-peak, left-peak, or right-peak) and uses a rainfall intensity curve to determine the hourly rainfall intensity.

In fact, rainfall has strong regional characteristics, and rainfall designs have to consider the actual conditions. Similar to that reported by Pilgrim and Cordery, we determined the position of rainfall peak and other rainfall factors by statistical analysis of recorded rainfall events in this area. A histogram was constructed based on the recorded rainfall events (Fig. 34). It was determined that most of rainfall peak occurred at the center position, and the distribution of the rainfall peak was similar to normal distribution. Then, in the rainfall simulation, for the determination of position of rainfall peak, we have two options of using the average value such as that reported by Pilgrim and Cordery or fitting the distribution of rainfall peak and simulating the value from the distribution.

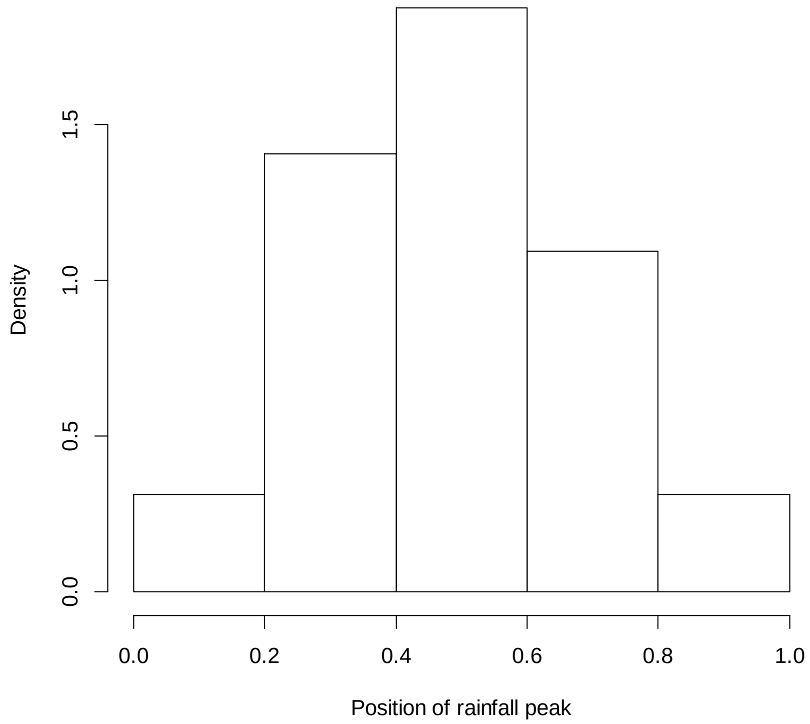

Figure 34 Density histogram of rainfall peak. The length of the rainfall record is treated as 1, and the value of the horizontal axis is the position of rainfall peak in the length of the rainfall record

The ratios between peak rainfall and other parts of rainfall can be calculated from recorded rainfall events. These ratios can were used complete the rainfall events in our research. For example, when designing a 6 h rainfall event, the position of rainfall peak was set at the third hour; the second hour rainfall and the fourth hour rainfall were determined by the copula model. This 3 h rainfall is the core of rainfall that may be the main cause of flood disasters. The first, fifth, and sixth hour rainfalls were determined by the ratios between peak rainfall and these events.

Therefore, to summarize the above discussion, the following procedure for rainfall event generation is proposed:

1. Simulate significant rainfall from a copula-based joint distribution model.

2. Simulate a rain peak position by statistical study of rainfall records and plot the simulated significant rainfall at this position.

3. Complete the other parts of rainfall by the ratios between peak rainfall and these other parts.

This is procedure it create a complete rainfall event is not the only option. For example, in the second step, one can determine the position of rainfall as center-peak, left-peak, or right-peak. Further, in the third step, one can use other methods to determine the other parts of rainfall. In addition, a typical rainfall pattern can be used to complete the rainfall event, except for significant rainfall parts.

To show the rainfall event generation, five cases of rainfall events according to a once in 20 years return period were generated. Table 7 shows the joint probability and marginal probability of 1 h, 2 h, and 3 h rainfalls. From this table, it is clear that joint probability was the same and marginal probability and rainfall value both differed significantly.

Table 7 Simulated cases according to the once in 20 years return period

Case Number	Joint probability	Probability of 1 h rainfall	Probability of 2 h rainfall	Probability of 3 h rainfall
1	0.950	0.961	0.968	0.969
2	0.950	0.970	0.960	0.961
3	0.950	0.954	0.981	0.982
4	0.950	0.953	0.982	0.983
5	0.950	0.979	0.954	0.955

From table 7, the significant rainfall can be calculated and combined with the procedure discussed above to generate a rainfall event. Figure 35 shows rainfall events generated from the above significant rainfall. The horizontal direction shows different rainfall value of different rainfall cases, and the vertical direction shows the variation in rainfall pattern due to changes in the position of peak rainfall. In fact, in the vertical direction, the position of other 2 h rainfall can change within 3 h significant rainfall durations, creating six cases. In the figure, the occurrence of significant rainfall is assumed at the center part of the rainfall event. Without this assumption, many more cases can be expected. However, for flood risk assessment, as is emphasized in this thesis, significant rainfall duration is the first concern. Rainfall events here consider only the variation in the position of rainfall with significant duration.

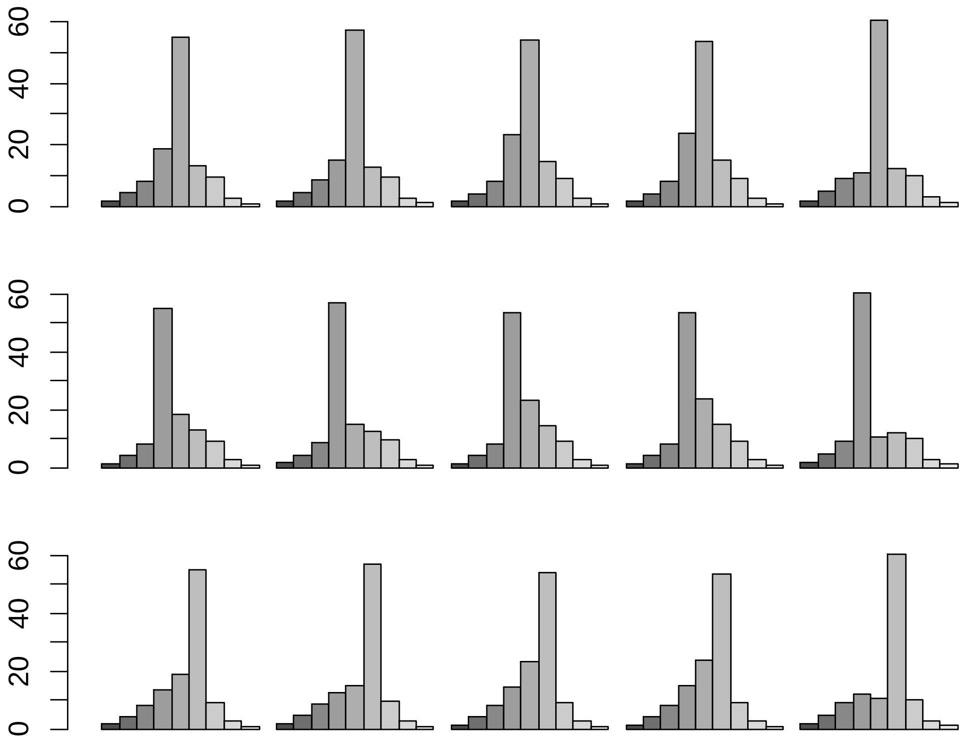

Figure 35 Rainfall events according to the once in 20 years return period. The horizontal direction shows different rainfall values of different rainfall cases; the vertical direction shows the variation in rainfall pattern due to changes in the position of peak rainfall

4.4 Discussion

In this chapter, the definition of basin rainfall and local rainfall from the perspective of overall basin representative rainfall was first proposed, and a copula-based methodology was presented to analyze rainfall dependence and generate correlated rainfall data for flood risk assessment. The case study in the Otsu River Basin, Osaka prefecture, Japan, demonstrates the feasibility of this methodology. Other factors worth discussion are summarized in the following points:

1. Because direct definition of basin rainfall and local rainfall will increase the complexity of rainfall correlation analysis, the concept of representative rainfall for the entire basin was adopted. Spatial correlation of rainfall in the sub-basin was therefore transformed to temporal correlation of representative rainfall in the entire basin. This compromise method is subject to the complexities of considering spatial and temporal correlation together.

2. The copula method is an effective for build joint probability distribution and offers a way for free-scale measuring of dependence and for constructing families of joint distribution. One of the main advantages provided by the copula is that the process of the dependence between varieties and the choice of the marginal distributions can be done independently. For rainfall analysis, this method enabled us to capture the dependence structure and to analyze rainfall distribution by different datasets. It is quite suitable for basin rainfall analysis because in a basin, the length of the rain gauge record can differ significantly, as shown in our case study.

3. Concentration time is used in this paper to indicate statistical units of rainfall duration because the concentration time of flooding can be thought as the duration contributing to flood peak volume. The rainfall within the concentration time of flooding is defined as significant rainfall. Analysis of significant rainfall is proper for flood risk analysis concerned with flood peak. Various correlated rainfall events were generated with the method proposed in this paper, which offers rainfall information for flood simulation under an assumption of rainfall types.

4. This study has clearly shown that even though joint probability was the same, marginal probability can differ significantly. Therefore, it is necessary to consider joint probability rather than only a single marginal distribution. Joint probability offers more cases of rainfall events, which is quite important for flood risk assessment. The traditional method of rainfall design is essentially only one case of this method.

References

[1] Nelsen R. 2006. An Introduction to Copulas, Second edition, Springer, New York.

[2] Bouyé E, Durrleman V, Nikeghbali A, Riboulet G, Roncalli T. 2000. Copulas for finance—a reading guide and some applications. Available at SSRN 1032533.

[3] Salvadori G, Michele De C. 2004 Frequency Analysis Via Copulas: Theoretical Aspects and Applications to Hydrological Events. Water Resour Res. 40, W12511.

[4] Zhang L, Singh V P. 2006. Bivariate flood frequency analysis using the copula method. Journal of Hydrologic Engineering, 11(2):150-164.

[5] Ghosh S. 2010 Modeling Bivariate Rainfall Distribution and Generating Bivariate Correlated Rainfall Data in Neighbouring Meteorological Subdivisions Using Copula. Hydrol Process. 24: 3558-3567.

[6] Salvadori G, De Michele C, Kottegoda N T, Rosso R. 2007. Extremes in nature: an approach using copulas (Vol. 56). Springer.

[7] Genest C, Favre A C. 2007. Everything You Always Wanted to Know about Copula Modeling but Were Afraid to Ask. J Hydrol Eng. 12 (4): 347-366.

[8] Serinaldi F. 2009. A multisite daily rainfall generator driven by bivariate copula-based mixed distributions. Journal of Geophysical Research: Atmospheres (1984–2012), 114(D10).

[9] Sklar A. 1959. Fonctions de repartition an dimensions etleursmarges. Publ Inst Statist Univ Paris 8:229-231.

[10] Joe H. 1997. Multivariate Models and Dependence Concepts. Chapman &Hall, London.

[11] Aas K, Berg D. 2009. Models for construction of multivariate dependence—a comparison study . The European Journal of Finance, 15(7-8): 639-659.

[12] Whelan N. 2004. Sampling from Archimedean copulas . Quantitative finance, 4(3): 339-352.

[13] Savu C, Trede M. 2010. Hierarchies of Archimedean copulas . Quantitative Finance, 10(3): 295-304.

[14] Czado C. 2010. Pair-copula constructions of multivariate copulas /Copula theory and its applications. Springer Berlin Heidelberg: 93-109.

[15] Kurowicka D, Cooke R M. 2007. Sampling algorithms for generating joint uniform distributions using the vine–copula method . Computational Statistics & Data Analysis, 51(6): 2889-2906.

[16] Aas K, Czado C, Frigessi A, et al. 2009. Pair-copula constructions of multiple dependence . Insurance: Mathematics and Economics, 44(2): 182-198.

[17] Hughes J P, Lettenmaier D P. 1981. Data requirements for Kriging: Estimation and network design . Water Resources Research, 17(6): 1641-1650.

[18] Dairaku K, Emori S, Oki T. 2004. Rainfall amount, intensity, duration, and frequency relationships in the Mae Chaem watershed in Southeast Asia . Journal of Hydrometeorology, 5(3): 458-470.

[19] Huff F A. 1967. Time distribution of rainfall in heavy storms . Water Resources Research, 3(4): 1007-1019.

[20] Coles S, Pericchi L R, Sisson S. 2003. A fully probabilistic approach to extreme rainfall modeling . Journal of Hydrology, 273(1): 35-50.

[21] Choroś B, Ibragimov R, Permiakova E. 2010. Copula estimation /Copula theory and its applications. Springer Berlin Heidelberg: 77-91.

[22] Berg D, Bakken H. 2006. Copula goodness-of-fit tests: A comparative study. Preprint. Norwegian Computing Centre. http://www. danielberg. no/publications/CopulaGOF. pdf, 4.

[23] Genest C, Rémillard B, Beaudoin D. 2009. Goodness-of-fit tests for copulas: A review and a power study . Insurance: Mathematics and Economics, 44(2): 199-213.

[24] Brechmann E C, Schepsmeier U. 2013. Modeling dependence with C- and D-vine copulas: The R-package CD Vine . Journal of Statistical Software, 52(3): 1-27.

[25] Dan'azumi S, Supiah S, Rahman A A. 2010. Probability distribution of rainfall depth at hourly time-scale. Proceedings of International Conference on Environmental Science and Engineering, Singapore, August 26–28, 2010. World Academy of Science Engineering and Technology.

[26] De Michele C, Salvadori G. 2003. A Generalized Pareto intensity–duration model of storm rainfall exploiting 2-Copulas . Journal of Geophysical Research: Atmospheres (1984–2012), 108 (D2).

[27] Kao S C, Govindaraju R S. 2007. A bivariate frequency analysis of extreme rainfall with implications for design . Journal of Geophysical Research: Atmospheres (1984–2012), 112(D13).

[28] Guoping C, Jin S, Rongsheng F. 1998. Research on Rainfall Pattern of Urban Design Storm, Advances in Water Science, Vol. 9, No. 1, Mar.

[29] Yen B C and Ven T C. 1980. Design Hyetographs for Small Drainage Structures, Journal of the Hydraulics Division, ASCE, Vol. 106, No. HY6.

[30] Keifer, C J, Henry H C. 1957. Synthetic Storm Pattern for Drainage Design, Journal of the Hydraulics Division, ASCE, Vol. 83, No. HY4.

[31] Pilgrim D H, Cordery I. 1975. Rainfall temporal patterns for design floods. Proceedings of American Society of Civil Engineers, Journal of the Hydraulics Division, Vol.100, 81-95.

[32] Kibler D F. 1982. Urban Storm Water Hydrology. American Geophysical Union, Water Resources, Monograph 7, 48–60.

Chapter 5 Development of an integrated rainfall–runoff–inundation model for spatial flood risk assessment

5.1 Introduction

In past research, inundation models have been used for simulating flood events and for calculating flood risk. These models take the output of other runoff models as input and are able to simulate inundation scenarios under various situations in an area. However, such models treat upstream and downstream or city and region areas independently and fail to consider the upstream–downstream and city–region relationships, which are important in flood risk assessment. For the upstream–downstream relationship, it is obvious that flood risk downstream is influenced by upstream flooding. For the city–region relationship, the main concern is that flood risk in a city may originate from multiple sources in the region such as rivers and mountains, as was explained in chapter 1.

Studies of integrated rainfall–runoff–inundation models are not as plentiful as those of separate models. Sayama developed a rainfall–runoff–inundation model based on 2D diffusion wave equations and created rainfall–runoff–inundation analysis of the 2010 Pakistan flood in the Kabul River Basin [1]. Kobayashi developed a distributed rainfall–runoff–inundation (DRR/FI) simulation model based on a 1D dynamic wave equation for river routing and a 2D shallow water equation for surface flow simulation [2]. Both of these models were based on raster data and used the same resolution for runoff and inundation.

There are two shortcomings with this type of model. The first is that the raster model uses regular mesh sizes, which makes it difficult to describe land surface features, particularly in urban areas. The second is that using the same resolution for runoff and inundation for flood risk assessment in a large area can lead to the consequence that either the resolution is too low or the calculation is too slow. Therefore, to overcome these shortcomings, this research used irregular vector mesh sizes, and runoff and inundation were separately considered for building an integrated rainfall–runoff–inundation model. However, for the flood risk assessment in city areas, although river basins should be considered, more attention should be paid to the inundation of the city area. Thus, in our model, hydrological analysis was adopted in the river basin to simplify the process of runoff, which made calculation reasonable and faster. Then we simulated high resolution in the city area with no concern on the time-consuming runoff part. The GIS helped to build this model, which included mesh generation, data preprocessing, and result visualization.

In this chapter, a GIS-based visualized, simplified rainfall–runoff–inundation model for flood risk assessment is developed. The hydrological analysis and spatial analysis of GIS provided a basic database, and kinematic wave equations and simplified shallow water equations constituted the calculation framework. The runoff area was divided by hydrological analysis, and the kinematic wave equation was adopted according to sub-basins. The inundation area was simulated by a 2D model based on simplified shallow water equations. The integration of runoff and inundation was controlled by joining the runoff mesh and the inundation mesh, and time steps were coordinated by interpolation.

5.2 Mathematical equations

In flood risk assessment areas, water may come from multiple sources such as rainfall, rivers, drainage, and nearby mountains. All of these factors can be integrated into an overall model, and taking rainfall as input, runoff and inundation are calculated at the same time. To simplify the calculation, kinematic wave equations were adopted to model the rainfall runoff process, and simplified shallow water equations were adopted to model inundation.

5.2.1 Runoff model

The runoff model in our simulation is based on a kinematic wave model. Assuming that the bed slope and friction slope terms of the Saint Venant equation are dominant, the following 1D governing equations are applied for the slope area [3]:

$$\frac{\partial h}{\partial t}+\frac{\partial q}{\partial x}=r_{\mathrm{e}} \tag{1}$$

and

$$q=\sqrt{\sin\theta_s}\,/\,N*h^m, \tag{2}$$

where t is the time independent variable, x is the longitudinal direction, h is the water depth, q is the water discharge per unit width in the slope area, r_e is the effective rainfall, θ_s is the angle of slope, and N is the equivalent roughness; *m* is defined as m = 5/3.

For the river flow, the following equations were applied:

$$\frac{\partial h}{\partial t}+\frac{\partial q_*}{\partial x}=\frac{q_s}{B} \tag{3}$$

and

$$q_s=\sqrt{\sin\theta_1}/n*h^m, \tag{4}$$

where q_* is the water discharge per unit width in a river, q_s is the lateral inflow discharge per unit width from the slope, B is the river width, θ_1 is the angle of the river bed, and n is the Manning roughness coefficient; *m* is defined as m = 5/3. The equations were easily discretized by using the control volume method.

Infiltration was calculated from an empirical formula based on Horton's equation [4], in which infiltration starts at a constant rate, f_0, and decreases exponentially with time t. After some time when the soil saturation level reaches a certain value, the rate of infiltration will level off to the rate f_c:

$$f_t=f_c+(f_0-f_c)\mathrm{e}^{-\mathrm{kt}}, \tag{5}$$

where f_t is the infiltration rate at time t; f_0 is the initial infiltration rate or maximum infiltration rate; f_c is the constant or equilibrium infiltration rate after the soil has been saturated, or the minimum infiltration rate; and k is the decay constant specific to the soil.

5.2.2 Inundation model

The inundation flow model is more complex than the runoff model because it should consider a 2D model to represent flow on flat ground. The most commonly used governing equations are those for shallow water. The governing equations for 2D unsteady flow are

the continuity equation

$$\frac{\partial h}{\partial t}+\frac{\partial M}{\partial x}+\frac{\partial N}{\partial y}=\mathrm{q}, \tag{6}$$

and the momentum equations

$$\frac{\partial M}{\partial t}+\frac{\partial (uM)}{\partial x}+\frac{\partial (uM)}{\partial y}+gh\frac{\partial H}{\partial x}+\frac{gn^2u\sqrt{u^2+v^2}}{h^{\frac{1}{3}}}=0 \tag{7}$$

and

$$\frac{\partial N}{\partial t}+\frac{\partial (uN)}{\partial x}+\frac{\partial (uN)}{\partial y}+gh\frac{\partial H}{\partial y}+\frac{gn^2 v\sqrt{u^2+v^2}}{h^{\frac{1}{3}}}=0 \quad , \tag{8}$$

where h is the water depth; H is the water level; q is a source term representing rainfall in this model; M and N are the discharges per unit width in the x and y directions, respectively; u and v are the components of the flow velocity in the x and y directions, respectively; n is the coefficient of roughness; and g is acceleration due to gravity.

It is not necessary, however, to solve the full equation for inundation. Here, we adopt a simplified strategy developed by the China Institute of Water Resources and Hydropower Research whereby the flux is calculated by various simplified equations according to the type of passage. The three main passage types considered include river passage, defined as that between river meshes; land passage, that between land meshes; and special passage, that between land meshes and river meshes. In addition, water obstructions such as railways and dykes can be treated as special passages.

For river passages, the acceleration, gravity, and resistance terms in the momentum equation are reserved:

$$\frac{\partial M}{\partial t}+gh\frac{\partial H}{\partial x}+\frac{gn^2 u\sqrt{u^2+v^2}}{h^{\frac{1}{3}}}=0 \tag{9}$$

and

$$\frac{\partial N}{\partial t}+gh\frac{\partial H}{\partial y}+\frac{gn^2 v\sqrt{u^2+v^2}}{h^{\frac{1}{3}}}=0 \cdot \tag{10}$$

A discrete equation is achieved by using the control volume method:

$$Q^{t+\Delta t}=Q^t-gh\frac{|H_1{}^t-H_2{}^t|}{L}\Delta t-gn^2\frac{|Q^t|Q^t}{h^{7/3}}\Delta t \cdot \tag{11}$$

For river passages, the gravity and resistance terms in the momentum equation are reserved:

$$gh\frac{\partial H}{\partial x}+\frac{gn^2 u\sqrt{u^2+v^2}}{h^{\frac{1}{3}}}=0 \tag{12}$$

and

$$gh\frac{\partial H}{\partial y}+\frac{gn^2 v\sqrt{u^2+v^2}}{h^{\frac{1}{3}}}=0 \cdot \tag{13}$$

A discrete equation is achieved by using control volume method:

$$Q^{t+\Delta t}=\frac{1}{n}h^{5/3}\left(\frac{|H_1{}^t-H_2{}^t|}{L}\right)^{1/2} . \tag{14}$$

Owing to complex ground conditions, some surface features are defined as water hindrances. To calculate flow from such ground surfaces, the following weir flow equation is used:

$$Q_j = m\sigma_s \sqrt{2g} h_j^{3/2} , \qquad (15)$$

where Q_j is the discharge per unit width, m is the discharge coefficient, σ_s is the submergence coefficient, and h_j is water depth at the weir crest.

Urban drainage can be simulated by 1D unsteady flow if detailed drainage information is available:

$$\frac{\partial Q}{\partial t} + \frac{\partial}{\partial l}\left(\frac{Q^2}{A}\right) + gA\frac{\partial H}{\partial l} = -gAS_f , \qquad (16)$$

where Q is discharge, A is area of the water section; and S_f is friction slope.

In some areas, however, detailed drainage information was not available. In such cases, a simple average formula can be used to identify drainage for each mesh:

$$d_i = \frac{D_o}{A_o} * A_i , \qquad (17)$$

where d_i is the drainage capacity of mesh *i*, D_o is the drainage capacity of the overall area obtained by survey of pump stations, and A_o and A_i are overall drainage area and mesh area, respectively. Details for the inundation model have been reported by Cheng, Li, and Tan [9][10][11].

5.2.4 Scheme of model

In the model, the study area was separated into inundation and runoff areas. To simplify the calculation, the runoff area was divided into sub-basins according to DEM and river sections by hydrological analysis that implied no water exchange on the edges of the sub-basin. Then, for each sub-basin, the runoff was calculated.

In the inundation area, the study area was divided into irregular meshes according to rivers, streets, roads, railways, and slopes. To ensure that the irregular meshes effectively represented the surface feature of the inundation area, they were made manually. The river meshes should follow actual river shapes and directions, and the information of dykes can expressed at the edges of the river meshes. The drainage and pump stations can also be considered because meshes with drainages will drain away water to rivers through pump stations.

The junction of the runoff and inundation areas follows the nature direction, and the outlet of the runoff was treated as an inlet of inundation. It is not necessary to keep the same time step in the calculation because the runoff model is more stable than the inundation model. If a large time step for the runoff model is used, the two parts can be coordinated by interpolation. Figure 36 shows a scheme map of this model.

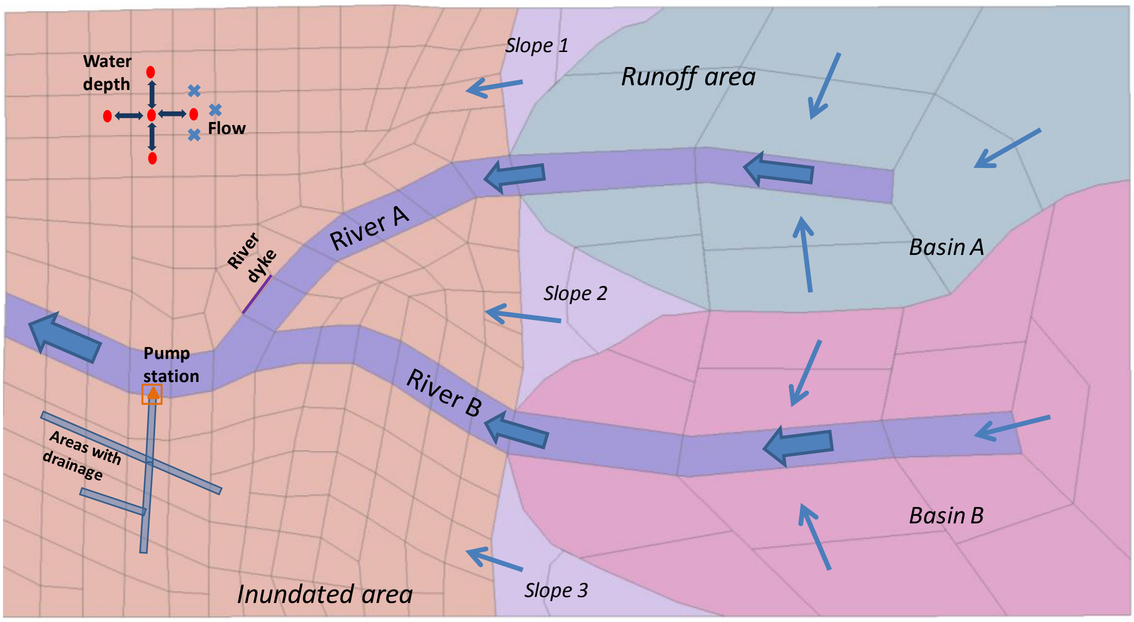

Figure 36 Scheme map of integrated rainfall–runoff–inundation model

This model was solved by the control volume discrete and staggered method. We calculated the water depth at the center of mesh (red points in figure 36) and the discharge at the edges of meshes, which are called passages (blue x marks in figure 36), at half time steps apart.

5.3 GIS-based model construction

5.3.1 Role of GIS in modeling

GIS can play an important role in flood simulation model construction [5][6][7][8] and can be applied for data management, data processing, and visualization. According to the scheme in the preceding section, the model calculates the water depth at the center of the mesh and the discharge at the passages. For this type of staggered calculation, a method for model construction reported by Li (2002) and Cheng (2009) uses lines as passages and connects the nodes of the lines to create meshes by programming [9][10]. Passages, meshes, and nodes lie at the same layer. In our research, we took advantage of the data structure of ArcGIS, such that the mesh and passage were treated as two different layers. The mesh layer and passage layer are treated as polygon-shaped and a polyline-shaped files, respectively. Nodes are not necessary in this structure. The connectivity between meshes and passages are built through spatial analysis.

The role of GIS in this model is shown in figure 37. GIS plays an important role in data management. All collected data including DEM, images, city map, and location of rain gauge stations are transformed to the ArcGIS format and are saved in a computer for convenience of management and processing. Then, the meshes and passages for the model can be generated in ArcGIS taking other geographic data as the base map. By applying spatial analysis and other GIS functions, the connectivity matrix and parameters used in simulation can be easily extracted. ArcGIS also offers automatic processing for developing a data processing procedure for flood and inundation simulation on irregular meshes. By following a button-by-button pattern, preparations for flood and inundation simulation can be achieved. The processed mesh and passage data are then converted to text files as input of a calculation program. The calculation program follows a hydrology process such that rainfall, water concentration, and drainage and execution flow are linear; parameter reading, data reading, and looping are conducted through time steps. The calculated water depth and discharge are also exported as text files such as csv format and are added to the layers in the ARCMAP program to realize the visualization [12].

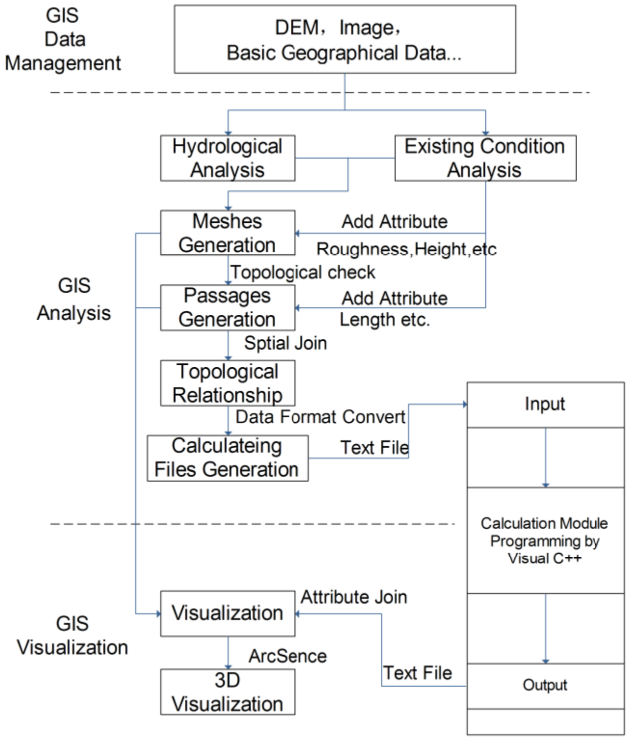

Figure 37 Role of Geographic Information System (GIS) in modeling

5.3.2 GIS-based data preprocessing

In this model, the mesh layer is treated as polygon-shaped file, and the passage layer is treated as a polyline-shaped file. The connectivity between meshes and passages are built through spatial analysis, and parameters used in calculation are saved as attributes of the polygon and polyline. A question arose concerning how to realize this proposal in GIS. Two important parts should be realized for quick extraction of model parameters: mesh and passage generation and topological relationship construction.

5.3.2.1 Mesh and passages generation and connectivity construction

The staggered method was adopted to solve our equations. The water depth was calculated at the center of the mesh, and the discharge was calculated at the passages. To construct the staggered grid, a set of codes should be used; however, a clearer method by taking advantage of GIS is to build a polygon layer as the mesh and a line layer as passages. The topological relationship between meshes and passages and their parameters can be expressed by layer attributes. For the basin area, the counter line layer and mesh layer can be generated through the DEM based hydrological analysis offered by GIS in addition to the river layer, and then the passage layer can be converted. For the inundated area, taking the remote sensing image, administrative map, and land use map as a base map, the mesh layer can be generated manually or automatically. To ensure that the irregular meshes effectively represent the surface features of the inundation area, they are made manually. Then, the passages layer can be converted.

Due to the code-free mesh and passage generation, we did not consider the basic data structure of the vector polygon and line; therefore, the topological relationship between the mesh layer and the passage layer should be built. Here, an ARCGIS spatial analysis-based procedure is offered to construct connectivity between meshes and passages. When a mesh is chosen, the passages around the mesh should be known, and vice versa. If the passage chooses the mesh, from the polygon to line function, the mesh ID around the passage is automatically added to the attribute of passages. If the mesh chooses the passage, through the line to point function, the passage line can be converted to passage points because they share the same ID. Then, a buffer is made for passage points by the buffer function so that the passage points can touch the meshes at both sides. The spatial join function is used to obtain the ID of passages for the meshes. Finally, a small code is used to removes duplicate IDs to clarify the topological relationship. The tools can be easily integrated and developed by Python in ARCMAP. Then, we need only click the button. This procedure is shown in figure 38.

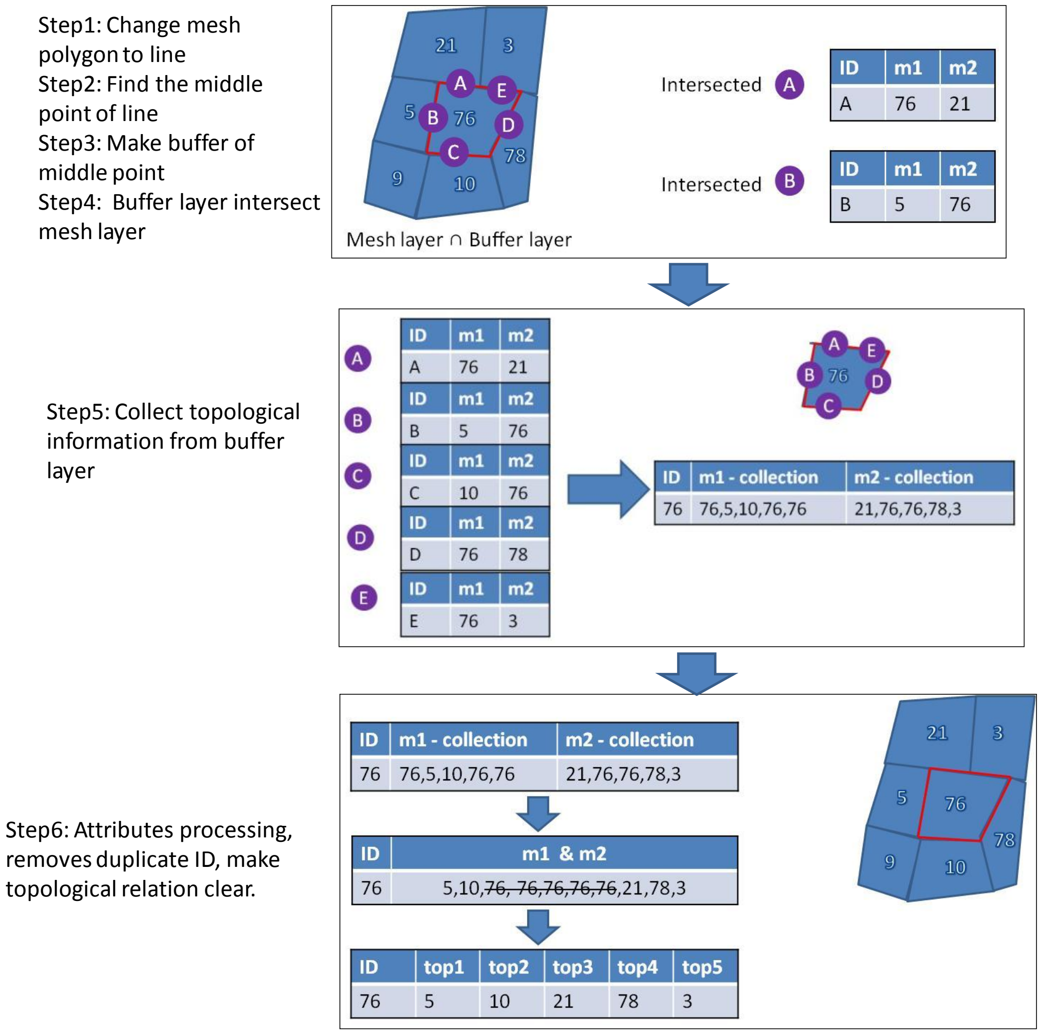

Figure 38 Procedure for construction of connectivity between meshes and passages through spatial analysis

5.3.2.2 Quick extraction of model parameters

Next is parameter extraction. Taking other information layers as the base map, through the overlay or other spatial analysis functions, information can be extracted into the mesh and passage layers. The area of the mesh, length of passage, height, and roughness are the most important parameters in this model. The area and length in the projected coordinate system can be calculated by geometry. The height can be calculated by zonal statistics of DEM. For the roughness, each type of land use has a certain value. In one mesh, the roughness is calculated by area weighting. The mesh layer overlying the land use layer is used to obtain the area of each type of land use. Then the area is taken as weight to calculate the roughness in each mesh.

Most of the parameters such as area, height, and length can be extracted directly through a single function offered by ArcGIS. Other parameters can be extracted by combining some functions. For example, the calculation of distance between the centers of meshes should first convert the mesh to center points, then the distance between points can be calculated, and the calculation result and combined with the passage attributes. Some parameters may not be directly extracted by existing functions. For example, in the last step in connectivity construction, small programming with python and Arc objects in ArcGIS can help to realize the function. Figure 39 shows the results of connectivity information and extracted parameters. All of these data are saved as attributes of meshes and passages and are then converted to text files that can be used directly in calculation programs.

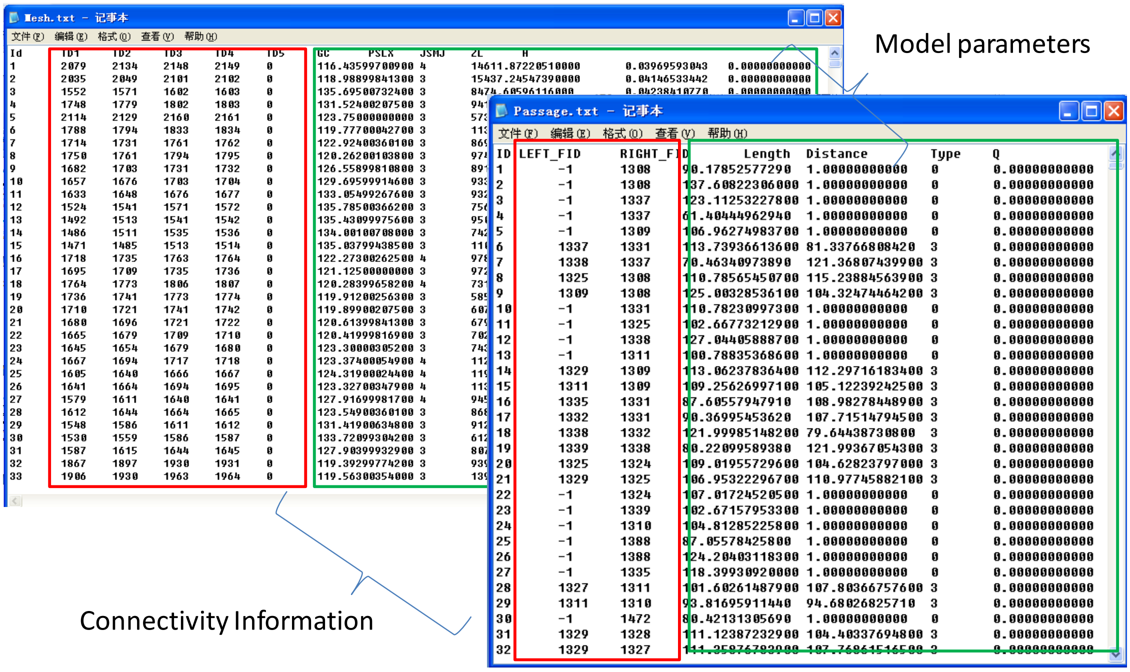

Figure 39 Results of connectivity and attributes extraction

5.3.2 Calculation of module programming

The calculation module is programmed at the platform of visual C++. The calculation procedure is quite straightforward. First, the mesh data and passage data prepared as text files are read. In the program, two structures are built to receive the input mesh data and passage data; classes are also fine. Structure pointers are used to call up the data. Second, the rainfall data saved as an array in the program are read. Then, the program goes to the main part and is looped through time steps. In the time loop, the program will first loop through passages to calculate discharges of each passage using water depth of meshes calculated at the last time step, then it loops through the meshes to calculate the water depth of each mesh by using the discharge of passages calculated previously. The calculation ends after looping through all time steps. Finally the program writes the calculation results such as final water depth, final discharge, water depth and discharge each hour, water depth of specified mesh, and discharge of specified passage to the csv file. The procedure for calculation of the model programming is shown in figure 40.

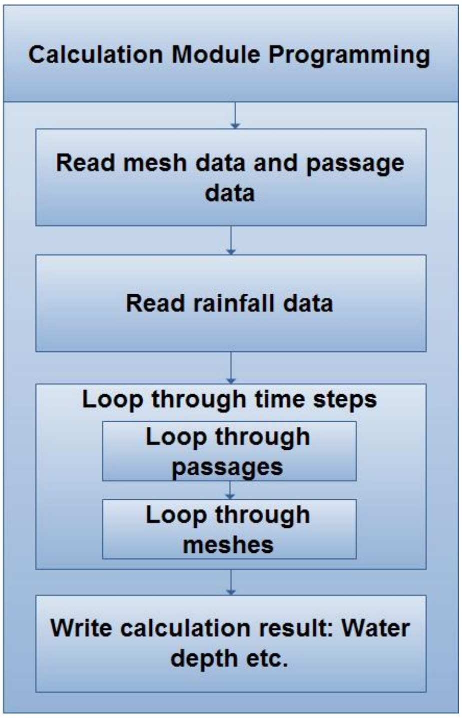

Figure 40 Procedure for calculation of model programming

5.4 Validation of model

The integrated rainfall–runoff–inundation model is difficult to validate because the entire process of rainfall–runoff and inundation is rarely measured in realty, and it is difficult to compare the model with measured data. There are few integrated model developed, which makes it difficult to compare the model with other models. Our model, however, is a combination of runoff and inundation models; therefore, we can separate the model into runoff and inundation parts for respective validation. The runoff data is easily measured in reality. Therefore, the runoff model can be validated by actual water levels or discharge data. A case study in the Marayama River Basin, Japan, was conducted to validate the rainfall–runoff part of the model. However, because the inundation data is not easily measured, this part is validated by comparison with other models. The inundation part of the model in this case was validated by comparison with the results simulated by the LISFLOOD model in Buscot, UK.

5.4.1 Runoff simulation in Maruyama River Basin, Japan

The study area is located in the southern part of the Maruyama River basin, Hyogo prefecture, Japan, as is shown in figure 41, and consists of two sub-basins of the Maruyama River. The entire study area is approximately 218 km^2 with an average elevation of 370 m. Two rain gauge stations known as Wadayama and Nii are located in the study area, and a discharge gauge station known as Kyouguchi is located at the outlet. Because rainfall data, discharge data, and geographic data of this area are easily accessed, this area was selected as the case study area. Our integrated model can be treated as a rainfall–runoff model when the inundation part is closed. In the study area, the model was adopted to calculate the rainfall flowing from the ground surface into the river.

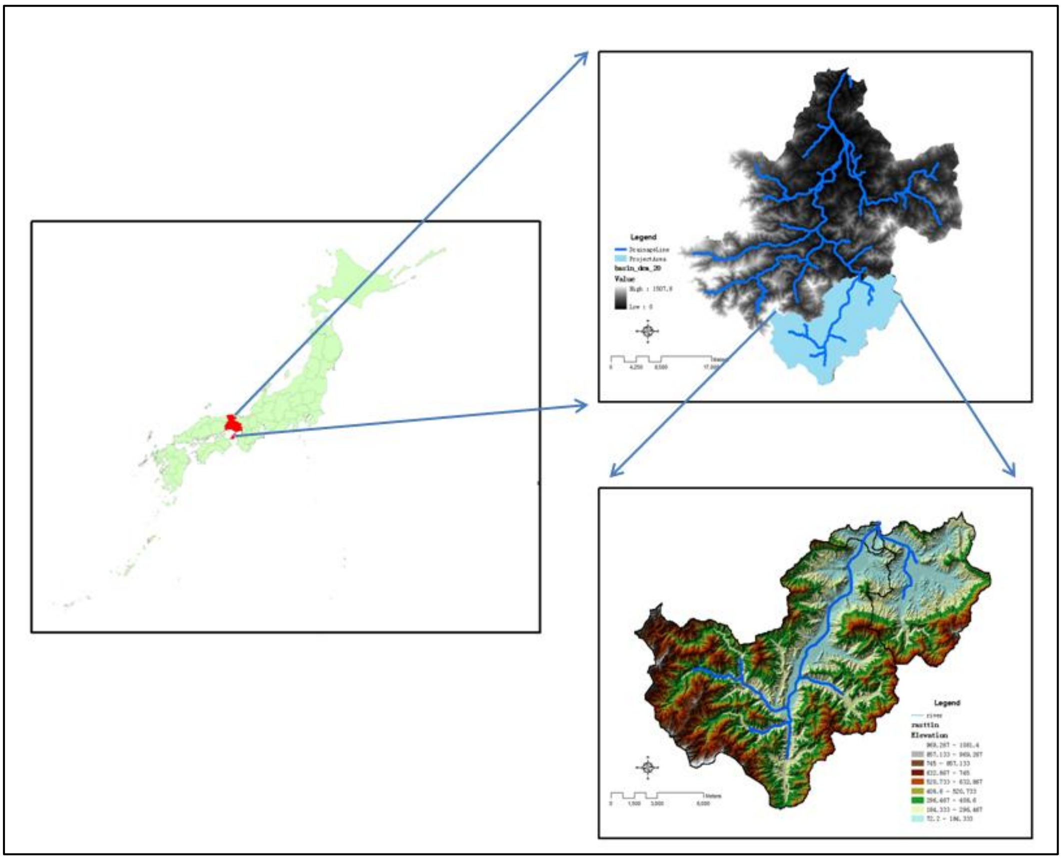

Figure 41 Map of the study area

After setting up the model in this area using the method introduced in previous sections, a rainfall event that occurred from 18:00 to 4:00 (UTC + 9 hours) on August 30–31, 2004, was used for input data. the rainfall and flow gauge data are summarized in table 8. The model was validated by comparison with the observed flooding at the outlet and the simulation results.

Table 8 Rainfall and flow gauge data used for the runoff model

Time (UTC + 9 hours)	Rainfall in sub-basin 1 (mm)	Rainfall in sub-basin 2 (mm)	Q (m^3/s)
8/30/2004 18:00	5	2	1.53
8/30/2004 19:00	2	1	2.64
8/30/2004 20:00	13	15	5.74
8/30/2004 21:00	25	34	31.54
8/30/2004 22:00	36	15	214.27
8/30/2004 23:00	16	28	398.81
8/30/2004 24:00	17	29	1023.63
8/31/2004 1:00	2	5	913.05
8/31/2004 2:00	1	2	739
8/31/2004 3:00	0	0	593.49
8/31/2004 4:00	0	0	472.96

Figure 42 shows a comparison of the observed and simulated discharge amounts; the red points in the figure represent observed discharge, and the black line represents the simulated discharge. From this figure, it is clear that the performance of our model is acceptable, particularly for the simulation of peak discharge. From the fifth to eighth hour, this model accurately simulated the peak discharge caused by heavy rainfall. In the last two hours, the simulated results were smaller than observed discharge, which may be attributed to the influence of ground water. In our model, ground water was not considered.

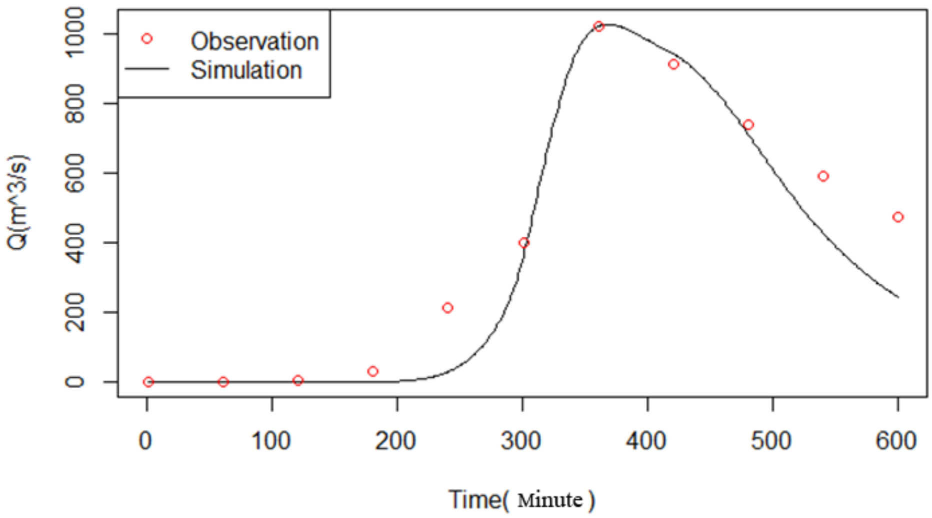

Figure 42 Comparison of observed and simulated discharge

Although this case study is not a complex study, it demonstrates the ability of runoff simulation of our model. It performed well, particularly in the simulation of peak discharge caused by heavy rainfall, and meets the requirements of integrated flood risk assessment. The details of this case study can be found in reference [13].

5.4.2 Inundation simulation in Buscot, UK

Compared with that of the runoff model, validation of the inundation model is more difficult owing to the lack of actual cases and observed data. Therefore, an alternative to validation was selected in which comparisons were made with other models. The LISFLOOD-FP developed by Bristol University was chosen as the candidate model for several reasons. Developed in 1999, the LISFLOOD-FP has more than 10 years of history and is continually being updated. Many papers have been published on this model, which proves its ability. In addition, it was developed for the purpose of research and can be downloaded free from the web site [14]. The final reason for using this model is that as a research scholar, I visited Bristol University for three months and worked with the author of the model, professor Paul Bates, and his group. Thus, any questions about this model could be answered directly.

The case study of Buscot is an example case released with the LISFLOOD-FP model. The case study area is located between Oxford and Bristol with River Thames passing through. The location of the study area is shown in figure 43. The model domain was set up between the gauge station at Buscot weir, which provides a measure of flow for the upstream boundary condition, and the weir in the right side in figure 43.

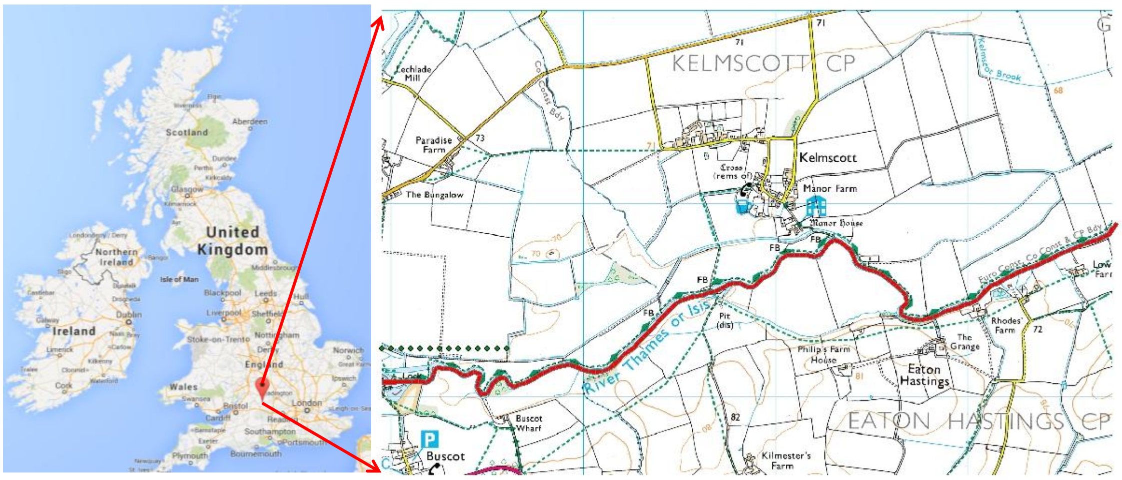

Figure 43 Sketch map of study area

To make a comparison with the LISFLOOD-FP model, a case study in Buscot using our model was conducted. The same geographic data, initial inputs, and parameters as those used by LISFLOOD-FP were used in our model, and the output results were compared.

The basic geographic data was DEM, which was constructed for the area using stereo air photogrammetry. This information was provided as a raster grid with a resolution 50 m and vertical accuracy of about 25 cm. The LISFLOOD-FP model is based on raster data directly. The raster data was used as input for their model; however, our model is based on vector data. Thus, the meshes for simulation were generated, and the river meshes followed the direction of river. To make a comparison with the raster-based model, we modified the overlap part between the river and the inundation area by using irregular meshes and kept the rectangle of other parts. The DEM used in the LISFLOOD-FP model and the meshes used in our model are shown in figure 44 and figure 45, respectively.

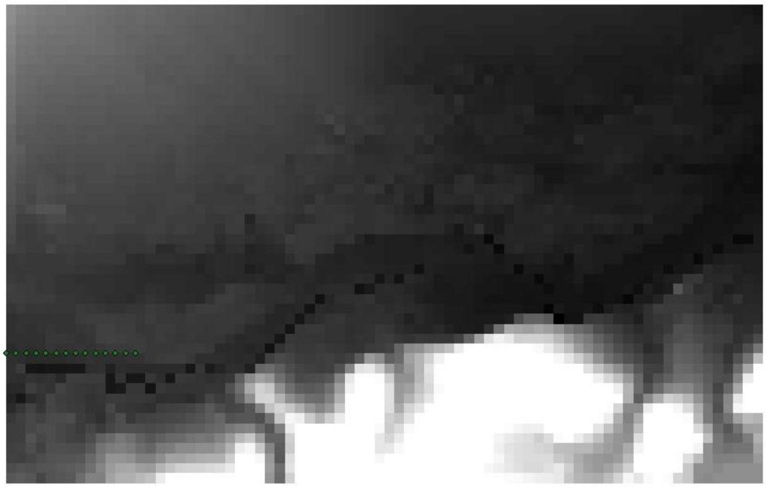

Figure 44 Digital elevation model (DEM) used in LISFLOOD-FP model

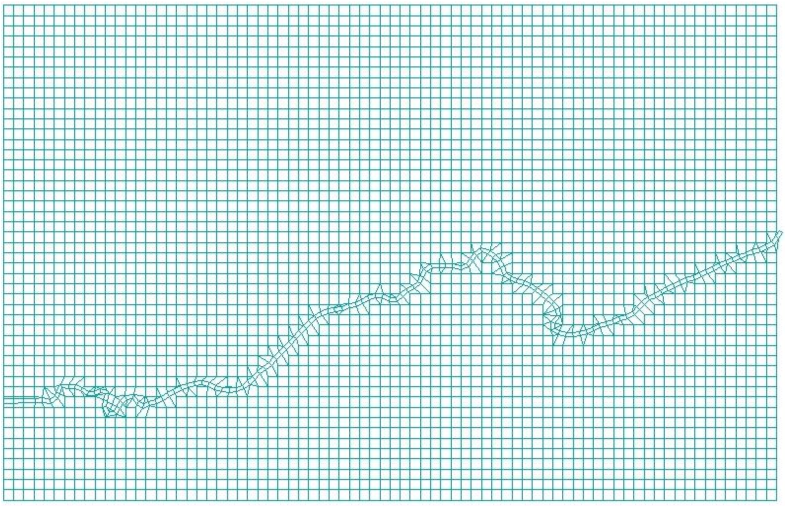

Figure 45 Meshes used in simulation model

The boundary conditions, initial conditions, and parameterization were set following the Buscot case study of the LISFLOOD model.

Boundary conditions:

(Qin) – Constant discharge 73 m^3s^{-1}.

(Qout) – Free outflow, fixed water surface elevation 68.43 m. Side boundaries, zero flux.

Initial conditions:

Water contained in channel only, 2.0 m deep with zero velocity (Qout = 0 m^3s^{-1}).

Parameterization:

Spatially lumped into two zones for friction, spatially uniform for channel (0.03) and floodplain (0.06).

The results of the simulation are shown in figure 46. The blue areas indicate inundation simulation by LISFLOOD, and red areas represent that by our model.

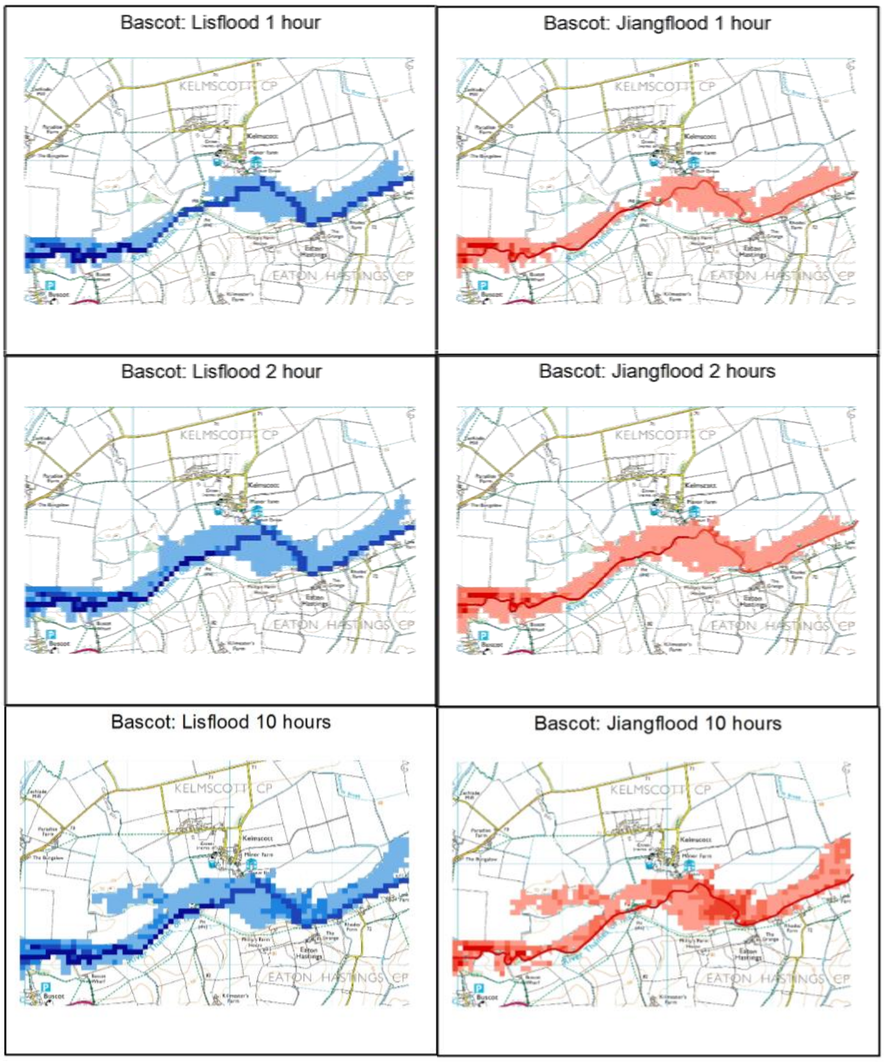

Figure 46 Comparison of simulation results

From the figure 46, the differences between the two model are not obvious. After 10 h of simulation, 95% of inundated area simulated by the two models was the same. The difference in simulated inundation water heights between the models were within the interval [-0.5, 0.3]. However, some detail parts differed. After discussed with professor Bates, the following two reasons were identified:

1. Because the two models had different DEM processing procedures, the height of the bank in LISFLOOD was set as the height of neighboring raster cell of the river cell, although the width of the river is smaller than the size of raster. In our model, however, we used vector data and represented the river as its actual width and height.

2. The LISFLOOD-FP model is a separate model with a 1D model for river routing and a 2D model for inundation. In our model, 1D and 2D data were integrated to represent the process of river routing and inundation together. For different models, different parameters should be considered by calibration. However, in this case study, our model used only the parameters of the LISFLOOD-FP model, which may be not appropriate.

Detailed difference between the two models is not our main focus. More importantly, this case study demonstrates the ability of inundation simulation of our model. Our model performed as well as LISFLOOD-FP and meets the requirements of integrated flood risk assessment. Additional applications of the inundation model can be found previous studies [13][15].

5.5 Integrated simulation in Otsu River Basin

After validation of runoff and inundation parts, the integrated model was applied to the main study area in the Otsu River Basin. The basic information of study area was presented in chapter 3. In this section, the model and its calibration and application are introduced.

5.5.1 Mesh division

As discussed in section 5.3, GIS is used to manage and process data. By using GIS functions, the study area was firstly divided into runoff and inundation parts according to topography and distribution of the residential area. The inundation part includes lower parts of the river basin and most of the residential areas. The runoff parts are the upper and middle stream of rivers, which are mountainous regions with very few residential areas. The inundation area was then divided into small irregular meshes following the shapes of the river, slopes, and street direction. The average size of the irregular meshes was about 50 m × 50 m. The meshes are mainly quadrangles with a few triangles and pentagons in the junction area. The runoff area was divided into sub-basins by hydrological analysis. The procedure for basin division based on DEM is modularized and integrated in Arc Hydro [16]. Figure 47 shows the mesh divisions.

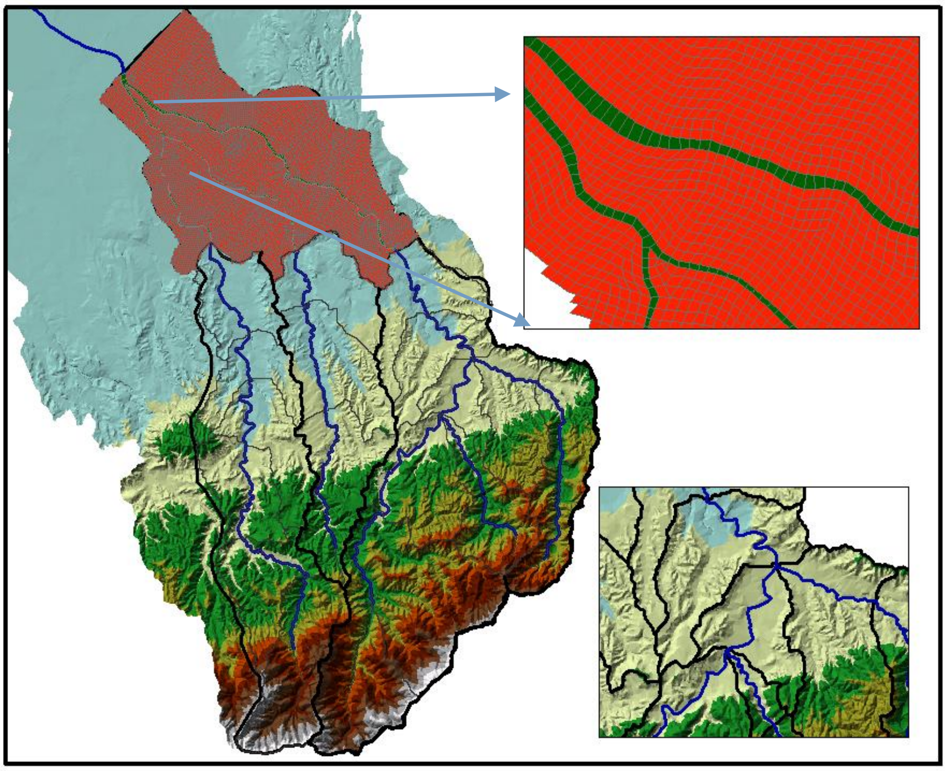

Figure 47 Mesh and sub-basin divisions of the study area

5.5.2 Model coding

The model was constructed following the methods introduced in section 5.3. Here, some specifications of the model are explained. Table 9 shows the attributes of meshes adopted in the calculation. ID is a unique number used to identify meshes. P1 to P6 store the connectivity information between meshes and passages. The numbers in P1 to P6 are the ID numbers of passages. If the number is -1, that means no passages are surrounding the mesh. In the following case, the first seven columns describe a mesh with ID 0 surrounded by passages with ID 74, 75, 76, and 82, which is a quadrangle. The next four columns are the parameters. Area is the area of the mesh, and type is the type of mesh. Table 10 lists the codes of mesh type in this case study, including basic and additional types. For the additional types of meshes, we generally treated these structures as passages. However, if they are big enough or if special care is needed, they could also be treated as meshes. Elevation is the average elevation of mesh, and roughness is area-weighted roughness. Manning's *n* roughness coefficient according to land use type was introduced by Kalyanapu [17], as listed in table 11. Depth is the inundated water depth.

Table 9 Attributes of meshes adopted in the calculation

ID	P1	P2	P3	P4	P5	P6	Area	Type	Elevation	Roughness	Depth
0	74	75	76	82	-1	-1	2500	2	72.72	0.06	0

Table 10 The code of mesh type in this case study

	Types of meshes	Code
Basic types	Identity of basin area	1
	Identity of inundated area	2
	Identity of river	3
	River in basin area	13
	River in inundated area	23
Additional types	Dam	5
	dyke	6
	Railway	7
	others	...

Table 11 Manning's *n* roughness coefficient according to land use type

Description	Manning's n
Developed, open space	0.0404
Developed, low intensity	0.0678
Developed, medium intensity	0.0678
Developed, high intensity	0.0404
Barren land	0.0113
Deciduous forest	0.36
Evergreen forest	0.32
Mixed forest	0.40
Shrub/scrub	0.40
Grassland/herbaceous	0.368
Pasture/Hay	0.325
Woody wetlands	0.086
Emergent herbaceous wetlands	0.1825

Table 12 shows the attributes of passages adopted in the calculation. M1 and M2 store the connectivity information between passages and meshes. The numbers in M1 and M2 are the ID numbers of meshes. If the number is -1, this passage is a border and there is no mesh on one side. In the following case, this first three columns describe a passage with ID 0 connecting meshes with ID 13 and 20. The next four columns are the parameters. Table 13 lists the code of passage type in this case study. Type is the type of passage; length is the length of passage; distance is the distance from one mesh center to the next mesh center; weir describes the height of the dyke or weir; and flow is the discharge in the passage.

Table 12 Attributes of passages adopted in the calculation

ID	M1	M2	Type	Length	Distance	Weir	flow
0	13	20	14	50	50	2	0

Table 13 Codes of passage type in this case study

	Types of passage	Code
Basic types	Identity of basin area	1
	Identity of inundated area	2
	Identity of boundary	3
	Identity of river	4
	Interface between basin area and inundated area (water exchange)	12
	Boundary of basin area	13
	Interface between basin area and inundated area (no water exchange)	123
	Interface between basin and river (dyke in basin area)	14
	Interface between river sections (river in basin area)	144
	Boundary of inundated area	23
	Interface between inundated are and river (inundated area)	24
	Interface between river sections (river in inundated area)	244
Additional types	Dam	5
	Bridge	6
	Railway	7
	others	...

5.5.3 Application of model to flood simulation

The model was applied to simulate a rainfall event that occurred on July 4, 1995. The recorded maximum point rainfall reached 46 mm/h at the Yokoyama rain gauge station. Because of this rainfall event, more than 70 houses were inundated. This rainfall event can be used to calibrate our model because it was a recent serious flood event, and compared with previous large flood disasters, it is closer to the current situation. Figure 48 shows the basin rainfall and corresponding observed discharge at Kawanakabashi gauge station and Yamadaibashi gauge station with model-simulated discharge. The locations of gauge stations are given in chapter 3.

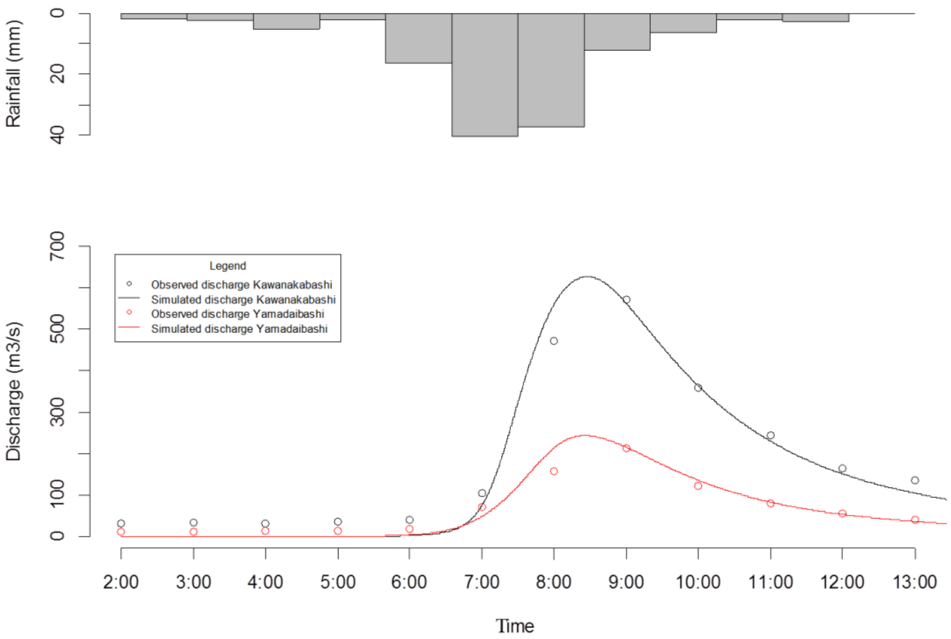

Figure 48 Basin rainfall and corresponding discharge at Kawanakabashi gauge station and Yamadaibashi gauge station with simulated hydrograph

The upper part of the figure shows the rainfall process. The solid lines in feature 48 represent simulated discharge, and points represent observed discharge. Because the base flow was considered, observed discharge is larger at beginning than simulated discharge. As the rainfall became larger, the fitness of observed discharge and simulated discharge improved.

For the inundation part, we adopted precise river section data rather than raw DEM, which may have made our simulation more reasonable. Figure 49 shows the simulation results of the integrated rainfall–runoff–inundation model overlying a satellite image. The figure shows the spatial distribution of water depth in the risk assessment area caused by the rainfall event. In this rainfall event, three large inundated areas were noted in the inundation simulation that were caused by overtopping in addition to one large inundated area caused by urban drainage and several small inundated areas. Ushitaki River was easily overtopped. The water depth in each inundated area was less than 0.5 m in most areas.

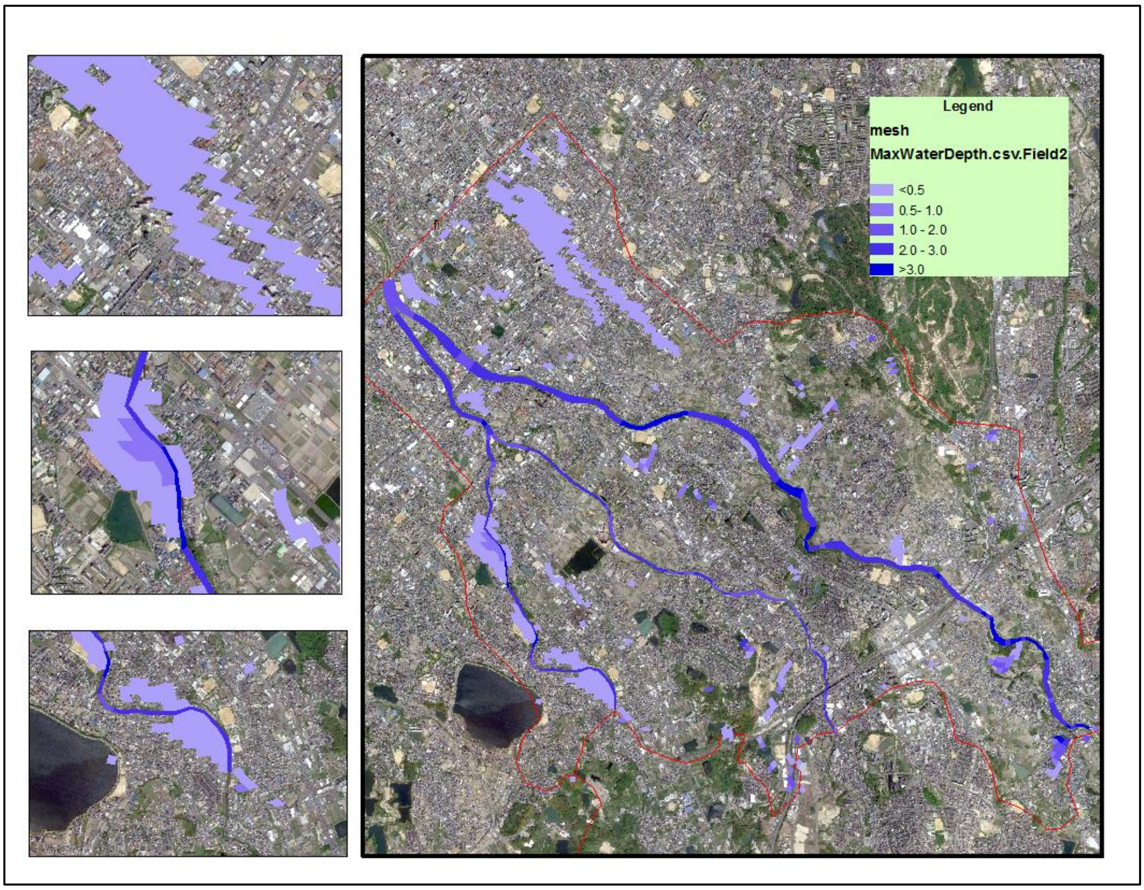

Figure 49 Spatial distribution of water depth caused by flooding and inundation

Usually, it is difficult to find observation data for validating the simulation results of spatial distribution of inundation. Fortunately, after this rainfall event, Osaka prefecture made a field survey of inundated locations [18], as shown in figure 50. The results of this survey were used for comparison with our simulation results. Eight inundated areas were recorded. In our simulation results six locations agreed with the field survey record. The imperfect match may be because the rainfall event occurred in1995, the river section data was measured in 2001, and land use data and other geographic data are more recent. The differences in river and land surface situations may have been caused by differences between simulated result and the survey record.

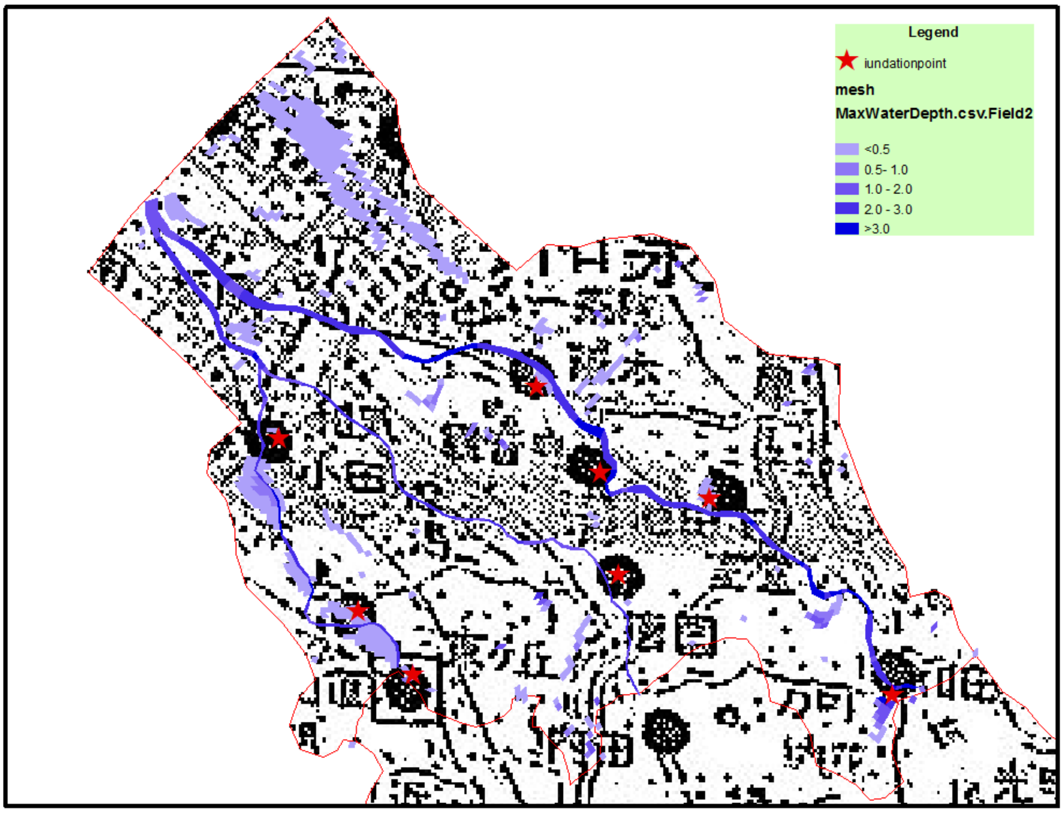

Figure 50 Comparison of the simulation results with the location of inundation reported in field survey

5.6 Discussion

In this chapter, a GIS-based, visualized, simplified rainfall–runoff–inundation model for flood risk assessment was developed. In this model, we emphasized the integration of flood and inundation simulation and used GIS as the operating platform for data management, data processing, and visualization. Visual C++ was the programming platform.

The adoption of GIS significantly decreased the work of the flood simulation, which followed the data processing procedure to enable easy access of mesh and passage files and parameter files for flood and inundation simulation. However, in this study, the irregular meshes were drawn on ARCGIS by hand since there is no better algorithm for irregular mesh generation that considers DEM in addition to information of roads, rivers, buildings, or other necessary data. This issue is a good topic for further study.

Simplified 2D unsteady flow equations were used to simulate flood and inundation in the risk assessment area. Simplification was unnecessary regardless of calculation time. All of the simplified equations could be updated to full equations according to the requirements of the actual work. The model can be improved under the current framework with development of additional knowledge.

References

[1] Sayama T, Ozawa G, Kawakami T, et al. 2012. Rainfall–runoff–inundation analysis of the 2010 Pakistan flood in the Kabul River basin . Hydrological Sciences Journal, 57(2): 298-312.

[2] Kobayashi K. 2013. Development of a Large-Scale Distributed Rainfall–Runoff/Flood Inundation Model for the Flood Risk Management. Journal of Disaster Research Vol. 8(1): 117-125.

[3] Mascarenhas F C B, Toda K, Miguez M G, Inoue K. 2005. Flood Risk Simulation. Chapter 2.WIT Press, UK.

[4] Horton R E. 1933. The role of infiltration in the hydrologic cycle. Trans. Am. Geophys. Union. 14th Ann. Mtg: 446-460.

[5] Wan H, Zhou C, Wan Q, Liu S. 2001. Integration of Geographical Information System Technology and Hydrological Model. Adv Water Sci. 12 (4), 560-568.

[6] Knebl M R, Yang Z L, Hutchison K, et al. 2005. Regional scale flood modeling using NEXRAD rainfall, GIS, and HEC-HMS/RAS: a case study for the San Antonio River Basin Summer 2002 storm event . Journal of environmental management, 75(4): 325-336.

[7] Liu Y B, Gebremeskel S, De Smedt F, et al. 2003. A diffusive transport approach for flow routing in GIS-based flood modeling. Journal of Hydrology, 283(1): 91-106.

[8] Jain S K, Singh R D, Seth S M. 2000. Design flood estimation using GIS supported GIUH Approach . Water Resources Management, 14(5): 369-376.

[9] Cheng X. 2009. Urban Flood Prediction and Its Risk Analysis in the Coastal Areas of China. Beijing, China, pp.142-161.

[10] Li N, Qiu J, Cheng X, Lu J. 2002. Study on Simulation System of Rainstorm Inundation in Tianjin City. Natural Disasters. 11 (2), 112-118. (in Chinese)

[11] Tan W. 1998. Shallow Water Hydrodynamics—Application of Finite Volume Method. Tsinghua University, Beijing, China, pp. 62-95. (in Chinese)

[12] Jiang X, Tatano H, Zhang J. 2011. Data Processing Procedure for Irregular Mesh Inundation Simulation Models: Toward Development of a GIS based Inundation Simulation System. ISSN: 1345-8507, Proc. of the Thirteenth International Summer Symp. JSCE.

[13] Jiang X, Tatano H, Tomoharu H. 2013. A Methodology for Spatial Flood Risk Assessment Taking Account of Spatial–Temporal Characteristics of Rainfall . IDRiM Journal, 3(1).

[14] Bates P D, De Roo A P J. 2000. A simple raster-based model for flood inundation simulation . Journal of Hydrology, 236(1): 54-77.

[15] Chen P, Zhang J, Jiang X, et al. 2012. Scenario simulation-based assessment of trip difficulty for urban residents under rainstorm waterlogging . International Journal of Environmental Research and Public Health, 9(6): 2057-2074.

[16] Maidment, D R.(Ed.). 2002. ArcHydro: GIS for water resources. ESRI, Inc.

[17] Kalyanapu A J, Burian S J, McPherson T N. 2010. Effect of land use-based surface roughness on hydrologic model output. Journal of Spatial Hydrology, 9(2).

[18] Osaka prefecture, historical heavy rain disaster records, http://www.pref.osaka.lg.jp/kasenseibi/keikaku/ootsukihon.html.

Chapter 6 Flood risk assessment considering multiple flood sources

6.1 Spatial distribution of economic data and fragility curve

6.1.1 Spatial distribution of economic data

According to the definition presented in this thesis, flood risk is produced by two components: probability of inundation and the associated consequences. In this thesis, consequences are defined as direct economic losses caused by flood events. The economic conditions of the study area, represented by four categories including house assets, household item assets, depreciable assets and stock assets of business, and depreciable assets of household for agricultural and fishery, are calculated from basic census data and economic census data [1][2][3]. Since the calculation of spatial distribution of flood risk is the focus of this thesis, the spatial distribution of economic data is required.

In Japan, the economic census is takes advantage of a standard areal mesh system (grid square system or longitude and latitude system). In this system the entire area of the country is divided into areal meshes of equal size with the aid of the specified longitude and latitude lines [4]. There are three basic levels of meshes. The primary area partition is denoted by 40′ of latitude and 1° of longitude (about 80 km). The secondary area partition is denoted by dividing the primary area partition into 64 (8×8) equal parts vertically and horizontally (about 10 km), and the basic grid square is denoted by dividing the secondary area partition into 100 (10×10) equal parts vertically and horizontally (about 1 km). Then, the basic grid square is divided into 4 (2×2) equal parts reaching the fourth level (about 500 m) or 16 (4×4) equal parts reaching the fifth level (about 100 m).

The economic census data is based on fourth level 500 m meshes and is provided in the csv format. To use the data, four steps of data processing are adopted. Most of the economic census data, which includes huge amounts information, are not relevant to this calculation. Therefore, only columns that can be used to calculate assets should be selected. Then, according to formulas, various types of assets can be calculated. However, because 500 m resolution is not sufficient for flood risk assessment, the 500 m mesh was recoded into 100 m mesh. When combined with 100 m land use meshes downscale, the census data can be realized. Each 500 m economic census contains 25 land use meshes. The economic census data is then distributed into 100 m land use meshes considering different type of land use. The flowchart of spatial distribution of economic data is shown in figure 51.

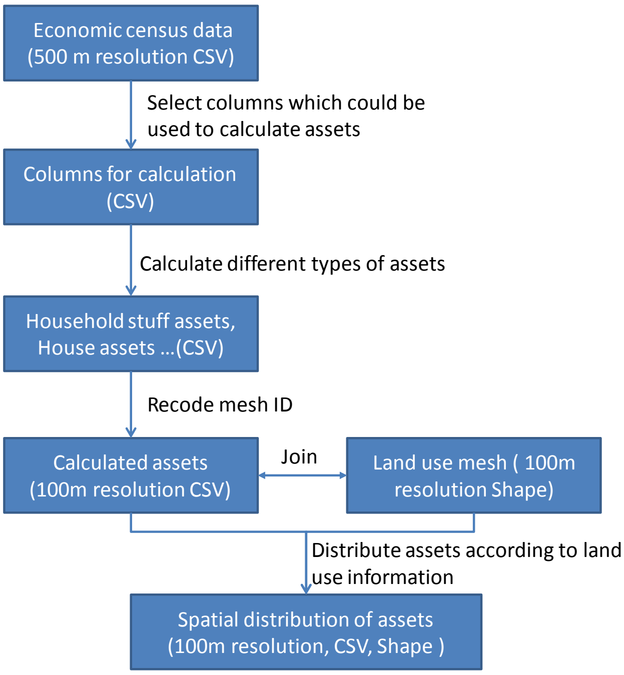

Figure 51 Flowchart of spatial distribution of economic data

The formulas used in the calculation of assets are summarized as follows:

House assets = House area × house value per square meter

Household item assets = Number of households × item value per household

Depreciable assets of business = Sum (number of employees per business sector × depreciable assets per employee of each business sector)

Stock assets of business = Sum (number of employees per business sector × stock assets per employee of each business sector)

Depreciable assets of agricultural and fishery = Number of household of agricultural and fishery × depreciable assets per household of agricultural and fishery

Stock assets of agricultural and fishery = Number of household of agricultural and fishery ×

stock assets per household of agricultural and fishery

For house area, the number of households, employees per business sector, and households of agricultural and fishery, can be found directly or by simple calculation of census data [1][2][3]. For house value per square meter, item value per household, depreciable assets per employee of each business sector, stock assets per employee of each business sector, depreciable assets per household of agricultural and fishery, and stock assets per household of agricultural and fishery can be found in the appendix of reference [5]. Detailed description of the calculation methods can also be found in reference [5].

Figures 52–57 show the spatial distribution of household item assets, house assets, depreciable assets and stock assets of business, and depreciable assets and stock assets of household of agricultural and fishery, respectively.

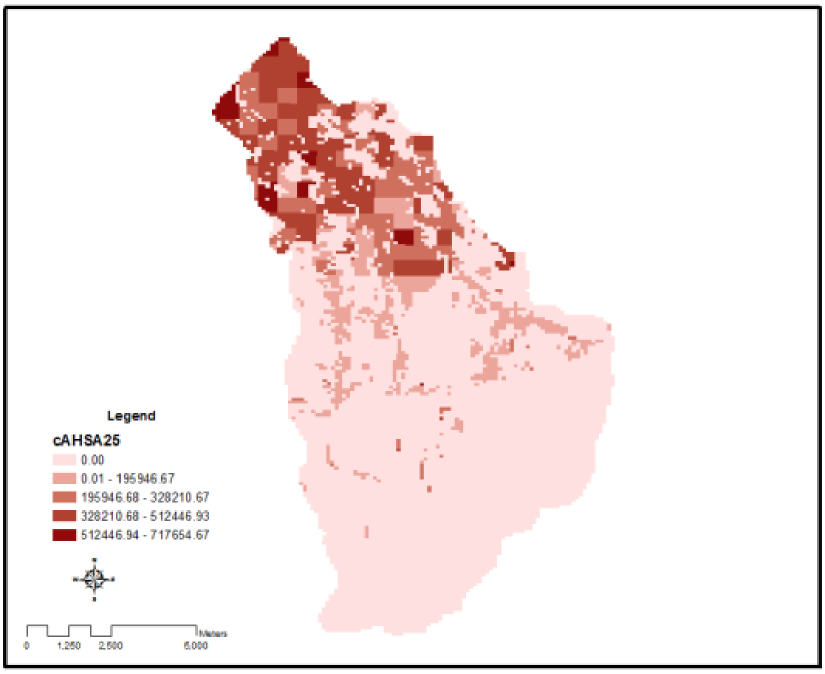

Figure 52 Spatial distribution of household item assets

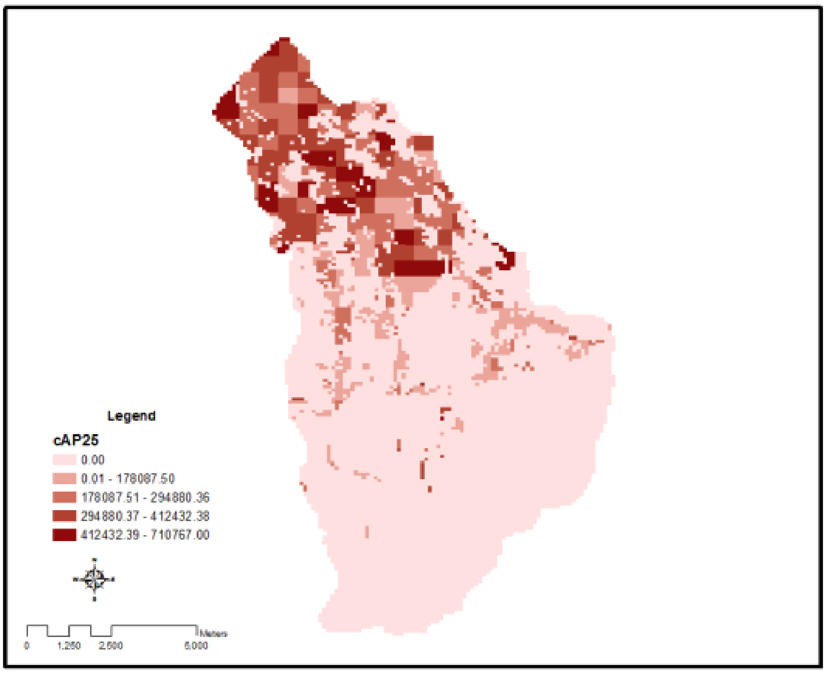

Figure 53 Spatial distribution of house assets

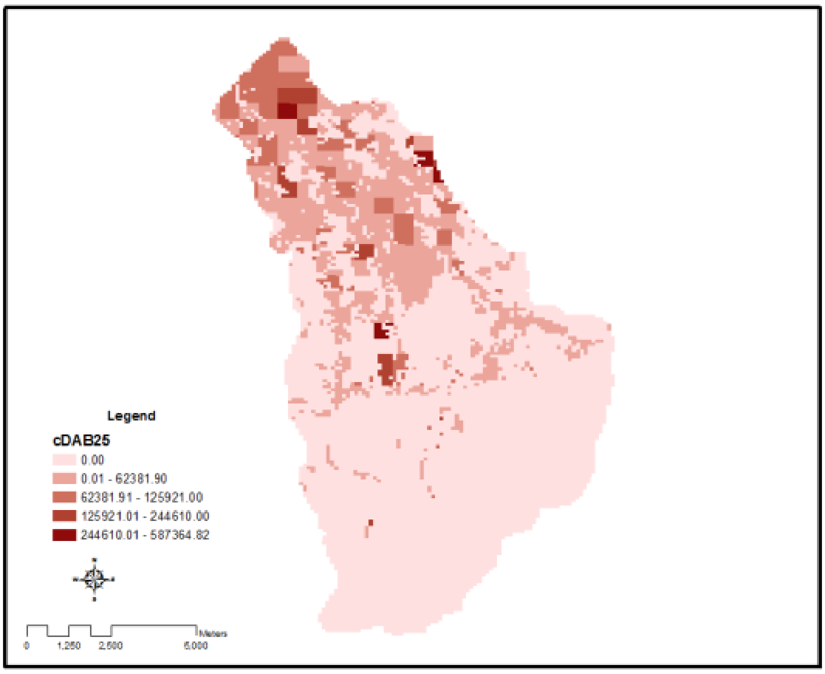

Figure 54 Spatial distribution of depreciable assets of business

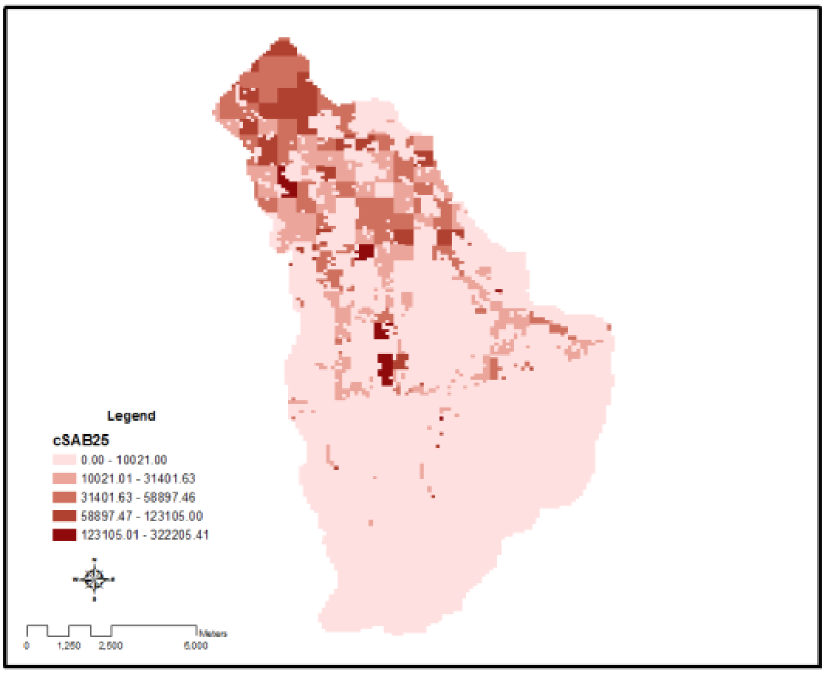

Figure 55 Spatial distribution of stock assets of business

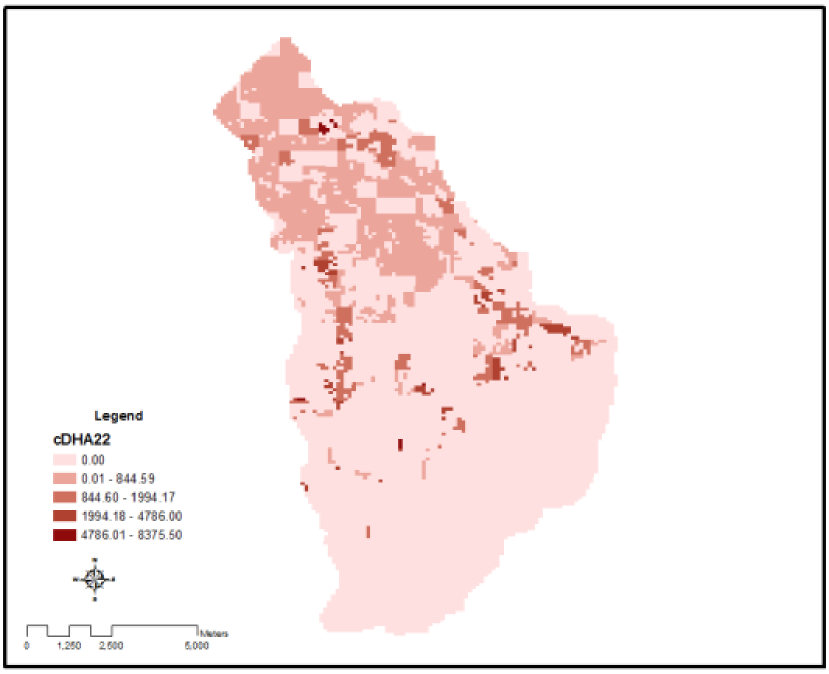

Figure 56 Spatial distribution of depreciable assets of household of agricultural and fishery

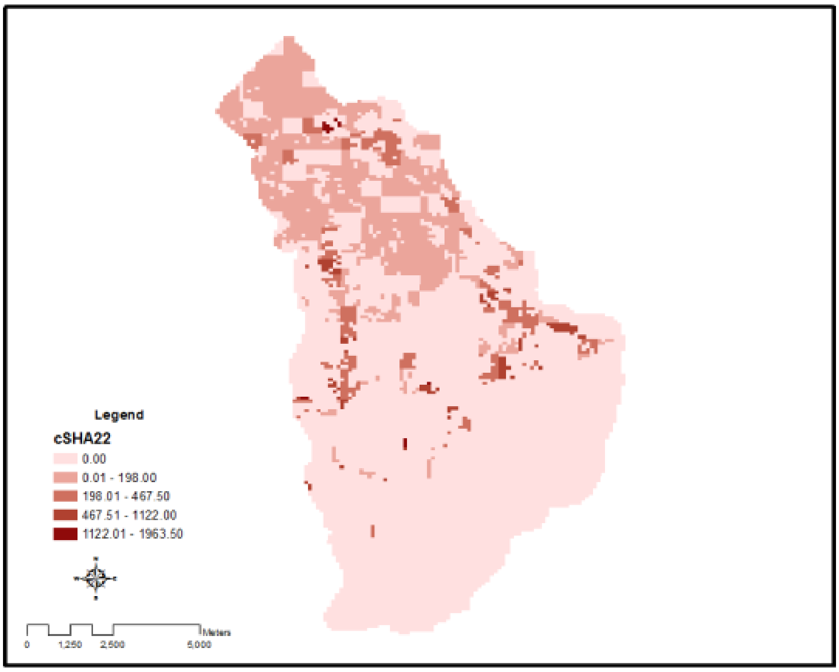

Figure 57 Spatial distribution of stock assets of household of agricultural and fishery

6.1.1 Fragility curve

Although some studies on fragility curves of flood have been conducted [6][7], there is no standard fragility curve for all areas. It is obvious that the fragility curve can differ significantly because of the differences in factors such as house type and structure code. In this study, the empirical fragility curves recommended by the Ministry of Land, Infrastructure and Transport of Japan were adopted. In accordance with six categories of assets, the fragility curves were also summarized as six categories, as shown in tables 14–17. A more detailed description of fragility curves can be found in reference [5].

For the loss rate of house assets, the house is divided into three types according to the slope. The slope of group A is smaller than 1/1000, that of group B is from 1/1000 to 1/500, and that of group B is larger than 1/500. The loss rate of assets for each type of house is shown in table 14. This table was created based on flood damage reported in field surveys conducted from 1993 to 1996.

Table 14 Loss rate of house assets

Water depth / Slope	Under floor	Above floor				
		<50 cm	50–99	100–199	200–299	>300 cm
Group A	0.032	0.092	0.119	0.266	0.580	0.834
Group B	0.044	0.126	0.176	0.343	0.647	0.870
Group C	0.050	0.144	0.205	0.382	0.681	0.888

The loss rate of household item assets is shown in table 15. This table was also created based on flood damage field surveys conducted from 1993 to 1996.

Table 15 Loss rate of household item assets

Water depth	Under floor	Above floor				
		<50 cm	50–99	100–199	200–299	>300 cm
Loss rate	0.021	0.145	0.326	0.508	0.928	0.991

The loss rate of depreciable assets and stock assets of business is shown in table 16. This table was also made based on flood damage field surveys conducted from 1993 to 1996.

Table 16 Loss rate of depreciable assets and stock assets of business

Water depth	Under floor	Above floor				
		<50 cm	50–99	100–199	200–299	>300 cm
Depreciable assets	0.099	0.232	0.453	0.789	0.966	0.995
Stock assets	0.056	0.128	0.267	0.586	0.897	0.982

The loss rate of depreciable assets and stock assets of household of agricultural and fishery is shown in table 17.

Table 17 Loss rate of depreciable assets and stock assets of household of agricultural and fishery

Water depth	Under floor	Above floor				
		< 50cm	50–99	100–199	200–299	>300 cm
Depreciable assets	0	0.156	0.237	0.297	0.651	0.698
Stock assets	0	0.199	0.370	0.491	0.767	0.831

It should be noted that in the flood risk calculation, a segmented fragility curve will create segmented loss. Thus, the tendencies are not always clear. Therefore, based on the loss rates presented above, loss rates according to certain water depth can be recalculated by piecewise linear interpolation.

6.2 Flood risk assessment

6.2.1 Monte Carlo simulation of rainfall event according to return period

The copula-based rainfall processing procedure and random rainfall generation were discussed in chapter 4. For the flood risk assessment, adoption of the full Monte Carlo method [8] is time consuming for flood simulation. For example, if we want include a 1/100 return period rainfall event, at least 1000 random points should be generated, and all rainfall events should be simulated by the rainfall–runoff–inundation model. An alternative strategy is direct generation of rainfall events according to the return period. Different from 1D probability distribution, in 2D dimensional probability distribution, the value at the return period is a counter line (surface in 3D probability distribution) rather than a single value. Therefore, it is possible to simulate random values according to counter lines.

The procedure for simulating random values according to counter lines is proposed as follows:

1. Generate extremely large numbers of random data from the copula model, such as more than 100,000. The algorithm for 2D copula random value generation was proposed by Nelson [9]; that for vines copula random value generation was proposed by Aas [10].

2. Select the point closest to the counter line by the following formula [11]:

$$(u,v) = \underset{C_{uv}(u,v)=t}{\operatorname{argmax}} \; f_{xy}(F_Y^{-1}(u)\,,\, F_X^{-1}(v)) \quad x = F_X^{-1}(u) \;\; y = F_Y^{-1}(v).$$

3. Select the point as a candidate point and delete the point from the original dataset.

4. Repeat step 2 and step 3 for *n* times, so that *n* points consistent with return period *t* can be selected. The selected points are rainfall events most likely to occur according to return period *t*. It should be noted that the precision is determined by the numbers of random data from the copula model; thus, it is recommended to generate large numbers rather than random values.

According to return periods of 1/200, 1/100, 1/50, 1/20, and 1/10, 10 rainfall events for each return period was generated following the above procedure. Figure 58 shows the generated rainfall events on 1 h rainfall and 2 h rainfall copula contour lines. The detailed information of simulated rainfall events is shown in table 18.

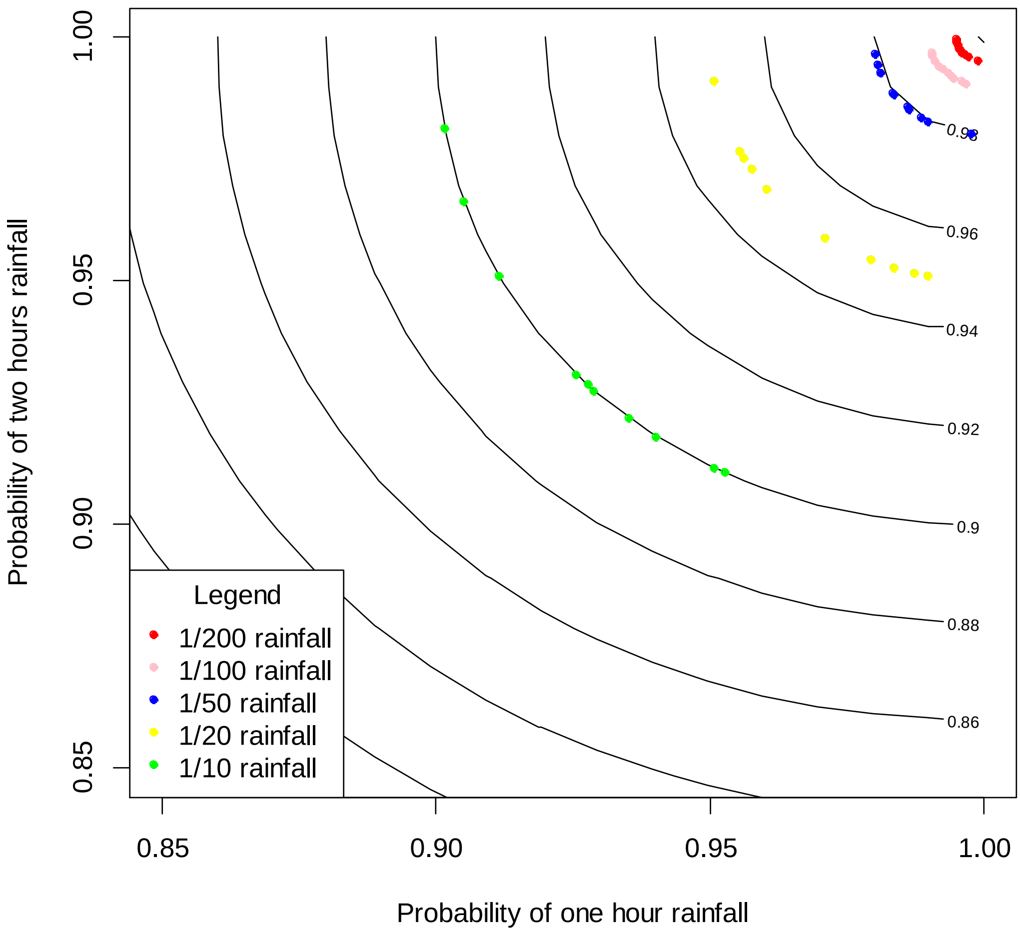

Figure 58 Generated rainfall events on 1 h rainfall and 2 h rainfall events copula contour

lines (10 rainfall events for each return period)

Table 18 Generated rainfall events according to return periods of 1/10, 1/20, 1/50, 1/100, and 1/200

Return period	Case Number	Joint probability	Probability of 1 h rainfall	Probability of 2 h rainfall	Probability of 3 h rainfall	1 h rainfall	2 h rainfall	3 h rainfall
1/10	1	0.9	0.91879	0.939225	0.941695	50	69	81
	2	0.9	0.911597	0.950728	0.953427	50	71	83
	3	0.9	0.963625	0.905985	0.906974	56	65	76
	4	0.9	0.910308	0.953206	0.955985	49	71	84
	5	0.9	0.921025	0.936088	0.938683	50	69	80
	6	0.9	0.973155	0.903307	0.903797	58	65	76
	7	0.9	0.901697	0.980941	0.982193	48	77	92
	8	0.9	0.976649	0.90252	0.902884	59	65	75
	9	0.9	0.930279	0.926294	0.928312	51	68	79
	10	0.9	0.948636	0.912918	0.914267	53	66	77
1/20	11	0.95	0.954936	0.977682	0.979032	54	76	90
	12	0.95	0.971929	0.958277	0.959073	58	72	84
	13	0.95	0.955524	0.976715	0.977845	54	76	70
	14	0.95	0.956502	0.974884	0.976025	54	75	89
	15	0.95	0.955797	0.975845	0.977319	54	76	90
	16	0.95	0.97613	0.955644	0.956443	59	71	84
	17	0.95	0.955492	0.976411	0.977907	54	76	90

	18	0.95	0.967443	0.961666	0.962575	576	7254	85
	19	0.95	0.964972	0.963624	0.964882	60	73	86
	20	0.95	0.971399	0.958697	0.959446	58	72	84
1/50	21	0.98	0.995654	0.980527	0.980557	64	79	94
	22	0.98	0.989213	0.983172	0.983425	68	78	92
	23	0.98	0.980948	0.994091	0.994293	63	80	94
	24	0.98	0.98143	0.992698	0.992972	78	77	91
	25	0.98	0.988885	0.983428	0.98365	73	77	91
	26	0.98	0.980182	0.996555	0.997561	63	80	95
	27	0.98	0.988066	0.984007	0.984251	62	81	97
	28	0.98	0.9839	0.987837	0.988535	61	89	109
	29	0.98	0.98707	0.984496	0.98507	62	82	98
	30	0.98	0.993136	0.981314	0.981365	67	80	92
1/100	31	0.99	0.991662	0.994403	0.994706	68	86	102
	32	0.99	0.993686	0.992282	0.992424	71	83	100
	33	0.99	0.996077	0.990852	0.990901	76	82	98
	34	0.99	0.994742	0.991544	0.991639	73	83	99
	35	0.99	0.991035	0.995683	0.995797	68	87	105
	36	0.99	0.990127	0.998024	0.998561	67	92	113
	37	0.99	0.990378	0.997507	0.997474	67	91	109
	38	0.99	0.991031	0.99578	0.995806	68	87	105

	39	0.99	0.99239	0.993647	0.993727	6947	8561	101
	40	0.99	0.990519	0.996449	0.997029	67	88	108
1/200	41	0.995	0.996649	0.996298	0.99639	77	88	106
	42	0.995	0.995028	0.999613	0.999532	73	101	122
	43	0.995	0.995315	0.998203	0.998366	74	93	112
	44	0.995	0.995483	0.997902	0.997975	74	92	111
	45	0.995	0.995028	0.999159	0.999531	73	97	122
	46	0.995	0.997792	0.995433	0.995575	82	87	104
	47	0.995	0.997145	0.99598	0.995979	79	88	105
	48	0.995	0.995637	0.997357	0.997677	74	90	110
	49	0.995	0.998268	0.995184	0.995354	84	86	104
	50	0.995	0.996114	0.997058	0.996969	76	90	107

6.2.2 Flood simulation

The generated 1 h rainfall, 2 h rainfall, and 3 h rainfall were adopted to make complete rainfall events following the method discussed in chapter 4. In this study, the duration of rainfall is determined as 9 h, and the rainfall pattern was determined as the center peak pattern. All of the rainfall events were taken as input of the integrated rainfall–runoff–inundation model, which was introduced in chapter 5.

Figure 59 shows a rainfall case of flood simulation. The rainfall simulation was repeated for each generated rainfall event, and the maximum inundation depth was recorded. The output of flood simulation was prepared for the calculation of event curve and risk curve.

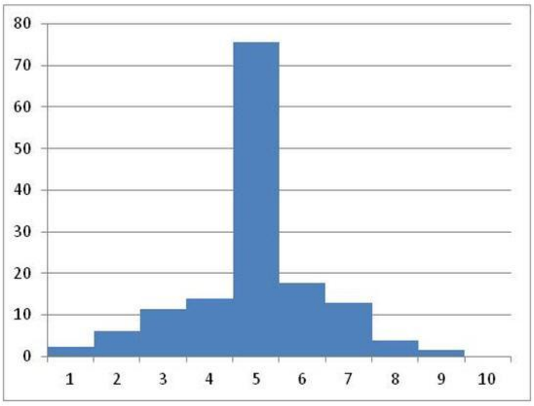
80
70
60
50
40
30
20
10
0
1
2
3
4
5
6
7
8
9
10

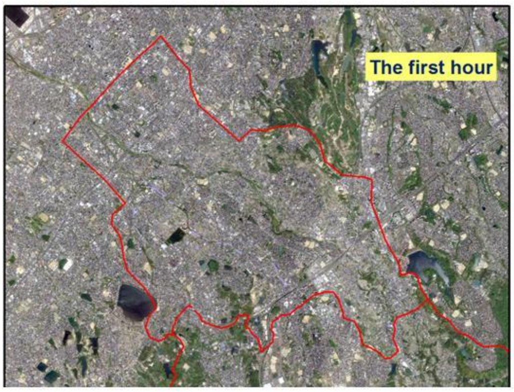
The first hour

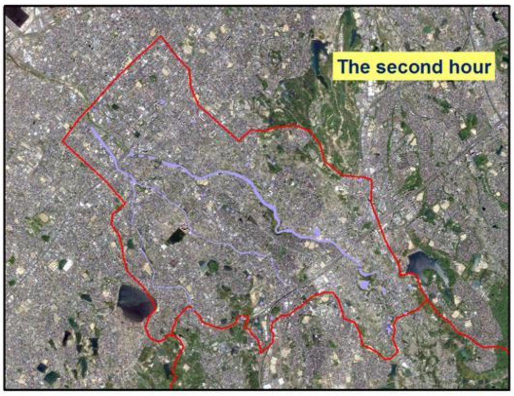
The second hour

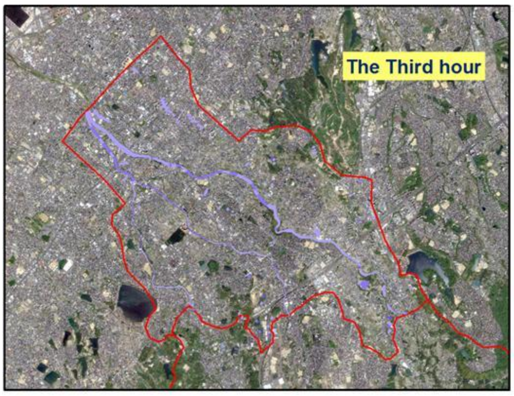
The Third hour


The four hour


The fifth hour

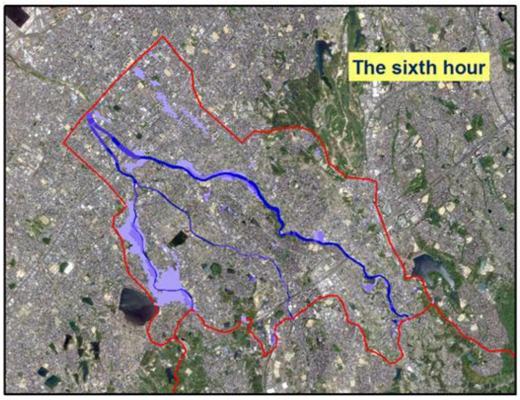
The sixth hour

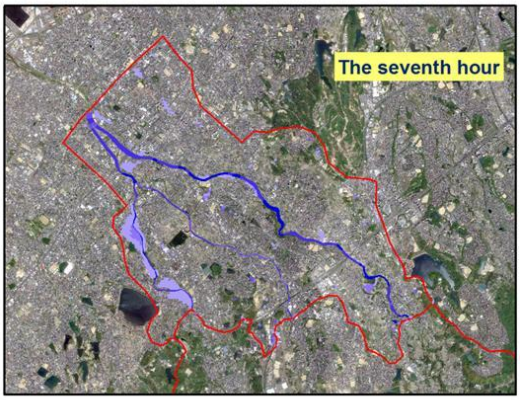
The seventh hour

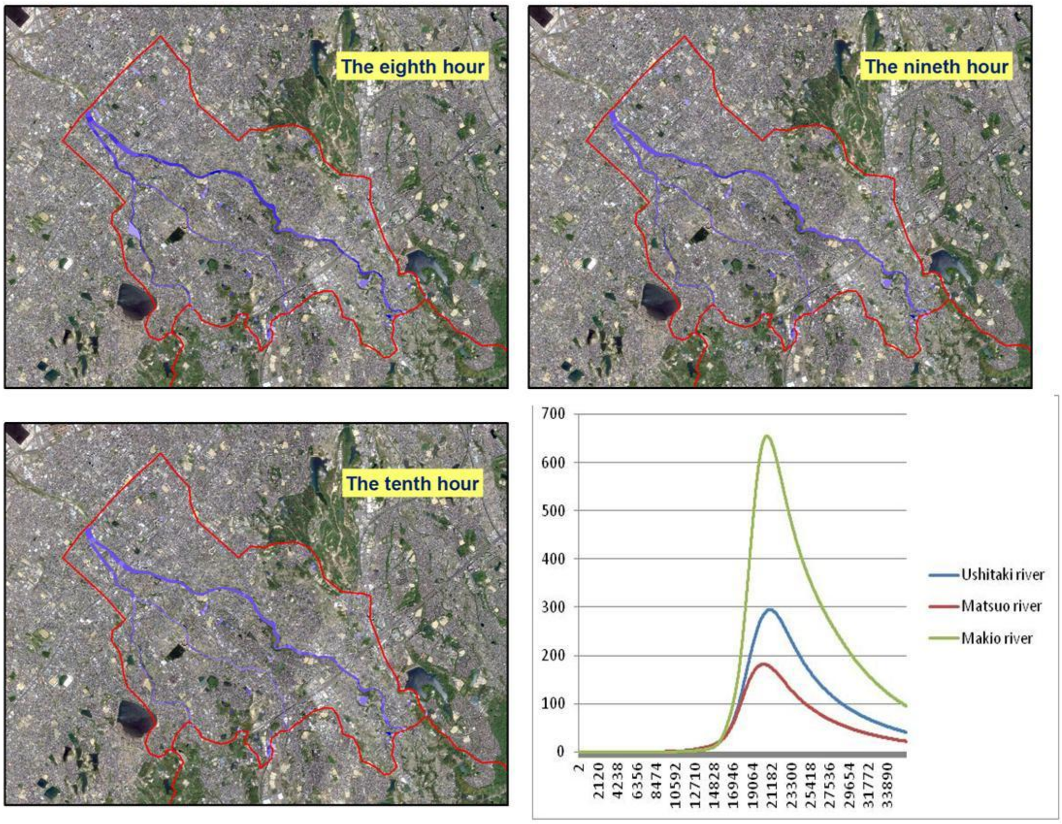

Figure 59 Flood simulation case by using generated rainfall as input. The first picture is the rainfall event used as input. The second picture to eleventh picture show the flood and inundation process in the risk assessment area. Because our model is an integrated rainfall–runoff–inundation model, the last image shows the runoff process from upper sub-basins

6.2.2 Event curve and risk curve

After spatial distribution of the economic data, the fragility curve is determined, and all rainfall scenarios are simulated, the loss for each rainfall event for each mesh can be calculated. Then, the flood event curve and risk curve can be calculated. The event curve is an event-based curve in which horizontal axis indicates the loss of event and the vertical axis indicates the expectance probability [12]. In our study, each flood scenario simulated from the generated rainfall according to a certain return period was treated as an event. The loss of event was plotted on the horizontal axis, and the return period was plotted on the vertical axis. For each mesh in the risk assessment area, a loss value was calculated for a rainfall event. Taking mesh No. 5548 for example, the loss and return period of events were plotted as shown in figure 60, and an event curve was drawn using the average loss of each return period.

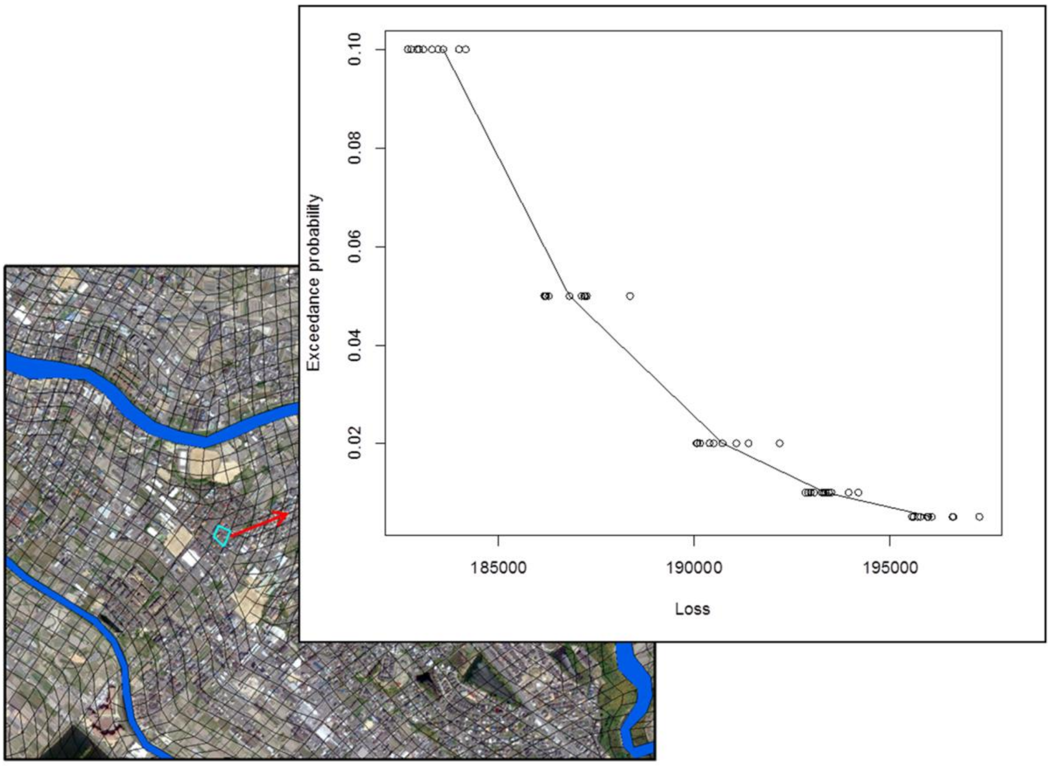

Figure 60 Location of mesh No. 5548 and its event curve

The event curve describes the relationship between loss and exceedance probability. However, as is shown in figure 60, in our study, many rainfall event could be generated according to a certain return period. These rainfall events of the same return period can be treated as uncertainty of flood risk. Risk curve considers such uncertainties to refine the event curve. It is possible to create a risk curve from an event curve through the following formula [12]:

$$EP(x) = \sum_i \left[\lambda_i \times P_i\left(x; \bar{x}, \sigma\right) \right],$$

where x is loss, $EP(x)$ is the exceedance probability of loss x, λ_i is the probability of event i, $P_i(X)$ is the exceedance probability of loss X, and σ is standard deviation. The risk curve of mesh No. 5548 was calculated, as shown in figure 61.

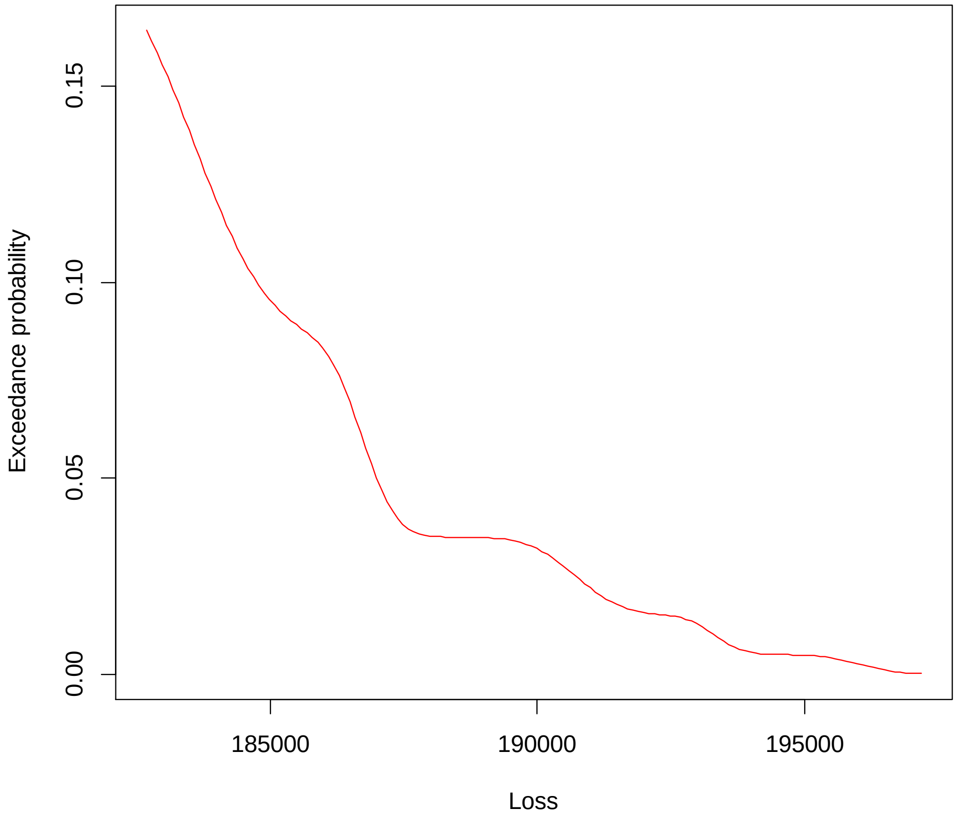

Figure 61 Risk curve of mesh No. 5548

6.2.3 Spatial distribution of flood risk

Our purpose was to study the spatial distribution of flood risk. In last several sections of this chapter, we have shown the methods and procedures of calculating the flood risk curve. The flood risk curve can be calculated in each mesh; therefore, when a mesh is selected, its risk curve can be presented. However, presenting a risk curve of each mesh is a 3D issue, which is slightly different from risk mapping. Sometimes it is necessary to show the flood risk on a map; therefore, the expected loss calculated from the risk curve of each mesh can be used for risk mapping. In figure 62 and figure 63, the spatial distribution of flood risk is mapped according to expected loss and expected loss ratio.

From these two figures, the spatial distribution of flood risk in this area can be understood. The flood risk caused by river flooding occurred mainly along the Ushitaki River, and that caused by inundation was mainly in the lower part of the river basin. This river flood risk is likely because the process of river improvement in the Ushitaki River is not completed, and the river capacity is relatively small. For the inundation flood risk, the lower part of the river basin is prone to inundation; however, the drainage in this area depends largely on pump stations, which were not considered in our simulation model. Therefore, the model could be improved in the future. Figure 63 shows that the expected loss ratio in this area is not high, likely because in the flood simulation, we assumed that all river dykes were safe enough so that no dyke collapsed. Water routed along rivers until reaching the height of the dyke, then overtopped. Some dyke break scenarios that may cause severe inundation were ignored. As previously stated, the model could be improved in the future.

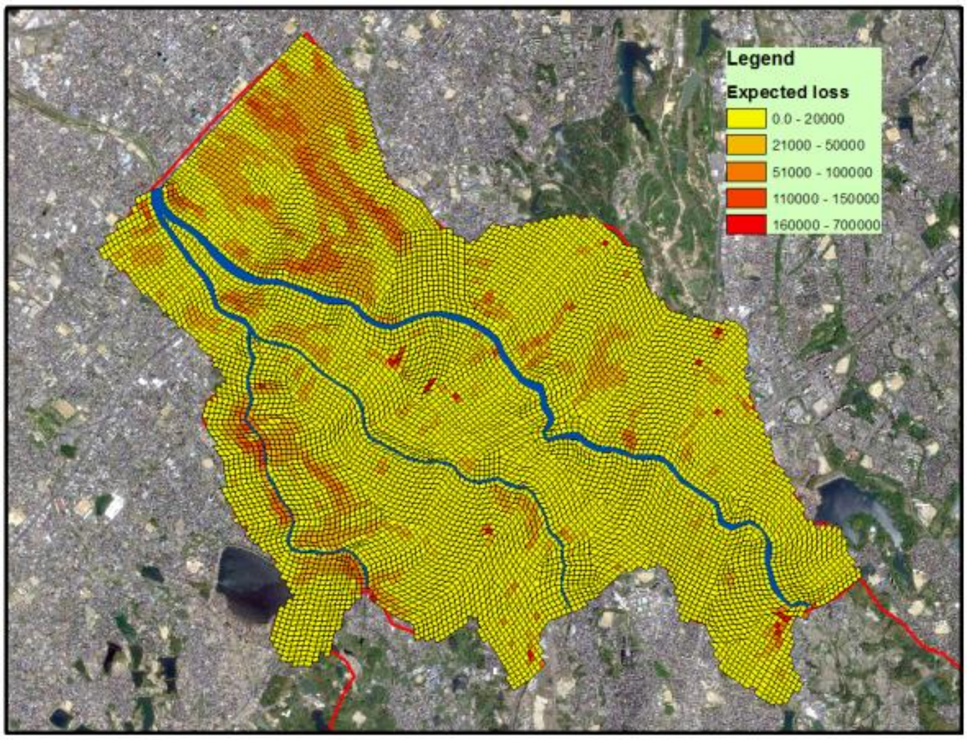

Figure 62 Map of spatial distribution of flood risk in terms of expected loss

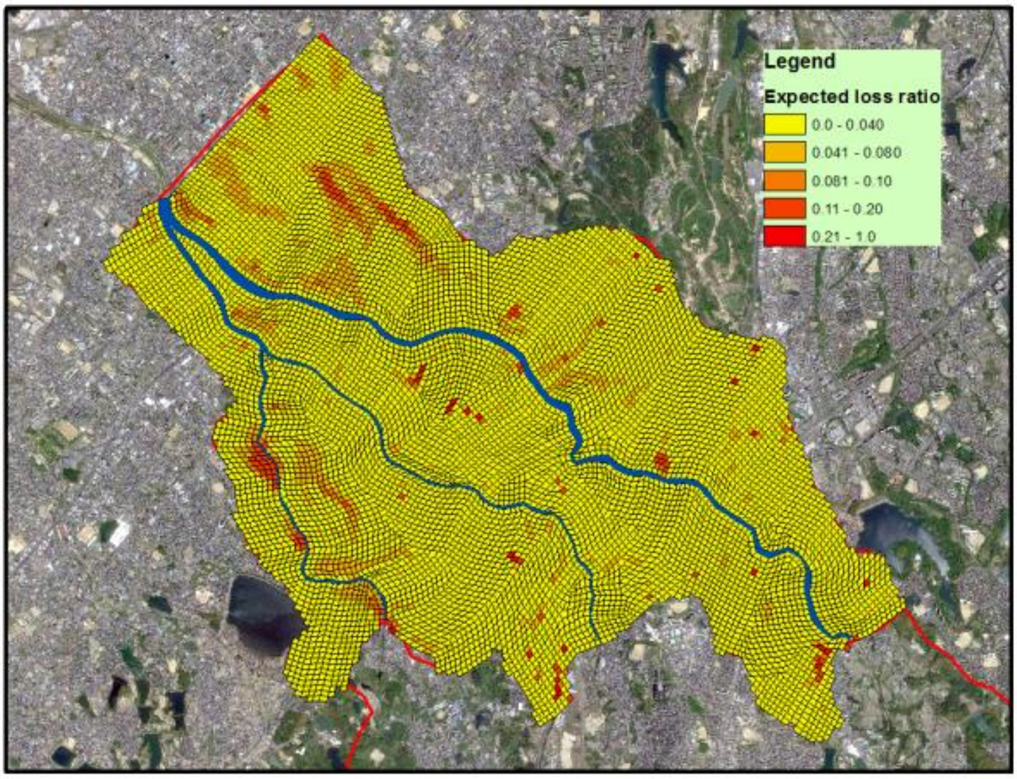

Figure 63 Map of spatial distribution of flood risk in terms of expected loss ratio

6.3 Discussion

This chapter adopted all achievements introduced in former chapters to conduct spatial flood risk assessment. Rainfall events were generated based on the copula method, and flood scenarios were simulated by the integrated rainfall–runoff–inundation model. To calculate the spatial distribution of flood risk, economic data and fragility information were distributed over the risk assessment area. Finally, the risk curve of each mesh was calculated, and a risk map was made in terms of excepted loss and expected loss ratio.

As proved in the case study, multivariate distribution of probability of occurrence of rainfall offers a reasonable way to generate the variation of rainfall events even in the same return period. The multivariate distribution of probability of occurrence of rainfall, which includes significant information of important rainfall duration for inundation and important rainfall duration for river flooding enabled us to consider inundation and river flood risk analysis from a statistical perspective. The risk assessment in the area, particularly the meshes that are prone to be flooding by river flooding, could be improved because local inundation is also included through the rainfall analysis.

In this case study, the phenomenon that a mesh is simultaneously affected by flooding from two rivers was not found, which does not mean that this phenomenon will not occur in this area. In fact, in the flood simulation, we assumed that all the river dykes were safe enough so that no dyke collapsed. Water routed along rivers until reaching the height of the dyke, then overtopped. Some dyke-break scenarios that may cause severe inundation were ignored. If the failure of dyke is considered, the phenomenon that a mesh simultaneously affected by flood from two rivers can be expected, particularly at the river junction area, which may cause severe damage. This also could be improved in future work.

References

[1] Sinfonica. 2010. Areal mesh based census of Japan. (in Japanese)

[2] Sinfonica. 2009. Areal mesh based economy census of Japan. (in Japanese)

[3] Sinfonica. 2006. Establishment and enterprise census of Japan. (in Japanese)

[4] Statistics Bureau, Ministry of Internal Affairs and Communications. 2009. A Guide to the Statistics Bureau, the Director-General for Policy Planning (Statistical Standards) and the Statistical Research and Training Institute.

[5] Ministry of Land, Infrastructure and Transport. 2005. Manual of economic survey for water management.

[6] Hall J W, Dawson R J, Sayers P B. 2003. A methodology for national-scale flood risk assessment . Proceedings of the ICE-Water and Maritime Engineering, 156(3): 235-247.

[7] Gouldby B, Sayers P, Mulet-Marti J, et al. 2008. A methodology for regional-scale flood risk assessment . Proceedings of the ICE-Water Management, 161(3): 169-182.

[8] Neal J, Keef C, Bates P, Beven K, Leedal, D. 2013. Probabilistic flood risk mapping including spatial dependence. Hydrological Processes, vol. 27, pp. 1349-1363.

[9] Nelsen R. 2006. An Introduction to Copulas, Second edition. Springer, New York.

[10] Aas K, Czado C, Frigessi A, et al. 2009. Pair-copula constructions of multiple dependence . Insurance: Mathematics and Economics, 44(2): 182-198.

[11] Gräler B, van den Berg M J, Vandenberghe S, et al. 2013. Multivariate return periods in hydrology: a critical and practical review focusing on synthetic design hydrograph estimation . Hydrology and Earth System Sciences, 17(4): 1281-1296.

[12] Tatano H, Takagi A. 2005. Economic analysis of disaster prevention: policy and evaluation of risk management. Keisoshobo Press. (in Japanese)

Chapter 7 Conclusion

7.1 Summary of research findings

This thesis proposed a methodology for assessment of spatial distribution of flood risk considering multiple flood risk sources. Compared with traditional flood risk assessment procedures, this proposed methodology emphasized two key points: (1) estimation of the joint probability of flood occurrence from multiple sources and (2) requirement of integrated simulation of the process from multiple sources to inundated water depth. For the first point, in this study, a copula-based method was proposed to estimate the joint probability of flood occurrence through spatio–temporal correlated rainfalls. To reduce the complexity of rainfall analysis, the concepts of basin rainfall and flood concentration time were adopted. For the second point, a GIS-based integrated rainfall–runoff–inundation model was developed. The model applied unstructured irregular meshes and simplified 2D shallow water equations to flood and inundation simulation in the risk assessment area. Moreover, it applied hydrological analysis and 1D kinematic wave equations to rainfall–runoff simulation in the runoff area and was able to simulate runoff, flooding and inundation together. GIS is fully adopted in data management and data processing as well as result visualization. Spatial flood risk assessment was realized through Monte Carlo generation of correlated rainfall events according to several return periods and the simulation of consequences of corresponding rainfall events. Spatial flood risk was represented as a risk curve for each mesh in the risk assessment area. A case study in the Otsu River Basin, Osaka prefecture, Japan, was conducted to demonstrate the feasibility of the methodology.

Because the study of flood risk assessment considering multiple flood sources is relative new, few studies have focused on this topic. Several research questions were encountered during the study and are worth summarization.

The first question is the definition of multiple flood sources. In this thesis, flood sources refer to the direct sources from which water originates. For example, a river is a source of river flooding, although the water of the river is the root of basin rainfall. The rainfall for river flooding is the root hazard. Under this definition, one can directly study the joint behaviors of multiple flood sources without consideration of their root hazards. For example, if we study the joint effects of two rivers on the flood risk at a junction area, only the discharge or water level of two rivers is enough [1]. In our case study, because the inundation from drainage was also included, it was difficult to build the joint probability distribution of drainage inundation and river flooding directly. Thus, we traced the root hazards of local rainfall and basin rainfall to estimate their joint probability.

The second question is the definition of flood risk. Although it was summarized in the first chapter, different people may have different ideas for the concept of risk. In this study, risk is defined as flood consequence with probability [2]. Under this definition, statistical calculation of flood risk was conducted. To analyze the factors contributing to the flood risk, the definition of flood risk as an interaction of hazard, exposure, and vulnerability was given [3]. These two definitions emphasized the different aspects of risk.

The third question considered how to define local rainfall and basin rainfall joint distribution of the occurrence of local inundation and river flooding, such as that in the case study. An intuitive way is for each basin and risk assessment, a representative rainfall was assigned. Then joint distribution of these rainfall events was made to evaluate the joint distribution of the occurrence of local inundation and river flooding. However, the rain gauge stations are not always well distributed in river basins, and the interpolated representative rainfall for each sub-basin and risk assessment area is not always reliable. On the other hand, even if representative rainfall of each sub-basin can be calculated from sufficient rain gauge stations, the complexity of the joint spatio–temporal correlation of rainfall will make risk analysis difficult to implement. Therefore, in the case study, we assumed that rainfall in the entire study area could be represented by one representative rainfall, and the hourly rainfall could be treated as local rainfall that causes local inundation. The rainfall amount for the duration of the concentration time could be treated as basin rainfall that causes river flooding. The joint probability of occurrence of flood from multiple sources became joint probability of occurrence of rainfall amounts in different durations.

The fourth question is the problem of building high dimensional joint distributions. Two popular methods were introduced in this thesis: *n*-dimensional Archimedean copula and the vine trees method. For the former, only the free specification of $d - 1$ copulas and the same Archimedean copula families are required in the nested process, and the degree of dependence expressed by the copula parameter must decrease with the level of nesting [4]. For the latter, they are based on a decomposition of a multivariate density into $d(d - 1)/2$ bivariate copula densities, of which the first $d - 1$ are unconditional and the rest are conditional [5]. For both methods, the higher dimensional joint distributions are built, the more information will be loss. Thus, for our study, although one can build 12 dimensional copula to represent the temporal structure of 12 h rainfall, it is not necessary to do so. Only focusing on the significant rainfall duration is enough.

The fifth question relates to the integrated rainfall–runoff–inundation model. Some arguments from Europe scholars indicate that it is not necessary to develop an integrated rainfall–runoff–inundation model and that only an inundation model is enough for flood and inundation risk assessment. This is may be true in Europe because most places in that region are relatively level, and it is not necessary to emphasize the runoff from mountains far away; thus, the rainfall–runoff is just an input of the inundation simulation model. However, in Japan, most areas are mountainous. Rainfall can easily root from mountainous areas to urban areas, which are just located at the foot of mountains. In this case, runoff from mountains is also important. The spatial correlation between rainfall in the runoff area and that in the urban area will significantly influence the inundation and river flooding of the urban area.

Finally, the method of sampling of rainfall events from joint distribution according to a certain return period directly influences the shape of the final flood risk curve. In the case study, although a procedure for sampling rainfall events was proposed, the question arose of how many rainfall events are enough for a risk curve construction. Definitely, the more rainfall events generated, the better the risk curve. The flood simulation is a time-consuming work, particularly for unstructured irregular mesh-based flood and inundation simulation models.

Other research findings could be addressed.

The biggest achievement for this thesis is the methodological framework for flood risk assessment considering multiple sources. It is a systemic work that includes rainfall analysis, runoff simulation, flood inundation simulation and as flood risk assessment and integrates knowledge from disciplines such as copula from statistics, runoff simulation from hydrology, flood inundation simulation from hydrodynamics, risk assessment from economics and implementation from geography and informatics.

The feasibility of the methodology was demonstrated by the case study in the Otsu River Basin, Osaka prefecture, Japan. More case studied could be expected with improvement by following the proposed procedure.

As the main chapter, the copula-based method was proposed to estimate the joint probability of occurrence of flood through rainfall. To reduce the complexity of rainfall analysis, the concepts of basin rainfall and flood concentration time were adopted. This idea worked well in the case study and is convenient for flood risk assessment considering multiple sources.

A GIS-based integrated rainfall–inundation simulation model was developed, and a procedure of data processing for model construction on GIS was proposed. This will significantly change the idea of simulation modeling [6]. Through GIS functions, the modeler can obtain the mesh and parameter information without considering basic data structures, and it is convenient for people not majoring in hydrodynamics [7].

Finally, the procedure of spatial flood risk assessment was given. From the spatial distribution of economic data and the fragility curve, Monte Carlo simulation of rainfall, cascading flood simulation to the event curve, and risk curve calculation, C++ code and R code were made, which can be used in the future.

7.2 Future research

Although the methodology for spatial flood risk assessment considering multiple sources was basically achieved, it is just a small step of this study. In future researches, the works should be continued.

First, the components in the methodological framework could be updates with the development of knowledge. For example, improvement of the copula method to deal with multivariate distributions can result in a faster and more stably integrated rainfall–runoff–inundation model to simulate rainfall events.

Second, in this thesis, the flood risk sources are only considered as river floods and local inundation. The methodology should be expanded to cover storm surge, tsunamis, and other flood risk sources to realize a general methodology. During the process of expansion, research topic will appear for further research.

For many reasons, current, flood risk management should become more integrated to deal with different types of countermeasures, multiple stakeholders, and authorities. The purpose of our research is provide a scientific platform to assess the present situation in a target river basin and to evaluate the efficiency of integrated countermeasures. Therefore, applying our research to actual work and practical issues, such as urban planning, evacuation directions, etc. is a significant in the future study.

As is presented in the thesis, the assessed spatial flood risk from our methodology are probability distribution of loss at each place in a basin. Compare with qualitative risk assessment, the methodology provides statistically reliable and generalisable results of risk information; Compare with traditional quantitative analysis, the methodology provides the information of "risk as probability distribution" rather than "risk as a number", allow decision makers to access to more possibilities of loss scenarios which may help them for better decision making; Compare with traditional method of probabilistic flood risk analysis, the methodology considering multiple flood risk sources, provides more precise risk information at each place of a basin.

Local government officers may utilize the risk information provided by the methodology to optimize the choice of the portfolio of countermeasures, for example, build dyke for small rivers and make evacuation planning or land use restriction for large river, etc. Enterprises may utilize the risk information provided by the methodology to make better decision on factory location selection, flood prevention investment, etc. Communities may also utilize the hazard map or risk map provided by the methodology for risk communication and risk education, because this methodology considering flood risk from multiple flood sources, people in the communities will have a better understanding of flood may occur from multiple sources and have a direct recognition of spatial flood risk. Many ways are available for applying our research into social world. In the future , some actual case studies are expected.

References

[1] Neal J, Keef C, Bates P, Beven K, Leedal D. 2013. Probabilistic flood risk mapping including spatial dependence. Hydrological Processes, vol. 27, pp. 1349-1363.

[2] Conrow E H. 2003. Effective risk management: Some keys to success. Aiaa.

[3] Hagihara Y, Okada N, Tatano H. 2006. Introduction to Integrated Disaster Risk Management, Kyoto University Academic Press, pp. 141-143. (in Japanese)

[4] Savu C, Trede M. 2010. Hierarchies of Archimedean copulas. Quantitative Finance, 10(3): 295-304.

[5] Czado C. 2010. Pair-copula constructions of multivariate copulas, Copula theory and its applications. Springer Berlin Heidelberg: 93-109.

[6] Jiang X, Tatano H, Zhang J. 2011. Data Processing Procedure for Irregular Mesh Inundation Simulation Models: Toward Development of A GIS Based Inundation Simulation System. Proceedings of the Thirteenth International Summer Symposium, pp. 91-94.

[7] Zhijun T, Jiquan Z, Xinyu J. 2012. Urban Safety Geographic Information System, Peking University Press. (in Chinese)